ON PLANT MYOSIN

Thesis by

Paul On-Pong Ts'o

In Partial Fulfillment of the Requirements

for the Degree of

Doctor of Philosophy

California Institute of Technology

Pasadena, California

1956

This thesis is affectionately dedicated to

Amy and Paul S. F. Ts'o

ACKNOWLEDGEMENTS

The author wishes to acknowledge his gratitude to the people who have made this work possible, profitable and enjoyable.

Dr. James Bonner has directed the research and the educational program of the author in the Institute with far sightedness and great interest. He has whole-heartedly encouraged the author to study in the fundamental sciences of physics and chemistry. With special effort, he has made many facilities available for this training program and for this research project. Dr. Jerome Vinograd patiently and carefully taught the author protein physical chemistry and served as an adviser on this aspect of the work. He helped to design experiments and gave many hours in valuable discussion. It is also a pleasure to know him socially and personally. Dr. Luther Eggman has designed the viscometers, run the ultracentrifuge and helped out in many technical difficulties including the printing of all the photographs in this thesis. In association with him during these years, the author has acquired a higher standard of precision and perfection in experimentation. The three individuals mentioned above have been an integral part of this research program. It is only through their common efforts, including correcting this thesis, that this work is in its present form.

Dr. D. L. Caspar and Dr. W. A. Jensen have contributed

Appendixes I and II respectively in cooperation with the author. Dr. Jensen has proof-read the manuscript before typing. Drs. P. Y. Cheng, M. Delbrück, and A. W. Galston have discussed with the author different parts of this work.

Dr. D. H. Campbell and members of his group in the Chemistry Division have made their instruments available for this work and were always fully cooperative. Many friends and fellow students have made the life of the author at the Institute a stimulating and enjoyable one.

Mrs. Alethea Miller typed the manuscript and Miss Mary L. Slichter prepared most of the figures. Miss Muriel Wong filled in the equations and the diagrams in the text.

The author has received financial support from teaching assistantships and McCallum Summer Fellowship of the Biology Division and from the Frank Shu Scholarship.

Mrs. Doris T. C. Yip and Professor and Mrs. S. C. Lee have made the opportunity for advanced study possible for the author.

Finally, the author wishes to express his admiration and appreciation to the One who creates and takes care of the slime mold as well as the author.

ABSTRACT

A systematic study has been carried out both on the cellular and the molecular level of the mechanism of protoplasmic streaming in the slime mold, Physarum polycephalum. This study is based on the hypothesis that ATP-protein interaction is an important feature of the mechanism.

ATP has been found to have a liquefying effect on the gel structure of the streaming plasmodium. Furthermore, when ATP is allowed to react with protoplasmic material extracted from plasmodia under proper conditions, the viscosity of the solution decreases immediately. This abrupt decrease in viscosity of the protoplasmic solution is followed by a slow recovery.

The active protein which is responsible for ATP induced viscosity lowering reaction has been identified by studies of viscosity, electrophoresis and ultracentrifuge. It has been purified to 75% by salt precipitation and differential centrifugation. It is proposed that this protein be termed myxomyosin because of its similarity to actomyosin.

Myxomyosin is found to complex with RNA to ca. 9% of its own weight. The RNA does not appear to be essential for the ATP-protein interaction process. RNA does, however, exert a great influence on the physical states of myxomyosin in solution.

Myxomyosin preparations possess an ATPase activity. The turnover number of this enzymatic activity is small, namely, 30. A refractory state of myxomyosin has been found. Immediately after myxomyosin reacts with a large excess of ATP, the system enters into a refractory state which persists during the re-

covery of the viscosity level. In this state, the protein is not sensitive to ATP.

Viscosity, sedimentation, flow birefringence and electron microscopy studies reveal that myxomyosin is a rod-like molecule with a weight average molecular weight of 6 millions $\pm$ 10% and with a range of 4.9 to 10 millions. The molecule possesses a diameter of 50 Å $\pm$ 5 Å and a most frequent length of 4000 Å with a range of 3000 to 6000 Å.

The effect of ATP on myxomyosin has been investigated by viscosity, sedimentation, flow birefringence, electron microscopy and electrophoresis studies. There is no indication that myxomyosin breaks down into small units or suffers an extensive change in shape when it reacts with ATP. The present data are best understood on the basis that in the absence of ATP, myxomyosin aggregates in a concentration-dependent manner. The binding of ATP to the myxomyosin moiety reduces the aggregation of the monomers.

A proposed mechanism of protoplasmic streaming, suggested by the above observations is presented.

TABLE OF CONTENTS

I. INTRODUCTION

A. The Concepts.

The present research is based on two fundamental concepts developed over the last thirty years. The first is the concept of ATP (Adenosine Triphosphate) as a carrier of energy in biological systems while the second is the concept of the conversion of chemical energy to mechanical work by interaction of ATP and protein.

Through the findings of Meyerhof, Embden, Warburg, Kalckar, Ochoa, Krebs, Lippman, and others the mechanism of respiration and especially of oxidative phosphorylation has been elucidated. The general significance of phosphorylated organic compounds such as ATP was first clearly realized by Lippman who termed them energy-rich. The hydrolysis of these compounds to inorganic phosphate at physiological pH is highly exothermic and exergonic in nature. Among such materials, adenosine triphosphate has received most attention because it is present in larger amounts than the others and participates in many reactions. It was soon noticed that the large negative ΔF of ATP hydrolysis might be utilized to drive an endergonic reaction by suitable coupling of two systems provided only that the total sum of the free energies of the two reactions is negative. This type of coupling has been demonstrated not only to be the source

of energy for phosphorylations but also for the synthesis of fatty acids, the synthesis of small peptides, and in part for the photosynthetic reduction of CO_2. We now know that by the coupling of phosphorylation to electron transfer, ATP and similar compounds can be generated from their related esters and, that, by coupling the hydrolysis of energy-rich phosphate compounds to biosynthetic reactions other materials can be made. In a sense, ATP and similar compounds serve as energy carriers for the organism. Except for minor disagreements over details such as nomenclature, this concept permeates and dominates the field of biochemistry today. Not until recently, through the work of Millerd, Bonner, Laties, Stumpf, Albaum and others, was this idea conclusively extended to the biochemistry of the plant kingdom (1, 2, 3, 4, 5). A comprehensive and comparative review of the development of the concept in both the animal and plant world is given in the Ph.D. theses of Adele Millerd (1951) and Paul Saltman (1953), available at C.I.T.

Recent measurements of the enthalpy and free energy of ATP and pyrophosphate hydrolyses at pH 7 and 25°C temperature indicate that these values are lower than earlier believed (6, 7). The free energy for hydrolysis of ATP to ADP and inorganic phosphate is calculated to be 7900 calories by Meister (8) who studied the glutamine synthesis system and to be 6600 calories by Ouellet, Laidler, and Morales (9) who have studied the myosin system. These values are con-

siderably lower than the 10,000 to 12,000 calories previously believed to be correct (10, 11, 12). The new value for the free energy of ATP hydrolysis is however, still sufficiently high to account for the role of the substance biochemical reactions such as discussed above.

The second concept mentioned above is even more closely related to the present research. Evidently a living organism does many things in addition to synthesizing new compounds. These activities usually require a source of energy. Does ATP supply energy to endergonic but non-chemosynthetic reactions? The present research concerns only one, but an important, activity of all living organisms, namely, mechanical movement. It is not intended to review here the development of the physiology and chemistry of muscle. Many good reviews of the subject have appeared (13, 14, 15, 16, 17). The basic concept involved will, however, be presented below. The general approach of the muscle work has been adapted to this investigation and at the end of this thesis a comparison of the properties of the slime mold myxomyosin with the properties of actomyosin from the animal world will be made.

The early experiments of Muralt and Edsall (18) pointed out that large and highly asymmetric protein molecules can be extracted from muscle. The facts suggested that if these molecules were properly linked they might form the mechanical basis of muscle structure contraction. In 1940, the

school of Syent-Györgyi discovered the profound effect of salts and of ATP on the physical-chemical properties of the extracted muscle protein. Engelhardt and Ljubimova (19) at nearly the same time noticed that muscle proteins also have the ability to hydrolyze the terminal phosphate from ATP. The molecular physiology of muscle has flourished from the time of these two observations. Most of the studies can be categorized into four general classes as follows:

1. The contraction of the whole muscle fiber has been followed by chemical analysis, pH fluctuations, effects of inhibitors and stimulators, spectroscopy over a wide range of wave lengths, optical properties, thermal effects, electron microscopy, x-ray diffraction, mechanical properties, volume changes and others.

2. The muscle fiber is disassembled in solution as mildly as possible and the individual properties and interactions of constituent proteins are examined. Their enzymatic activities, physical states, chemical compositions, behavior toward salts, ions and other compounds have been described by methods such as chemical kinetics, titration measurements, optical studies, sedimentation and electrophoretic studies, hydrodynamic measurements, electron microscopy, x-ray diffraction, spectroscopy and others. Efforts are being made to reassemble the important constituent proteins into a unit capable of physical contraction, namely, a fiber, as close to the original living muscle

fiber as possible.

3. The notion that ATP is the direct causal agent in muscle contraction and the notion that the hydrolysis of the terminal phosphate of ATP directly or indirectly supplies the energy for contraction, have been investigated. Effects of ATP on living muscle fiber, on individual constituent proteins and their aggregates, on reconstituted fibers, the rate of hydrolysis of ATP, the reaction products, the specificity and effect of inhibitors, the amount and source of supply of ATP, etc. are examined in the light of chemical kinetics, thermodynamics, and modern colloid chemistry.

4. Models, theoretical and experimental, have been examined in order to demonstrate or support proposed theories of the mechanism of muscle contraction.

The above approaches themselves outline the basic concepts of modern muscle research. The great advances in the understanding of electron transfer, oxidative phosphorylation, and the biosynthetic pathways of cell metabolism are contributions of organic chemistry to the understanding of life. The significant advances of molecular muscle research are contributions of physics and of physical chemistry. Through these contributions parameters referred to space and structure are added to the description of the life process.

B. The Phenomena.

Many living organisms move around in various ways in addition to those employed by mammals. The idea that ATP may supply the energy for such non-muscular mechanical movement has been frequently put forward. Among the observations which suggest this hypothesis are: an effect of ATP injection on the movement of amoeba (20, 21), a correlation between the mobility of spermatozoan and the amount of ATP inside it (22), a relationship of ATPase activity to the mobility of leucocytes (23), and an effect of ATP on the physical properties of cytoplasm of sea urchin egg (24). It is indeed tempting to extend the concept as the basic mechanism for all kinds of mechanical movement in living organisms.

The phenomenon of protoplasmic flow has attracted many botanists since the discovery of the phenomenon by Cori in 1772 (25). The streaming rate of protoplasm ranges from 0.6 mm sec^{-1} in Physarum to 0.01 mm sec^{-1} in Elodea or even less in some species in special environments (25, 26, 27). Information concerning protoplasmic flow has also been collected from studies on the effects of physical agents such as temperature, light, electricity, shock, supersonic waves, pressure, torsion, and centrifugation on the protoplasm (25, 27). Effects of chemical treatment by drugs, alkaloids, dinitrophenol, anesthetic agents, salt, and acids on protoplasmic flow have also been reported abundantly

(25, 27, 28, 29, 30). That these reports are contradictory and confusing can be mainly attributed to two causes.

1. Inadequate knowledge of the primary reaction caused by the applied agents. The primary reaction caused by such treatments as x-ray, electricity, light, or auxin are far from being understood so the complicated effects of these agents on protoplasmic flow likewise cannot be understood. On the other hand, effects caused by heat, acids, or salts are too general to permit unique and concrete interpretation.

2. Inadequate control of the environment in which the measurements are made. Thus the experimental results are not reproducible, or comparable to each other.

Since the observations are based only on measurement of rate of flow, a resultant expression of several interacting forces, no specific information is provided regarding any particular physical property of the protoplasm such as viscosity or surface tension.

In the strife over the mechanism of protoplasmic streaming, one important but subtle point could be easily overlooked in the overall picture. It is rather obvious that the physiological function of muscle contraction in the animal kingdom is intended for little more than mechanical movement. But is this also true in the plant world? Mechanical movement may be still a major physiological function of the protoplasmic flow of slime molds and like organisms,

but it is highly unlikely that the protoplasmic streaming of green plant cells will serve this purpose. Most of the living cells of higher plants exhibit protoplasmic flow at all times or at certain times in their life history. The physiological function of protoplasmic flow is therefore uncertain. It may perhaps just circulate the cell contents, but it may also accomplish other important functions. For this reason, the recent proposal of Goldacre (31) is of interest. After Goldacre conclusively demonstrated an effect of injected ATP on amoeba, he went on to observe the absorption of vital dyes by amoeba, root hairs, and Neurospora filaments, especially with respect to the location of the dye in relation to protoplasmic movement. Through a rather extensive but unconvincing argument which is too long to be presented here, he suggests that protoplasmic streaming is motivated by an ATP mediated folding and unfolding of protein molecules, and that this change of configuration leads to active absorption of solutes. There is no clear evidence as yet which establishes a relationship between protoplasmic streaming and active uptake of solutes. The significance of proteins in relation to transport of ions is well recognized (32) and active ion uptake is an energy requiring process (33, 34, 35). Therefore, even though there is no clear evidence establishing a relationship between protoplasmic streaming and active uptake of solutes, the idea of transformation of chemical energy into

osmotic work through a ATP-protein coupled system is none-the-less an attractive one. This concept lies beyond the scope of this thesis which deals with the coupling of ATP to mechanical movement. However, because of the fundamental importance of active uptake process and the possibility that this process may be one of the physiological functions of protoplasmic flow, added interest is attached to the present research.

C. The Problems.

Attention will now be focused on the special problem of this thesis. The plasmodium of Myxomycetes, especially that of the species, Physarum polycephalum, has been a favorite experimental organism for research on protoplasmic structure and streaming. Its life history was first described by Howard in 1931 (36) together with some histological studies. Activities of some of the enzymes of the mold have been reported by Holter and Pollock (37), and by Ward (38). The cytology and structure of the plasmodia, especially in relationship to protoplasmic streaming, have been described by Camp (39), Andreson and Pollock (40), Lewis (41) and Seifriz (42). By injecting enzymes and salts into the plasmodium, Haas has obtained information about the effects of these substances in protoplasmic streaming and on the chemical nature of the protoplasm. Sponsler and Bath provide electron microscope picture of certain structural

components of the plasmodium (44). Most of the important observations on the protoplasmic streaming of Physarum have been summarized by Marsland, Lewis, Kamiya, and Seifriz in the monograph, The structure of Protoplasm, edited by Seifriz in 1942 (41, 42). Seifriz has also reviewed this subject thoroughly in 1950 (25). A few of the important facts concerning protoplasmic streaming will be summarized here so that they may serve as a reference for later discussion.

The plasmodial strand is surrounded by a structureless, slimy, and colorless sheath. This sheath consists of polysaccharides, waste products and contaminating microorganisms. The slime substance is left behind by the moving plasmodium. Closely under the sheath is a thin membrane, the plasmalemma, as in amoeba. The plasmagel, a rather stationary gel layer containing inclusion bodies lies underneath the plasmalemma. According to Lewis (41) and Camp (39), a layer of clear hyaline cytoplasm is sometimes found between the plasmalemma and the plasmagel as if the ground cytoplasm had filtered through the gel structure and reached the membrane. Embedded in the structure of plasmagel are much less viscous regions, the plasmasols, in which the protoplasmic streaming takes place. The streaming itself is made visible by the fact that particular inclusion bodies of various kinds are born along in the flow. The direction of protoplasmic streaming reverses periodically in a shuttle way and in the advancing

plasmodia, the streams may be seen to branch and fuse again. The following diagrammatic figure illustrates the main structure.

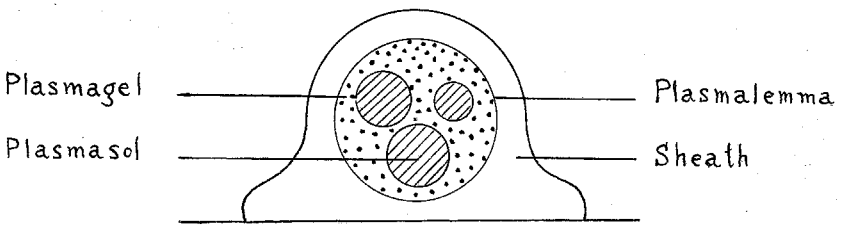

Diagrammatic drawing of a cross section of a vein of Physarum polycephalium on the surface of a liquid (from Pollock and Holter).

Marsland and Brown (44) have made a thorough study of the effect of high hydrostatic pressure on protoplasmic flow of amoeba and Elodea. They observed that with Elodea the streaming rate is reversibly and regularly decreased as pressure on the whole cell is increased up to 400 atmosphere. As the pressure goes up, the viscosity of the cytoplasm decreases which suggests that solation of the protoplams, i.e. conversion of gel to sol, is formed by high pressure. In the case of amoeba, increase of the pressure to 4000 lbs per square inch stops the movement and increases protoplasmic solation. Marsland and Brown also report that there is a

gradient of rigidity in the plasmagel structure, the rigidity decreasing from the base to the newly formed tip of the pseuodopodium. Since high pressures increase solation of protoplasm and decrease streaming rate in a proportional fashion, they conclude that the sol-gel transformation is an important factor in protoplasmic streaming.

With the help of a very ingenious method, Kamiya has recorded the rate of streaming, changes in direction and periodicity of streaming of the slime mold (45). By Fourier analysis, he demonstrated that these curves so obtained can be represented by a combination of sine wave components with different periodicities and different amplitudes. Kamiya measured the driving pressure of streaming as usually about 15 cm of water and he was able to accelerate, stop, or reverse protoplasmic streaming by applying an appropriate pressure differential. He also showed that the velocity distribution in the moving protoplasmic front is parabolic, being fastest in the middle of the strand and slowest along the sides as is expected in a capillary flow with peripheral resistance. These facts taken together led him to conclude that the protoplasmic flow is caused by rhythmic differences in pressure in different zones of the plasmodium (25). Lewis (41) has closely observed the changes inside the plasmodium during streaming and described them as follows.

> Contraction and partial solation of the posterior part of the gel layer forces the endoplasm forward through the tube and channels to the anterior end,

> where it forces out pseudopodia at weak places and builds forward the plasmodium at their bases. After about 30 seconds gelation sets in at the anterior end; the resulting contractile tension there, together with partial solation reverses the endoplasmic flow and expands the posterior weakened end. After about 30 seconds, gelation at the posterior end increases the contractile tension and reverses the flow and repeats the cycle. There is net gain at the anterior end and a net loss at the posterior end with each cycle.

Lewis assumed that the regulating mechanism depends on the tensions and turgor pressures of the different parts of the strand. Seifriz (42), using a camera, has made the following observations.

> If time-lapse moving pictures of the streaming protoplasm of the myxomycete, . . . , are made, a remarkable pulsation of the plasmodium is revealed. Pictures taken . . . , show the plasmodium undergoing rhythmic contraction and expansion when thus optically accelerated resemble the pulsations of a heart. At each contraction and relaxation the direction of protoplasmic flow reverses . . . . As the rhythmic contraction of the protoplasm is synchronized with the streaming . . . , from which the only constructive deduction to be made is that the flow is the result of the rhythmic movement. The mechanism of protoplasmic movement in slime mold is, then, one of rhythmic contraction and relaxation of the plasmodium with a total of 95 seconds for each pulsation, 45 seconds for systole and 50 seconds for diastole, the additional 5 seconds in time of outward flow account for advancement.

Seifriz disagreed, however, with the view that the driving force of protoplasmic flow is due to the contraction of outer cortical layer of the protoplasm, and proposed that the contraction is one of the whole protoplasm. The surface of the strand wrinkles as the strand contracts, which,

suggested to Seifriz that the outermost layer of the strand is not under tension. He also described some cases in which the contraction is not centered in the surface layer, but at a point or points some distance inside the protoplasm.

Further information in regard to the mechanism of protoplasmic streaming can hardly be obtained from descriptive observations on the cellular level. It is then necessary to break down the plasmodium and to study the phenomenon on a molecular level. In this case, however, the streaming can no longer be observed. Some new expression for the transformation of chemical energy to mechanical movement must be found, namely, reversible change in physical state of the extracted plasmodium in response to experimental treatment. Loewy in 1952 (46) has made a significant contribution to this aspect of the problem. He showed that the addition of ATP or of ITP (Inosine triphosphate) to crude extract of the plasmodia causes reversible changes of viscosity, changes resembling those induced by ATP in actomyosin solutions. Inorganic phosphate was liberated during the process. This has opened the door to physical and chemical studies of the nature of protoplasmic streaming on a molecular level. This matter is the subject of the present dissertation.

D. The approach.

The effect of ATP and related compounds on the streaming of plasmodium of the slime mold has been investigated. Crude extracts were then prepared by suitable methods and with these extracts reversible changes of the physical properties of the extract were found to be induced by ATP. The component of the extract chiefly responsible for the interreaction with ATP was then highly purified and was found to be a nucleoprotein. The chemical composition, the molecular dimensions, shape and molecular weight of this component have been extensively studied by several physical and chemical methods. Information pertinent to the interreaction of ATP and the active component have been collected. Finally, a model is suggested to explain the mechanism of protoplasmic streaming in relation to these new findings.

II. MATERIALS AND EXPERIMENTAL METHODS

A. Culture and Extraction of the Slime Mold Plasmodia.

Physarum polycephalum is cultured by a modified procedure of Loewy (46).* An inverted dish wrapped with a paper towel is sprinkled with oatmeal, and is inoculated with sclerotia or a growing culture of the organism. The dish is then placed in a pan containing a shallow layer of water. The pan is covered with a glass plate and incubated in dim light or total darkness at a constant temperature of 21° to 22° C. In 48 to 72 hours the multi-nucleate plasmodia are collected from the surface of the water and the walls of the pan, drained free of water, and frozen and stored at -10° C.

For the extraction, the frozen plasmodia not older than 2 months are first shattered into small pieces and the fragments ground to a slush in a cold mortar at *ca.* 0° C. The extraction medium, generally 1.4 ml per gram of frozen plasmodia, is added to this slush and extracted for one hour at -3° C to 2° C. The slurry is then centrifuged in the cold in a SS-1 Sorval centrifuge at 16,000xg for 20 minutes. The turbid supernatant solution is decanted through a filter pad of glass wool to remove particles and the lipid material which has coalesced at the top. It is

---

* The author expresses his gratitude to Dr. A. G. Loewy for the myxomycete culture.

then centrifuged a second time at 20,000xg for 20 minutes. The somewhat opalescent supernatant solution from the second centrifugation is termed the crude extract and usually contains about 1.5% by weight of trichloroacetic acid (TCA) precipitable material. The crude extract so obtained is the starting material for further purification as described in detail in Chapter IV.

B. Chemicals.

The dipotassium salts of adenosine triphosphate (ATP), adenosine diphosphate (ADP) (both from Pabst Co.) and adenosine monophosphate (from Ernst Bischoff Co.) were used without further purification. The solutions were neutralized to pH 7.0 with potassium hydroxide. All other reagents were of reagent grade.

C. Methods of Chemical Analysis.

Analysis of carbohydrates by the anthrone reagent. This method was employed for the estimation of polysaccharides which in these preparations derive principally from the slime. The method has been described by Morris (47).

Analysis of protein by biuret method. This method is seldom employed as a measurement of the protein content because of its low accuracy and also because the protein solutions are not colorless. It serves well, however, as a quick semi-quantitative method and also yields qualitative chemical evidence as to whether protein or polypeptides are

present in the preparation. The method described by Cornell, Bardawell, and David (48) was used.

The analysis of phosphorus by Allan's method with slight modification (49). This method is employed for the determination of total phosphate in the myxomyosin preparation and for study of the ATPase activity of the crude extract. A Beckman model B spectrophotometer was used and readings were taken at 650 millimicrons.

The determination of inorganic phosphate by the Lowry and Lopez method (50). The enzymatic hydrolysis of ATP by purified myxomyosin was followed by the analysis of inorganic phosphate. This method is very mild and does not hydrolyze phosphate esters such as creatine phosphate which are even more labile to acid than ATP and ADP.

D. Measurement of Concentration of Macromolecules.

Trichloroacetic acid precipitation method. This method for the measurement of concentration of macromolecules, mostly proteins, is employed in the investigation of the behavior of the crude plasmodial extract and the isolation of the myxomyosin as described in Chapter II and IV. The proteins in the solution were precipitated by addition of cold 1 N TCA to a volume ratio of 1:2. The precipitate was then centrifuged down after one hour or more at 0° C and washed twice with 0.5 N TCA. The washed precipitate was dried to constant weight at 100° C, usually about 72-100

hours. The range of dry weights was 10 to 20 mg per sample.

Differential refractometer method. This method was used for the measurement of protein concentration in the studies on the properties of purified myxomyosin. The advantages of this method are that it gives a precise and immediate answer, and that the solution is unchanged by the measurement. The solution must first, however, be thoroughly dialyzed. The principle and the instrumentation of the method are described by Brice and Hawler (51). The apparatus is that of the Phoenix Precision Company. It consists of an AH-3 mercury lamp, a filter which isolates 546 mu wave length band, a divided prismatic differential cell, a projection lens, a bilateral slit, and a filar micrometer microscope, all mounted on a horizontal optical bench. A parallel monochromatic beam of light is allowed to pass through a hollow prismatic cell which is divided obliquely into two equal compartments. If the solutions in the two compartments have the same index of refraction, n, the light path will suffer no deviation. If, however, the dialyzed protein solution is placed in one compartment and the buffer against which the protein was dialyzed in the other compartment, then the instrument is so designed that the slit image Δ d as determined by the filar micrometer is proportional to the difference in refractive index, Δn, of the two solutions.

$$\Delta n = K \cdot \Delta d$$

The proportionality constant K can be calibrated from the geometry of the instrument or from a solution of known concentration and known refractive index increment (dn/dc). The apparatus constant for the present instrument is 9.287×10^{-4}.* So, if the refractive increment, dn/dc, of any solute is known, the concentration can be calculated by the following equation:

$$\Delta n = \Delta c \cdot \frac{dn}{dc} = K \cdot \Delta d$$

For the time being, the dn/dc of myxomyosin at 546 mμ wavelength is assumed to be 0.185 (concentration in gm/cc) in accordance with the average value for most proteins. The working equation for the measurement of protein concentration in the myxomyosin system is

$$c = (0.502) \quad \Delta d$$

where c is in weight percent. It should be noted that both the methods employed for concentration determination yield values for total macromolecules content and may include small amounts of nucleic acid and polysaccharides as well as the major protein component.

---

* This constant was obtained by Dr. L. Eggman based on the calibration of KCl solution. The dn/dc value of KCl was taken from the data of Gosting (72: 4418, Jour. Amer. Chem. Soc. 1950).

E. Chromatography.

In order to demonstrate the presence of RNA in the myxomyosin preparation the chromatographic analysis method of purine and pyrimidines of Wyatt (52) was employed. The myxomyosin in the pellet obtained from centrifugation was lyophilized to dryness and then hydrolyzed with 70% perchloric acid at 100° C for one hour. The hydrolysate was neutralized with KOH to pH 2 to 5 and allowed to stand at 0° C. The sample was centrifuged to remove the debris and the potassium perchlorate precipitate. The supernatant solution was then concentrated in an oven at 50° C. The chromatography was done on Whatman No. 1 paper with an isopropyl alcohol-HCl solvent described by Wyatt. The positions of spots on the chromatogram were detected by ultraviolet photography (52). A RNA sample was treated in the same way as the myxomyosin in the presence and absence of salt and were co-chromatogramed with the myxomyosin as reference standards for the identification of the nitrogen bases.

F. Ultraviolet Spectroscopy.

The UV spectrum of the myxomyosin was obtained with the Cary recording quartz spectrophotometer model 11M manufactured by Applied Physics Corporation.* The UV

---

* The author expresses his gratitude to Dr. Makio Murayama for his valuable assistance with the Cary spectrophotometer.

spectrum of the yellow pigment was obtained with the Beckman spectrophotometer Model DU.

Since maleate ion absorbs strongly in the 240 mμ wave length region, it is necessary to completely remove maleate from the buffered solution in which the myxomyosin is normally prepared. The protein sample is dialyzed exhaustively against a large volume of 0.01 M KCl for 24 hours or more and the concentration and the spectrum of the sample against 0.01 M KCl was obtained. The sample was then redialyzed against fresh solution of 0.01 M KCl for another 24 hours and the concentration and spectrum again obtained. It was found that the spectrum and the magnitude of the extinction of the sample was the same after the second dialysis as after the first. It is concluded that all the maleate ions were removed except those which are tightly bound to the protein. For this reason, the absorption spectrum of maleate of known concentration and against 0.01 M KCl was also obtained to serve as a check on possible errors in the spectrum caused by bound maleate ions. The yellow pigment isolated from the dialyzed protein is assumed to be free of maleate.

G. Electrophoresis.

Theory of migration of charged particle in the liquid medium.

The main feature of this theory has been developed and surveyed by Gorin and others (53,54). A brief discus-

sion of some points in the theory pertinent to the problem of this thesis is presented here.

The mobility of the particle is defined as

$$U = \frac{V}{X}$$

V = velocity

X = field strength = $\frac{\text{voltage}}{\text{length}}$

The mobility of an isolated charged particle in a dielectric fluid is given by

$$U = Q \frac{D^*}{kT}$$

D* = diffusion constant

Q = charge

k = Boltzmann constant

T = absolute temperature

where the (D^*/kT) term is inversely proportional to viscous drag as is the electric mobility U. The mobility of a charged particle of intermediate size in an electrolyte solution may be shown on the basis of the diffuse double layer theory of Guoy and Debye and Hückel to be

$$U = \frac{\zeta D}{4\pi\eta}$$

$$\zeta = \frac{Q}{Dr} \quad \frac{1/K}{1/K + r}$$

$$U = \frac{Q}{4\pi\eta r} \quad \frac{1}{1 + Kr}$$

Q = charge on the particle

η = viscosity of the medium

D = dielectric constant of the medium

$1/K = d$ = thickness of double layer

$K = f\,(T, D, \sqrt{\text{ionic length}}\,)$

ζ = zeta potential

In the derivations of the foregoing equations it has been assumed that

1. The ratio of the effect of electrical energy to the effect of thermal energy on the distribution of ions is much less than unity.
2. That the particle is of spherical shape, that there is no field distortion, and that the radius of curvature of the particle is much larger than the thickness of its double layer.

If one considers the modification introduced by Henry's correction for the effect of distortion of the electric field by non-conducting particles, and by Gorin's correction for the finite size of ions in the double layer, then

the electric mobility of a sphere is given by the following equation

$$U = \frac{Q}{6\pi\eta r} \frac{f(\kappa r)(1 + \kappa r_i)}{(1 + \kappa r + \kappa r_i)}$$

r_i = radius of the ions

r = radius of the particle

$f(\kappa r)$ = Henry's function of κr.

If the particle is a long cylinder with length, l, and radius, a, rather than a sphere, the following relations are obtained (53,54).

$$U = \frac{\zeta DC}{\eta}$$

$$\zeta = \frac{2Q}{D(1 + 2a)} f(\kappa a)$$

C = the distortion effect by the cylindrical non-conducting particle to the electrical field

Finally, the electric mobility of a long cylindrical molecule is given by the equation:

$$U = \frac{2Q}{(1 + 2a)} f(\kappa a, \kappa r_i) \frac{C}{\eta}$$

$f(\kappa a, \kappa r_i)$ = the terms of ionic interference and effect of the thickness of the double layer.

Therefore, for molecules of the same shape and for the same ionic strength of the medium, the mobility of a rod shaped particle is directly proportional to its charge and inversely proportional to its length l, and radius, a.

Measurement of electrophoretic mobility.

The theory of the moving boundary method for the determination of electrophoretic mobility has been described in detail (55, 56, 57) and will not be repeated here.

The portable Tiselius electrophoresis apparatus Model 38 manufactured by the Perkin-Elmer Corporation with its 2 ml cell assembly is employed. The schlieren photographs were obtained with Longsworth scanning optics. The protein solution samples were dialyzed usually for 10 to 12 hours with constant stirring at 2° to 4° C temperature. The conductivities of the buffer and of the protein solution were found to be the same after the dialyses. The conductance of the buffer was measured at 1.5° C for the calculation of mobility. Two buffering solutions, 0.2 μ (ionic strength) K-maleate, or (0.1μ KCl + 0.1 μ K-maleate) have been used. Both buffers were adjusted to pH 7 unless specified otherwise.

$$u = \frac{d \cdot A \cdot K}{t \cdot I} = cm^2 \text{ volt}^{-1} \text{ sec}^{-1}$$

Where d = distance moved by boundary in time, t.

A = cross sectional area of the cell.

κ = specific conductance of the buffer in mhos.

t = duration of run in seconds

I = current in amperes.

H. Flow Birefringence.

Flow birefringence measurement may be used to determine rotary diffusion coefficients. The theory behind this application has been readily reviewed (57, 58). Since in our system we will encounter complications resulting from polydispersity and inter particle interaction, a brief summary of the principles of flow birefringence is given below to provide a basis for the discussion of the results obtained.

It is possible to orient a large asymmetric molecule in solution by applying a mechanical shearing force. The orienting force is opposed by randomizing thermal forces. The intensity of rotary Brownian movement of a molecule can be defined by its rotary diffusion coefficient, Θ,

$$\Theta = \frac{kT}{\zeta}$$

where k is the Boltzman constant, T, the absolute temperature, and ζ , the rotational frictional constant, is the torque necessary to maintain a unit angular velocity. Θ may be evaluated from the results of streaming birefringence

measurements by the following equation

$$\theta = \frac{G}{\alpha}$$

where G is the velocity gradient in the solutions, a quantity determined by the known dimensions and rotational speed attained in the instrument, and α is a measure of relative strengths of orienting forces due to the velocity gradient and the disorienting forces of Brownian movement. The term α, is a function of the extinction angle χ which is determined instrumentally. Scherage, Edsall and Gadd (59) have computed the values of α for various values of χ based on the Peterlin and Stuart equation, thus from any measured value of χ and G, the value of α may be immediately obtained. For a rigid, non-interacting ellipsoid, Perrin's equation relates θ to the molecular dimensions,

$$\theta = \frac{3kT}{16\pi\eta} a3 \quad (2\ln \frac{2a}{b} - 1)$$

where a, is the length of the ellipsoid, a/b is the axial ratio, and η , the viscosity of the solvent. The length a, can therefore be calculated using the value of a/b which is supplied from viscosity data. This assumes, of course, the correctness of a non-interacting rigid prolate ellipsoid model. For large axial ratios, the rotary diffusion con-

stant depends substantially on a, and is insensitive to changes in b. There are, however, complications to this determination as for example, interaction, polydispersity and deformation phenomena.

There is no quantitative theory to account for the dependence and hence of apparent particle length on the concentration of the solution. In the cases of DNA (57), θ is inversely proportional to concentration, while in case of fibrinogen (57, 60), the length, l, is proportional to concentration. The usual practice is to perform the experiment at a concentration low enough that these phenomena disappear. The concentration dependence is qualitatively visualized as resulting from inter particle interference of the asymmetric molecule which increases their observed rotational frictional constant, ζ .

Polydispersity of the sample has a large effect on birefringence data. At low shear gradients, only the longer molecules which have the low rotary diffusion constant are oriented. As the shear gradient is gradually increased, the shorter molecules with a higher rotary diffusion constant begin to be oriented. Thus the contribution of short molecules to the measurement will increase as the shear gradient increases.

Sadron (61) first derived an equation for the calculation of the total contribution by various components in a non-interacting heterogeneous system. Sadron's equation

has the form

$$\tan 2\chi = \frac{\sum_i \Delta n_i \sin 2\chi_i}{\sum_i \Delta n_i \cos 2\chi_i}$$

where Δn is the birefringence and the subscript i denotes the value of Δn and χ for the ith component. For the case of stiff rods for which the intrinsic and form anistropy is constant and independent of molecular weight, Donet (62) gives a limiting formula for the diminishing gradient,

$$\frac{1}{\Theta} = \sum \frac{C_i}{\Theta_i^2} \Big/ \sum \frac{C_i}{\Theta_i}$$

C being the volume concentration and Θ the apparent rotary diffusion constant at zero gradient. If the molecule is sufficiently elongated, the Θ will be sensitive only to the length a, and the average length measured from birefringence at zero gradient as denoted by $a_{f.b(0)}$ will be given by

$$a_{f.b(0)} = \left(\langle a^6 \rangle / \langle a^3 \rangle \right)^{1/3}$$

where the brackets denote weight average over the distribution. As indicated by the above equation the average length so obtained is weighted strongly in favor of the longer particles. Goldstein and Reichman have given a detailed discussion of this problem in relation to DNA (63).

The deformation effects of shear are important for

molecules which are not rigid. The shear tends to lengthen the molecule thereby increasing the value of the rotary diffusion constant. A sufficiently high shearing force may even break the molecule into smaller pieces. An increase of χ and θ at the same gradient with time indicates the occurrence of such breakage.

The birefringence instrument employed in this study was built at the California Institute according to the design of Edsall, Rich, and Goldstein (64). The dimensions of the apparatus and the equation for the calculation of the shear gradient, θ, are

Inner stator radius	R_1	1.8 cm
Rotor cup radius	R_2	1.1 cm
Height of the solution in the cup		4.0 cm
Gap (R_2-R_1)	d	0.1 cm

$$G \simeq \frac{R_1\omega}{d} \simeq \frac{R_2\omega}{d} = \frac{2\pi N\bar{R}}{d}$$

where N is revolutions per second, ω angular velocity of the rotor, and $\bar{R}$ is $\frac{R_1 + R_2}{2}$.

I. Viscosity.

Newton first defined the coefficient of viscosity η with the following equation

$$\tau = \eta \frac{dv}{dl} \quad A$$

where τ is the shearing force between two parallel planes in a liquid in relative motion, $\frac{dv}{dl}$, the velocity gradient perpendicular to the planes, and A is the area of the planes. The quantity, η, is expressed in units of poise and has the dimensions gm cm^{-1} sec^{-1}. The work spent in overcoming frictional resistance is transformed into heat. The heat, q, liberated per unit time in a unit volume at constant velocity is

$$q = \eta \left(\frac{dv}{dl}\right)^2$$

The introduction of large particles into a flowing liquid distorts the stream line so that an additional amount of work is required to maintain the gradient. This increase in viscosity has been related to the size and shape of the particles. The relationship, has however been derived for isolated particles randomly oriented in the fluid. When these conditions apply, it is possible to calculate the effective volume and the shape of the particle from viscosity data.

In the simplest case, for a very dilute solution of incompressible spheres in a fluid, the relation is, according to Einstein,

$$\lim_{\phi \to 0} \frac{(\eta/\eta_o - 1)}{\phi} = \frac{(\eta_{rel} - 1)}{\phi} = \frac{(\eta_{sp})}{\phi} = 2.5$$

where

η_o = solvent viscosity

η = solution viscosity

η_{rel} = relative viscosity

η_{sp} = specific viscosity

ϕ = volume fraction of the solute in the solution.

It should be noted that it is the volume fraction, not the size, of the solute particles which is related to viscosity. For molecules, other than ideal spheres, the viscosity of the solution is increased by at least two further factors; the resistance generated by the asymmetry in shape and by the volume increase caused by the hydration of solute. Simha has shown for rigid ellipsoids in the condition of overwhelming disorientation by Brownian moment, that the relationship between viscosity and the axial ratio, $P(= \frac{a}{b})$, is

$$\lim_{\phi \to 0} \frac{\eta_{sp}}{\phi} = \nu = \left[\frac{P^2}{15(\ln P - \frac{3}{2})} + \frac{P^2}{5(\ln 2p - \frac{1}{2})} + \frac{14}{15} \right]$$

The relations between ν and p for oblate and prolate ellipsoids have been tabulated (65). The volume fraction, ϕ, can be obtained from weight concentration, c, and the particle density, ρ , through the relationship $\phi = \frac{c}{\rho}$.

This presupposes, however, that the particle is neither internally or externally hydrated. It should be noted that Simha's equation can be applied only in the case of random orientation or $\alpha = \frac{G}{\theta} \ll 1$. The increase of viscosity of a solution over that of solutions of the ideal spheres of the same volume fraction can be assigned to the increase of volume of the solute in solution due to hydration. In this case, the volume ϕ becomes

$$\phi = \frac{c}{\rho}\left(1 + \frac{w\rho}{\rho_s}\right)$$

where w is the hydration in grams of solvent per gram of protein and ρ_s is the solvent density, which is here assumed to be the density of hydrating fluid. It is important to note that on the basis of viscosity studies alone, the contribution of viscosity due to the shape factor or the hydration factor cannot be separated. From the measurement of axial ratio, p, the frictional ratio, f/fo, of a prolate ellipsoid can be calculated by means of Perrin's equation

$$\frac{f}{fo} = \frac{(1 - p^2)^{\frac{1}{2}}}{p^{2/3} \ln \frac{(1+(1-p^2)^{\frac{1}{2}}}{p}}$$

The intrinsic viscosity of two non-interacting components (A and B) in a mixture can be calculated additively, if their weight fraction is known

$$C_T = C_A + C_B$$

where

C_T = total weight fraction

C_A = known weight fraction

C_B = known weight fraction

The reduced viscosity of the total mixture, $\frac{\eta_{sp}}{C_T}^T$ is then equal to the sum of the reduced viscosities of A and B. Thus

$$\frac{\eta_{sp}{}^T}{C_T} = \frac{\eta_{sp}{}^A}{C_A} \cdot \frac{C_A}{C_T} + \frac{\eta_{sp}{}^B}{C_B} \cdot \frac{C_B}{C_T}$$

If $\frac{\eta_{sp}{}^T}{C_T}$ is known and if $\frac{\eta_{sp}{}^B}{C_B}$ can be determined, these quantities together with the weight fractions of component A and B, permit calculation of the reduced viscosity of A, $\frac{\eta_{sp}{}^A}{C_A}$ by the above relationship.

When the viscosity of a solution is measured at finite concentrations, the interaction of the particles tends to increase the energy required to maintain the shear gradient and thus ordinarily increases the reduced viscosity. It is necessary here to distinguish between two modes of solutes interaction each of which increases the reduced viscosity. The first results from the crowding of solute particles in the volume of solvent necessary for the development of the

normal streamline pattern around each molecule. This effect may be observed at relatively low concentration for elongated solute particles and at higher concentration for symmetrical solute particles. The second kind of interaction involves actual aggregation of solute particles, so that the average particle is now larger. If this increase in size is accompanied by an increase in asymmetry or hydration a net increase in reduced viscosity will result. If, on the other hand, a decrease in asymmetry attends aggregation, a reduction in reduced viscosity will result. All systems which exhibit a concentration dependent aggregation of solute particles will then exhibit a concentration dependence of the reduced viscosity. The reduced viscosity at zero concentration may be obtained by extrapolation. Systems of the same reduced viscosity at infinite dilution may exhibit quite different slopes of their reduced viscosity vs. concentration curves due to differing degrees of aggregation. This situation will be encountered in Chapter VII below.

In the case of solutions which contain large and asymmetric molecules, orientation effects at high shear gradients reduce the viscosity of the solution; it is therefore desirable to extrapolate the data to zero shear gradient. With solute which aggregate by formation of bonds which are weak relative to the total mass involved in the aggregation reaction, high shear gradients may disrupt the aggregates

partially or completely thus tending to reduce viscosity. This phenomenon is referred to as the destruction of "structural viscosity."

The viscometers employed in the present work were of the Ostwald type and were built in this laboratory. The viscometers used in the early experiments on the crude extracts had the volumes of about 3.5 ml, flow time for water of 60-70 seconds and maximum shear gradients for water of approximately 1500 second^{-1}. The solutions examined were 2 to 3 times more viscous than water. Several viscometers were used in the studies of the molecular dimension of myxomyosin. They all possessed a bulb volume of ca. 1.3 cc, and maximum shear gradients for water of 90 sec^{-1} to 700 sec^{-1}. The kinetic energy corrections for these viscometers is small. The same relative viscosity was obtained with all viscometers including that of the lowest shear gradient (90 sec^{-1}). This viscometer was 118 cm in length, 0.5 mm radius, 5 cm high and a flow rate of only 1.4×10^{-2} cc per second. All viscosity measurements were made at a temperature $24.42 \pm 0.05^{\circ}$ C.

The calculation of the maximum shear gradient in a viscometer for a given liquid is made with the following equation

$$V = \frac{P}{4\eta l} (r^2 - a^2)$$

where V is the distribution of velocity in the liquid across the cylindrical tube of radius, r, length, l, pressure differential, P, and a is the distance from tube axis at any point. Differentiation of the above equation with respect to a gives

$$\frac{dV}{da} = -\frac{Pa}{2\eta l}$$

and the maximum shear gradient at the wall where r = a,

$$\frac{dV}{dr} = -\frac{Pr}{2\eta l}$$

From Poiseuille's law, the relation

$$V = \frac{\pi Pr^4}{8\eta l}$$

is obtained where V is the volume of liquid flowing through the tube in unit time. By substituting V into the shear gradient equation, the relationship

$$\frac{dv}{dr} = -\frac{4}{\pi}\frac{V}{r3}$$

is established.

Sample calculation,

Radius of the capillary $r = 0.051$ cm

$r^3 = 1.326 \times 10^{-4}$ cm^3

bulb volume, B = 1.22 cm^3

flow time, t, = 68.2 sec

$$V = \frac{B}{t} = \frac{1.22\ cc}{6.82\ sec} = 1.788 \times 10^{-2}\ cc/sec$$

then, the shear gradient

$$\frac{dv}{dr} = \frac{4}{\pi} \frac{1.788 \times 10^{-2}\ cc/sec}{1.32 \times 10^{-4}\ cc} = 171.7\ sec^{-1}$$

J. Ultracentrifugation and Related Measurements.

Preparative Ultracentrifugation:

The fractionation of proteins by differential centrifugation is performed in the preparative ultracentrifuge Model L, manufactured by the Specialized Instruments Corporation. The chamber and the #40 head are always refrigerated before and during the run. The theory of angle rotor centrifugation is presented by Pickels (66) and is unlike the non-convective, radial centrifugation of the analytical instrument. The operation procedure employed in this work is essentially empirical. In general the rapidly sedimenting component is the object of the isolation procedures, and is recovered in the form of a gelatinous pellet at the bottom of the centrifuge tube.

Analytical Utracentrifugation:

Sedimentation constant measurement.

The ultracentrifugal analysis of the protein samples in the isolation procedure studies (Chapter IV) were performed with the ultracentrifuge designed and built at this

Institute. A detailed description of the machine has been given in the Ph.D. thesis of Eggman (1953). The sedimentation studies on the myxomyosin (Chapter VII), were performed with the Ultracentrifuge Model E manufactured by Specialized Instruments Corporation.

In order to observe the area and the mobility of the slow moving boundary, the synthetic boundary cell has been used. This cell has been described by Schachman and Harrington (67) and also by the technical manual of the manufacturing company. Because of the nature of the cell and from other considerations, the samples were first dialyzed against the maleate buffer which is also used in the electrophoresis studies. The centrifuge runs were performed at temperatures between 20° and 25° C.

The sedimentation constant, S, is defined as (68)

$$S = \frac{dx/dt}{\omega^2 x}$$

where dx is the distance cm in the cell which the boundaries move in time (seconds) dt, ω is the angular velocity (radians/second) and x is the distance from the axis of rotation of the centrifuge head. The sedimentation constant, S, is expressed in units of 10^{-13} cm/sec/unit gravitational field or Svedbergs).

The sedimentation constant obtained at 20° C in the water medium was arbitrarily chosen as the standard value

by Svedberg and Pedersen (68). For the correction of experimental values of S obtained at any temperature and in any solvent to the standard value, the following corrections are used.

$$S_{w,20} = S_{B,t} \times \frac{\eta_{B,t}}{\eta_{w,t}} \times \frac{\eta_{w,t}}{\eta_{w,20}} \times \frac{1-\bar{V}\rho_{w,20}}{1-\bar{V}\rho_{B,t}}$$

The term $\eta_{B,t}/\eta_{w,t}$ corrects the viscosity of the experimental solvent at temperature to that of water at the same temperature. For ordinary buffers this usually is 1 to 2%. The second term, $\eta_{w,t}/\eta_{w,20}$ compensates the viscosity of water at the experimental temperature to that of water at 20° C, and is usually 2% per degree of difference from 20° C. The last term

$$\frac{1-\bar{V}\rho_{w,20}}{1-\bar{V}\rho_{B,t}}$$

corrects for the discrepancy in the buoyant forces due to the difference in density of the solvent at temperature t°, $\rho_{B,t}$, as compared to the density of water at 20°, $\rho_{w,t}$ $\bar{V}$ is the partial specific volume of the sedimenting component.

The integration of the above differential equation, yields that for the calculation of S,

$$S = \frac{1}{\omega^2}\int_{t_1}^{t_2}\int_{x_1}^{x_2} \frac{dx}{x}\,\frac{1}{dt} = \frac{\ln \frac{x_2}{x_1}}{\omega^2(t_2-t_1)}$$

Molecular weight calculation.

Since the rate of sedimentation of a molecule is related to its mass and to its partial specific volume, it can be shown that

$$M = \left(\frac{f}{f_o}\right) \frac{f_o \; S_{20,w}}{1 - \bar{V}\rho}$$

where M is the molecular weight, f, the molar frictional coefficient, (f/f_o) the frictional ratio, $\bar{V}$, the partial special volume of the anhydrous protein, and, ρ , the density of the solvent. From the Stoke's law calculation of f_o, the calculation of M can take the following form,

$$M = \left[\frac{6 \pi \eta N \left(\frac{3\bar{V}}{4\pi N}\right)^{1/3} S_{20,w} \left(\frac{f}{f_o}\right)}{1 - \bar{V}\rho} \right]^{3/2}$$

Partial Specific Volume Measurement.

Partial specific volume was measured by the method of difference in density of the solution and the solvent (69). The densities were measured with a pycnometer weighed to one part in ten thousand. It is assumed that the partial specific volume is independent of the concentration and is equal to apparent specific volume.

Anomalies in the sedimentation studies.

In sedimentation studies of asymmetric molecules, it is usual to observe that the apparent sedimentation constant depends on solute concentration and that the boundaries are sharp. Both these effects are attributed to the increase in friction encountered in the translational motion of an elongated molecule as a result of crowding. The apparent frictional coefficient at concentration c, can be expressed as a function of the frictional coefficient at infinite dilution multiplied by a power series in concentration, as

$$f_c = f_{c \rightarrow o} \left(1 + k_1 c + k_2 c^2 + \ldots . \right)$$

where $k_1, k_2, \ldots .$ etc. are the constants related to the concentration effect. Since the sedimentation constant is inversely proportional to the frictional coefficient, the relationship

$$\frac{1}{S_c} = \frac{1}{S_{c \rightarrow o}} \left(1 + K_1 c\right)$$

will apply, where S_c is the sedimentation constant at the measured concentration, $S_{c \rightarrow o}$, the sedimentation constant at infinite dilution, and K_1 is a proportionality constant involving the size, and shape of the molecule, and the viscosity of the solvent. It is evident that sedimenting molecules immediately behind the moving boundary will move

more rapidly than molecules just in front of the boundary. This results in a boundary sharpening effect as compared to boundaries formed by symmetrical particles.

For the concentration area analysis of a mixture which consists of a slow and a fast moving component, the complication of the Johnston and Ogston effect (70) enters in. This effect is based on the fact that the slow component sediments more rapidly in the region behind the boundary of the fast component. The concentration of the slow component tends therefore to be higher behind the fast-moving boundary and to be lower in front of the fast-moving boundary. The result is that in such a mixture, the optical measurement gives too high a value for the apparent concentration of the slow component and too low a value for the fast component. Since these phenomena are related to the retardation of the sedimentation constant of the slow component, Johnston and Ogston proposed the use of following relation

$$C_s^{obs.} = C_s^{o} \left(\frac{S_F - S_{s,mix}}{S_F - S_s} \right)$$

where C_s^{o} is the true concentration of the slow component, S_s is the sedimentation constant of the slow component when sedimenting alone, and S_F and $S_{s,mix}$ are the sedimentation constants of the fast and the slow component in the mixture (71). Trautman *et al.* with the aid of radial-dilution law and with the assumption that the effect of protein concentration on the sedimentation rates of both components

sedimenting in the presence of each other is the same, have obtained the relation

$$C_s^{obs.} \left(\frac{\bar{x}_s^{obs.}}{x_o} \right)^2 = C_s^{o} \cdot \gamma$$

$$\gamma = \frac{1 - \sigma}{1 - \dfrac{\ln \dfrac{\bar{x}_s^{obs.}}{x_o}}{\ln \dfrac{\bar{x}_F^{obs.}}{x_o}}} > 1 \quad \text{(if Johnston-Ogston effect is present)}$$

where

γ = Johnston-Ogston effect correction factor.

C_s^{o} = concentration of the slow component at zero time.

$C_s^{obs.}$ = " " " " " reported optically.

x_o = meniscus position from the axis.

$\bar{x}_s^{obs.}$ = position of the boundary of the slow component.

$\bar{x}_F^{obs.}$ = " " " " " " fast " .

$\sigma = \dfrac{S_s^{o}}{S_F^{o}}$ if the effect of concentration on both sedimentation constants is the same.

The effect of Johnston and Ogston can be estimated through these equations.

K. Electron Microscopy.

The electron microscope available for this work is the model EMU-2A, Radio Corporation of America, equipped with electromagnetically focussed lens. The magnification (10,000 x on tap 5) is calibrated with carbon replicas of a grid containing 30,000 lines per inch supplied by Ernest F. Fullam, Inc.* The details of the principle of electron microscopy are given by Wyckoff (72) and Hall (73).

Electron microscopy on myxomyosin was done as follows: The sample of proteins in 0.2 μ maleate buffer was first diluted to 0.2 mg/ml with 0.01 M KCl 3 to 5 minutes before use. This solution mixed with standard polystrene latex was sprayed with a nebulizer to a metal screen coated with collodion. The sample dries in air rapidly. The screens were shadowed with chromium or thorium as specified below with a shadowing angle of 5:1. The spherical polystrene particles (2600 Å in diameter) serve as a check of the magnification power as well as of the shadowing angle.

The measurement of the dimensions of the protein molecules were done on enlarged prints (5 or 10 x) of only those original negative (10,000 x) which were in critical focus.

L. Fiber Formation.

The fact that myxomyosin is a very long molecule in-

---

* The instrument was calibrated by Mr. E. Henderson of the chemistry department.

soluble in concentrated ammonium sulphate solutions suggests the possibility of forming myxomyosin fibers. The best possible way for forming an oriented fiber has not yet been determined because of the limited supplies of the pure material but the method described in the following paragraph yields a stable, rather stiff fiber which has been investigated in a preliminary way.

The myxomyosin is concentrated to 40-50% in a pellet form by centrifugation. The pellet is then put into a 1 cc syringe equipped with 19 gauge needle (approximately 0.7 mm in diameter) of 1.5 cm long. Saturated ammonium sulphate solution at neutral pH at room temperature is used as the precipitating solvent. Because of the high density of the ammonium sulphate solution, the protein solution is ejected upward from the bottom of the ammonium sulphate solution. The protein solution is slowly forced out from the needle and is immediately precipitated as a fiber which is held vertically by its buoyancy. This fiber can be stored in saturated ammonium sulphate solution in the refrigerator for several weeks.

M. Microinjection.

The P. de Forbrune micromanipulator manufactured by G. H. Beauadouin Company, Paris, was employed. Operations were carried out under a microscope with a mechanical state and at 100 to 200 x magnification. A 3-5 micron needle was

used for injection of solutions into the plasmodia. Observations with inert solutions, such as dilute phosphate solution, showed that the injection procedure caused no injury to the organism that could be observed after a one hour period.

III. THE EFFECT OF ATP AND RELATED COMPOUNDS ON PLASMODIAL STREAMING AND ON PLASMODIAL EXTRACTS

A. The effect of ATP on Plasmodial Streaming.

Microinjection of low concentrations of neutral ATP solutions into plasmodia under proper conditions partially liquifies the plasmagel and appears to increase the rate of protoplasmic streaming. A few seconds to a few minutes after microinjection, protuberances appear randomly on the periphery of the plasmodium and enlarge to clear hemispherical forms. Similar results are obtained if the ATP is introduced into the strand by diffusion from the medium. The time course of protuberance formation and morphology varies with the ATP concentration. The protuberances in low ATP concentrations are similar to an advancing pseudopodial tip. At higher concentrations of ATP, much of the plasmagel is liquefied, organized streaming stops, formation of protuberances is very rapid and high pressure appears to develop in them. One or more of the balloon-like protuberances soon rupture, leaving a definite membrane-like shell. The cytoplasm leaks out. Concurrently, expansion of other protuberances on the same strand stops. The protuberances may even shrink somewhat in size as if the pressure driving their growth had been relased. These effects of ATP on myxomycete plasmodia are similar in many respects to those on amoeba recently reported by Goldacre and Lorch (20).

The phenomena outlined above are largely specific for ATP although sodium triphosphate also causes the formation of protuberances on the strands as discussed below. Orthophosphate, ADP, and AMP are all without effect. Immersion of plasmodia into dilute solutions of detergents, organic solvents, acids and alkalies, kill the protoplasmic strand but without formation of protuberances or the accompanying intrastrand changes described for ATP.

Dinitrophenol (DNP) in the concentration of 1×10^{-3} M stops protoplasmic streaming of the immersed plasmodial strands within five minutes. DNP in a concentration of 2×10^{-4} M gradually slows the streaming which stops completely in 30 to 40 minutes. Those strands in which the streaming has stopped remain intact but appear to be dead. The streaming does not commence again when the strands are returned to water.

The above observations show that ATP has a unique and striking effect in liquefying the gel structure of the plasmodium, and thereby, in influencing protoplasmic streaming. It is known that the whole plasmodial strand is ordinarily under pressure and if one end of it is cut abruptly, the plasmosol rushes out through the strand as if driven by a pressure difference (36). These considerations suggest that excess amounts of ATP present at a particular region will tend to liquefy the gel at that region. The resistance to internal pressure as well as the viscosity of

the fluid in that area will be reduced. Plasmasol would then tend to flow to the area and a protuberance would be formed. Finally, in the continuous presence of an excess of ATP, the gel structure of plasmodium eventually dissolves to the extent that it can no longer retain the plasmosol.

No detailed studies have been made to compare the effect of ATP with that of sodium triphosphate. Qualitatively, in the presence of triphosphate, protuberances also occur except that they are smaller and form slower than in case of ATP at the same concentration.

DNP is known to act in uncoupling phosphorylation, though the mechanism of this action is not well understood. No simple conclusion can be drawn from the above experiment, however, since the plasmodium appears to be killed by the DNP. Whether the effect of DNP on plasmodia is solely on the inhibition of phosphorylation process or whether other processes are affected has not been determined.

Conclusion: ATP has a liquefying effect on the gel structure of the plasmodium. This is attended by a flow of protoplasm into the liquefied portion.

B. The Effect of ATP and Related Compounds on Plasmodial Extracts in Phosphate-KCl Buffer.

Further experiments were carried on with the extracts of plasmodia in which the system is capable of analysis by chemical and physical methods. It was soon found out that the nature of the extraction medium has a profound influence on the characteristics of the plasmodial solution.

Addition of 0.2 to 2.0 μM of ATP per ml to an extract prepared with 1.4 M KCl 0.1 M phosphate buffer (pH 7.8 to 8.0) or with 1.2 M KCl 0.1 M phosphate buffer (same pH), causes a small rise in viscosity (Fig. 1, curve A). This result is in marked contrast to that of Loewy (46) who found that similar amounts of ATP, 0.4 μM, produced sharp decreases in the viscosity of extracts prepared in the same medium. Since extracts prepared at higher concentration of KCl, 1.4 M, were more active than the others described below, extraction with 1.4 M KCl-phosphate buffer mixtures was routinely employed unless otherwise indicated.

AMP in concentrations of 0.04 to 2.0 μM per ml of extract causes an immediate rise in viscosity (Fig. 1, curves B and C). Subsequent addition of ATP to this AMP-treated system, however, evokes a sharp decrease in viscosity followed by a gradual recovery (Fig. 1, curve C). It would appear that certain physical properties of the extracts are changed by AMP, and that, therefore, the mode of action of ATP on the treated extracts is also changed. Thus,

Fig. 1. Effect of ATP and AMP and of Ca and Mg ions upon the viscosity of 1.4 M KCl-0.1 M phosphate (pH 7.9) extract. Reagents added at times indicated by arrows. Concentrations are in µM per ml of extract.

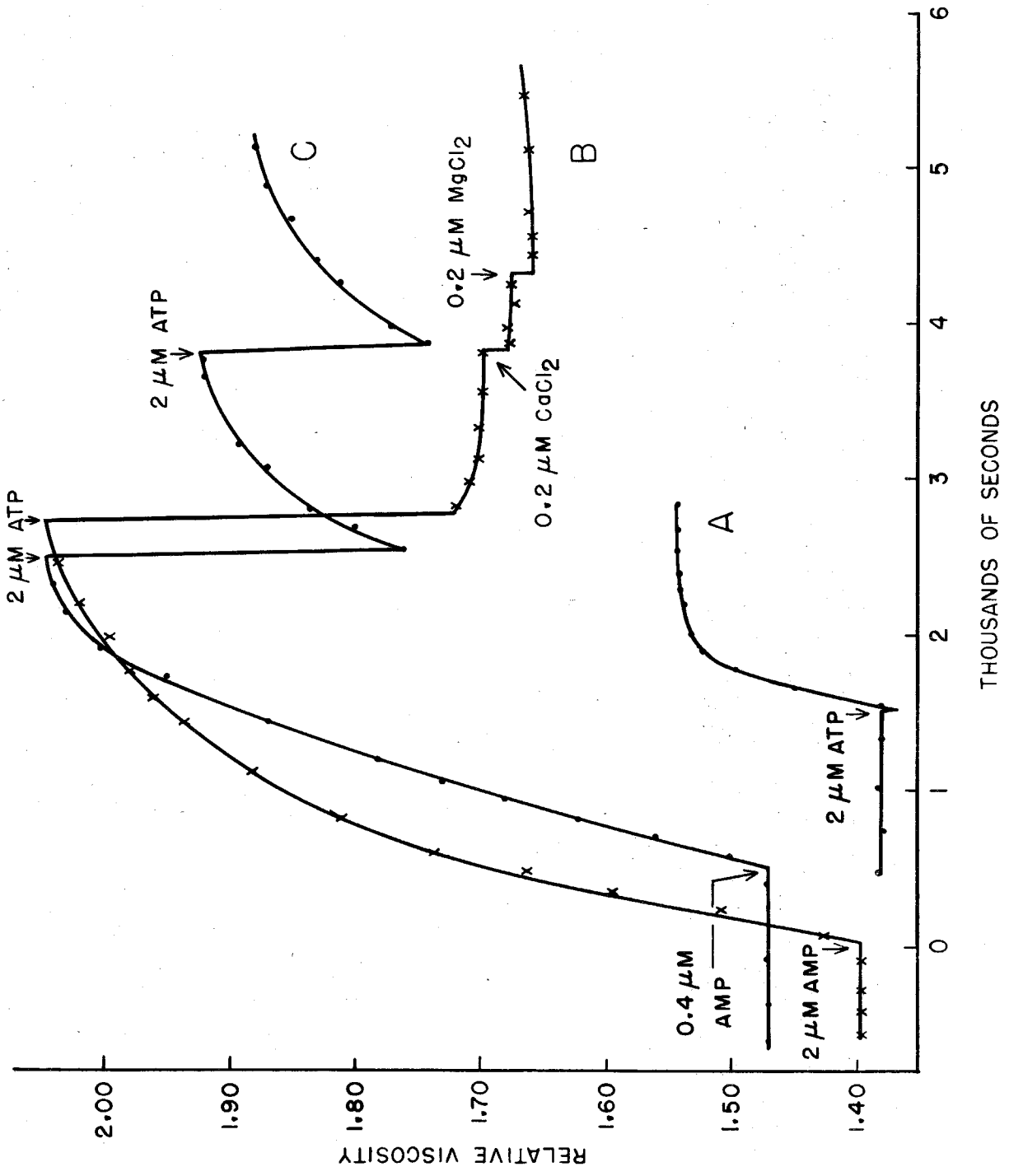
2 μM ATP
2 μM ATP
0.2 μM MgCl2
0.2 μM CaCl2
2 μM ATP
0.4 μM AMP
2 μM AMP
A
B
C
RELATIVE VISCOSITY
2.00
1.90
1.80
1.70
1.60
1.50
1.40
0
1
2
3
4
5
6
THOUSANDS OF SECONDS

before ATP can be effective in decreasing the viscosity of these extracts, the system must first be brought to a high viscosity level with AMP. Evidently, then the viscosity level of the extract is determined by the interaction of protein, AMP, and ATP, and is a function of their respective concentrations.

The minimum concentration of AMP which evokes a rapid and sizable rise in the viscosity of these crude extracts is 0.04 μM per ml while 10 times this amount elicits a near maximal response (Fig. 1, curve C). Still higher concentrations of AMP do not produce greater response but are definitely inhibitory to the recovery phase of ATP action (Fig. 1, curves B and C). A minimum of about 0.4 μM of ATP per ml is required to cause a decrease in viscosity of extracts previously treated with an optimal amount of AMP. Higher concentrations of ATP cause somewhat greater decreases in viscosity but lengthen the recovery period and reduce the extent of recovery. An ATP concentration of 2.0 μM per ml is sufficient to evoke a near maximal response but in many instances the system shows little tendency to return to a high viscosity state, especially in the presence of more than minimal amounts of AMP. Addition of more AMP to a system brought to a low viscosity level with excessive amounts of ATP does not again increase the viscosity, as it does in the original extract.

For AMP to be effective in raising the viscosity, it

must be added prior to addition of ATP. Even when AMP and ATP are added simultaneously, the AMP is ineffective in increasing the viscosity. For example, when 0.04 μM of AMP and 0.4 μM of ATP per ml are added simultaneously to the crude extract, a small increase in viscosity occurred, similar to that caused by addition of the same concentration of ATP alone to a crude extract in the absence of AMP (Compare Fig. 2, curve A with Fig. 1, curve A). Further addition of excess of AMP gives no great effect. However, when AMP was added separately to the same preparation (Fig. 2, Curve B), a great increase in viscosity is observed.

Magnesium and calcium ions (as the chloride salts) in concentrations up to 2 μM per ml either individually or jointly have no effect on the viscosity of the crude extract itself, nor do they have any qualitative effect upon AMP or ATP response of the system.

The magnitude of increase in viscosity caused by optimal amount of AMP and the subsequent magnitude of drop in viscosity caused by an optimal amount of ATP serves as a preliminary measure of the activity of the system.

Applying this criterion, it was found that the protein system extracted by 1.4 M KCl solution with the same amount of phosphate buffer (0.1 M) at the same pH (pH 7.9), is more active than the system extracted by 1.2 M or 0.6 M KCl (Fig. 3).

Fig. 2. Effect of AMP and of an AMP-ATP mixture upon the viscosity of a 1.4 M KCl - 0.1 M phosphate (pH 7.9) extract. AMP alone was added initially to solution of Curve B while AMP-ATP mixture was added to the solution of Curve A.

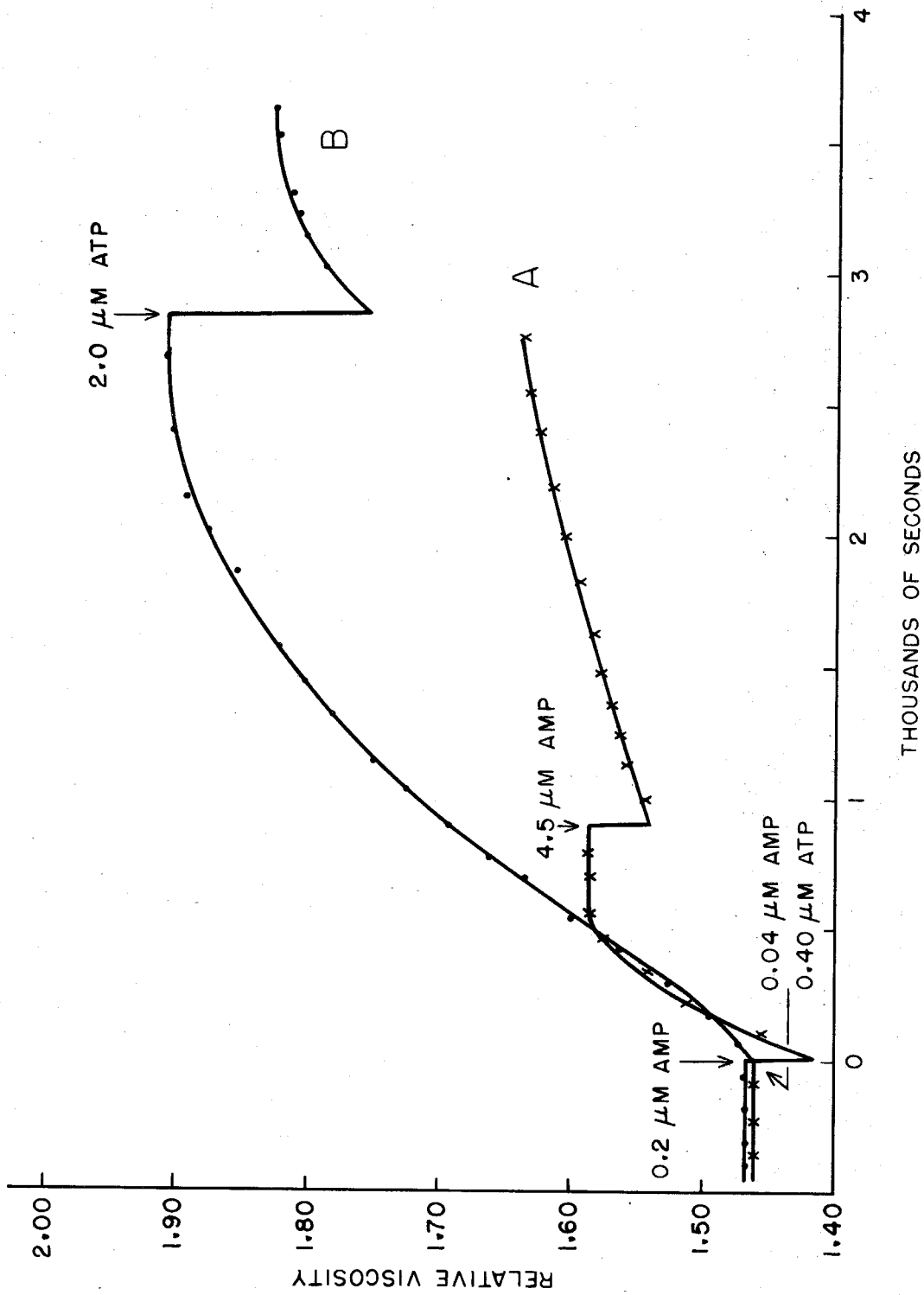
2.00
1.90
1.80
1.70
1.60
1.50
1.40
RELATIVE VISCOSITY
0
1
2
3
4
THOUSANDS OF SECONDS
0.2 μM AMP
0.04 μM AMP
0.40 μM ATP
4.5 μM AMP
2.0 μM ATP
A
B

Fig. 3. Effect of maximal amounts of ATP upon the viscosity of solutions prepared by extraction with buffered (pH 7.9) KCl solutions at several KCl concentrations.

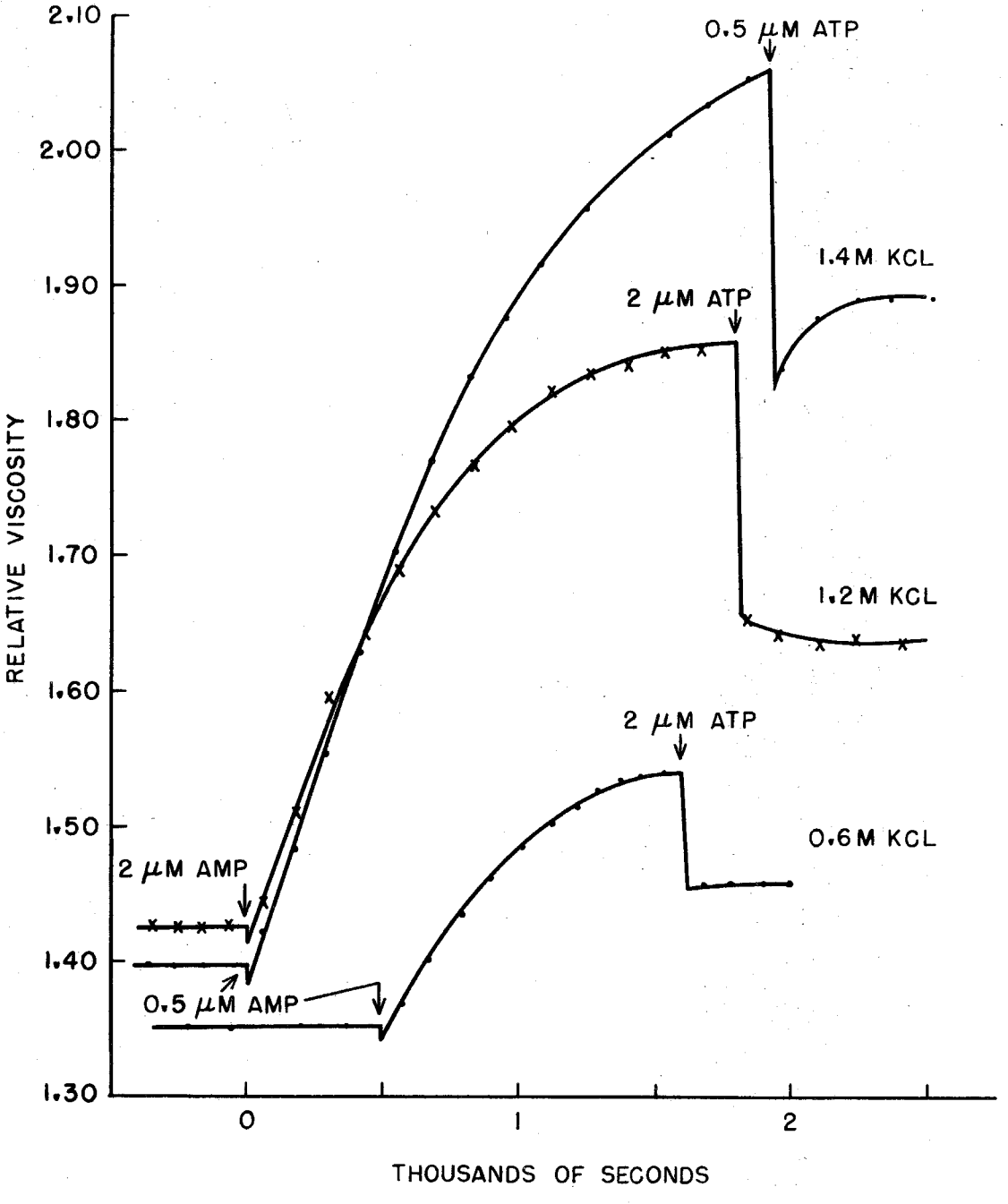
2.10
2.00
1.90
1.80
1.70
1.60
1.50
1.40
1.30
RELATIVE VISCOSITY
0
1
2
THOUSANDS OF SECONDS
0.5 μM ATP
1.4M KCL
2 μM ATP
1.2M KCL
2 μM ATP
0.6M KCL
2 μM AMP
0.5 μM AMP

When the plasmodia were extracted with and investigated in media containing 1.4 M KCl and 0.1 M phosphate buffer but at pH 8, pH 7.4 and pH 6.7, it was found that the protein system extracted as well as examined at pH 8 was more active than those obtained at pH 7.4 and pH 6.7.

Substitution of 0.1 M THAM buffer (Trihydroxylmethyl-amino methane) at pH 8.4 or 0.1 M potassium maleate buffer at pH 7.0 for the phosphate buffer in the extraction solution results in extracts which are completely inactive.

Conclusion: The plasmodial extract made in 1.4 M KCl - 0.1 M phosphate solution at pH 8 can be activated by AMP to give a solution of high viscosity. Subsequent introduction of ATP evokes a sharp decrease in viscosity followed by partial and gradual recovery of the viscosity level. The system therefore requires activation and is only partially reversible.

C. The Effect of ATP and Related Compounds on Plasmodial Extracts in Unbuffered KCl Solutions.

The plasmodial solution extracted by unbuffered 1.4 M KCl was found to possess a pH of 7. The properties of this neutral extract differ markedly from those of the extract obtained with KCl alkaline phosphate buffer.

ATP, AMP and phosphate ions all cause an increase in the viscosity of KCl extracts. The threshold concentration and the maximum effective concentration are different for each compound, AMP being the most effective on a molar basis.

The threshold requirement for AMP is 0.02 to 0.04 μM/ml. AMP in a concentration of 0.15 μM/ml evokes a fairly large increase in viscosity (Fig. 6, curve A). An initial addition of ATP to the original extract causes an increase in viscosity of the 1.4 M KCl extracts (Fig. 5, curve A), just as with extracts made in phosphate-buffered KCl (Fig. 1, curve A). Subsequent additions of ATP, however, evoke a reversible decrease in the viscosity (Fig. 5, curve A).

Addition of phosphate ions to the unbuffered KCl extract brings about an increase in viscosity which is more rapid and larger than that caused by any other reagent tested, although the concentration required is also higher. The nature of the response to phosphate ion is illustrated in Fig. 4, 5, and 6. Fig. 4 shows the effect of addition of pH 7.0 phosphate buffer to the extract to a final concentration of 0.05 M or 0.1 M. 0.1 M phosphate initiates a greater increase in viscosity than does 0.05 M phosphate. Addition of more phosphate to the 0.05 M solution to make the final concentration 0.1 M elicits some further increase in viscosity, but the addition of phosphate in two increments is not nearly as effective as a single addition of phosphate to the same final concentration.

When pH 9.2 phosphate buffer is added to a final pH of 8.0 and 0.1 M concentration of phosphate, there is no change in viscosity other than the small decrease due to

Fig. 4. Phosphate ion effect upon the viscosity of unbuffered 1.4 M KCl extracts. Protein concentration: *ca*. 10 mg/ml.

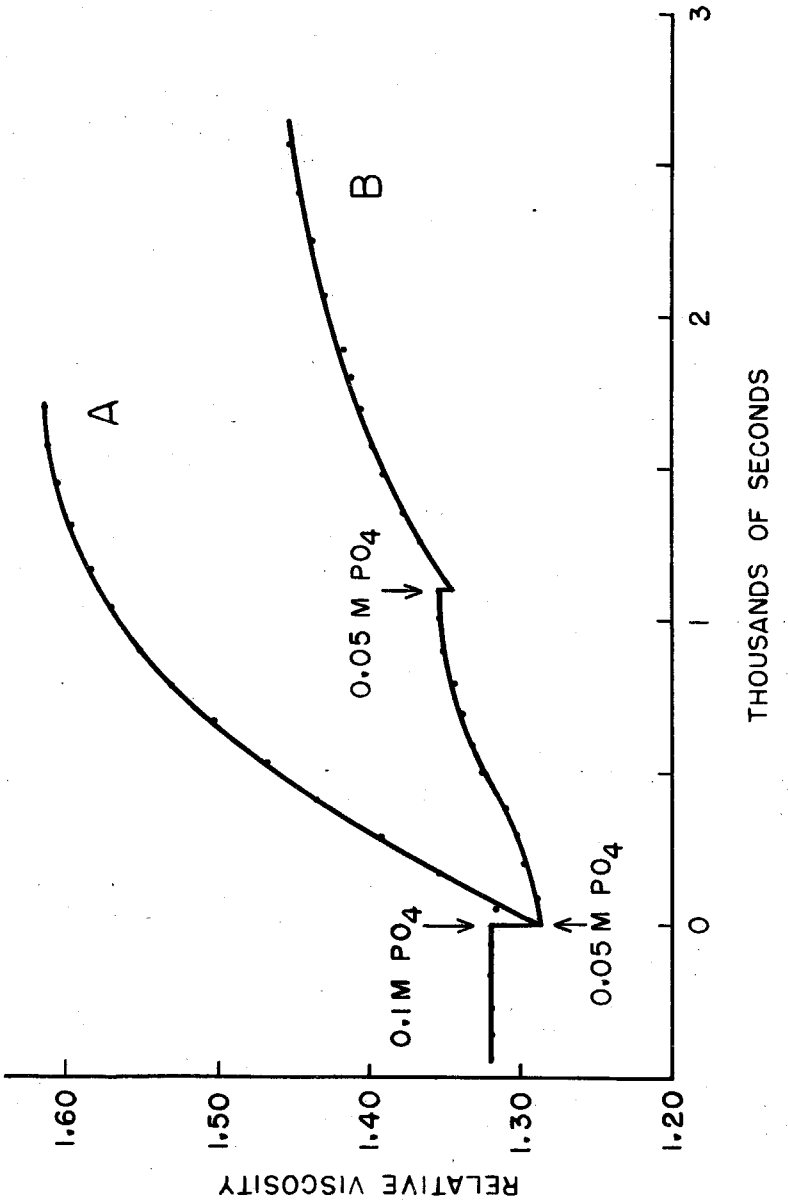
RELATIVE VISCOSITY
1.60
1.50
1.40
1.30
1.20
0
1
2
3
THOUSANDS OF SECONDS
A
B
0.1 M PO4
0.05 M PO4
0.05 M PO4

Fig. 5. Effect of phosphate ion and ATP upon the viscosity of an unbuffered 1.4 M KCl extract. Protein concentration: 14.5 mg/ml.

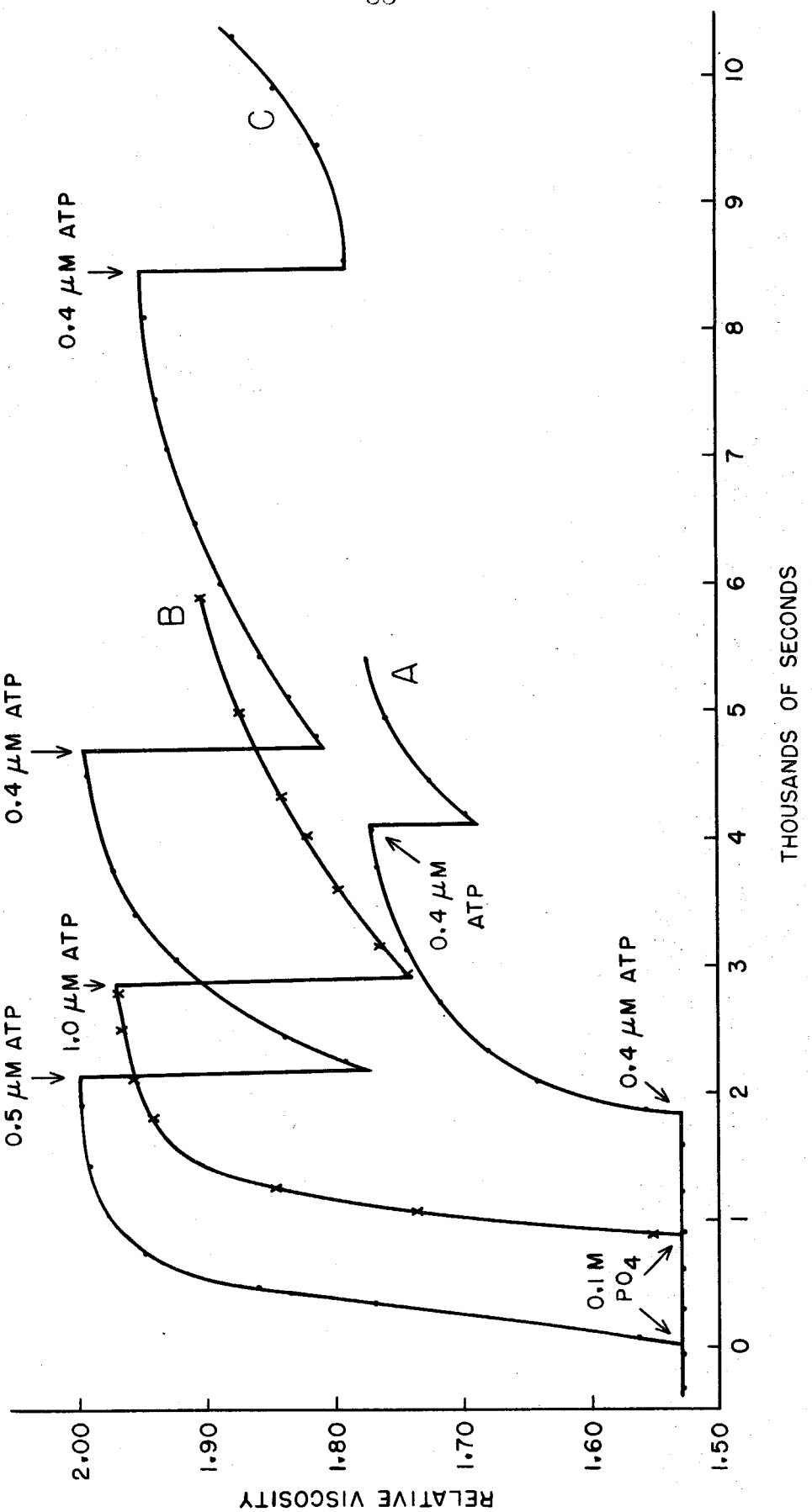
RELATIVE VISCOSITY
2.00
1.90
1.80
1.70
1.60
1.50
0
1
2
3
4
5
6
7
8
9
10
THOUSANDS OF SECONDS
0.1 M PO4
0.5 μM ATP
1.0 μM ATP
0.4 μM ATP
0.4 μM ATP
0.4 μM ATP
0.4 μM ATP
A
B
C

Fig. 6. Effect of phosphate ion, ATP and AMP upon the viscosity of unbuffered 1.4 M KCl extracts. Protein concentration: 14.0 mg/ml.

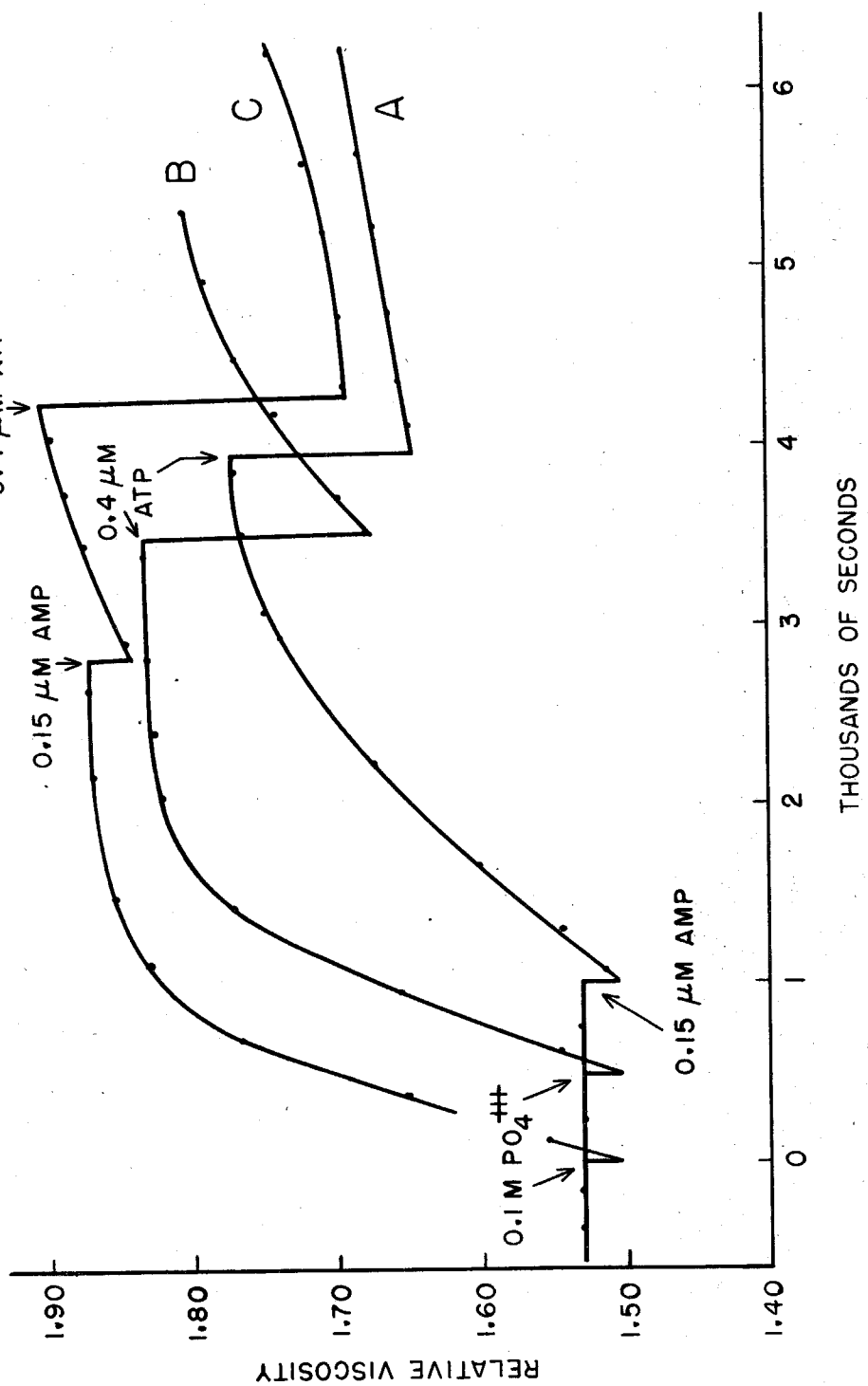
0.4 μM ATP
0.15 μM AMP
0.4 μM ATP
B
C
A
0.1 M PO4++
0.15 μM AMP
RELATIVE VISCOSITY
1.90
1.80
1.70
1.60
1.50
1.40
0
1
2
3
4
5
6
THOUSANDS OF SECONDS

dilution. Precipitation of the protein occurs in 20 to 30 minutes.

Addition of AMP to KCl extracts previously made 0.1 M in phosphate ion and already in the high viscosity state, causes a further small increase in viscosity (Fig. 6, curve C). If sufficient AMP is added to produce a maximal AMP response, subsequent addition of a previously optimal amount of phosphate causes little or no further increase in viscosity.

Concentrations of ATP which initiate only small increase in the viscosity of crude KCl extracts, evoke large and reversible decreases in the viscosity of solutions first brought to a high-viscosity state with 0.1 M phosphate or with AMP (Figs. 5 and 6). Continuous introduction of ATP into the system cause a maximum decrease in viscosity and maintain this low viscosity state for a longer period (Fig. 7). If AMP is used to raise the viscosity prior to addition of ATP, the AMP tends to inhibit recovery of the system to a high-viscosity level (Compare curves C with curve B, Fig. 6).

The specificity of the system constructed by addition of 0.1 M phosphate to the 1.4 M KCl extract has been tested briefly. Adenosine is without effect. ADP causes a small drop in viscosity (less than that caused by a similar concentration of ATP) but the recovery process is considerably slower than with ATP. Sodium triphosphate has no effect on a system initially in either a low or high viscosity state. Sodium pyrophosphate causes precipitation of protein in a few minutes.

Fig. 7. Effect of continuous addition of ATP to the viscosity of a buffered 1.4 M KCl extract after initial addition of phosphate ion.

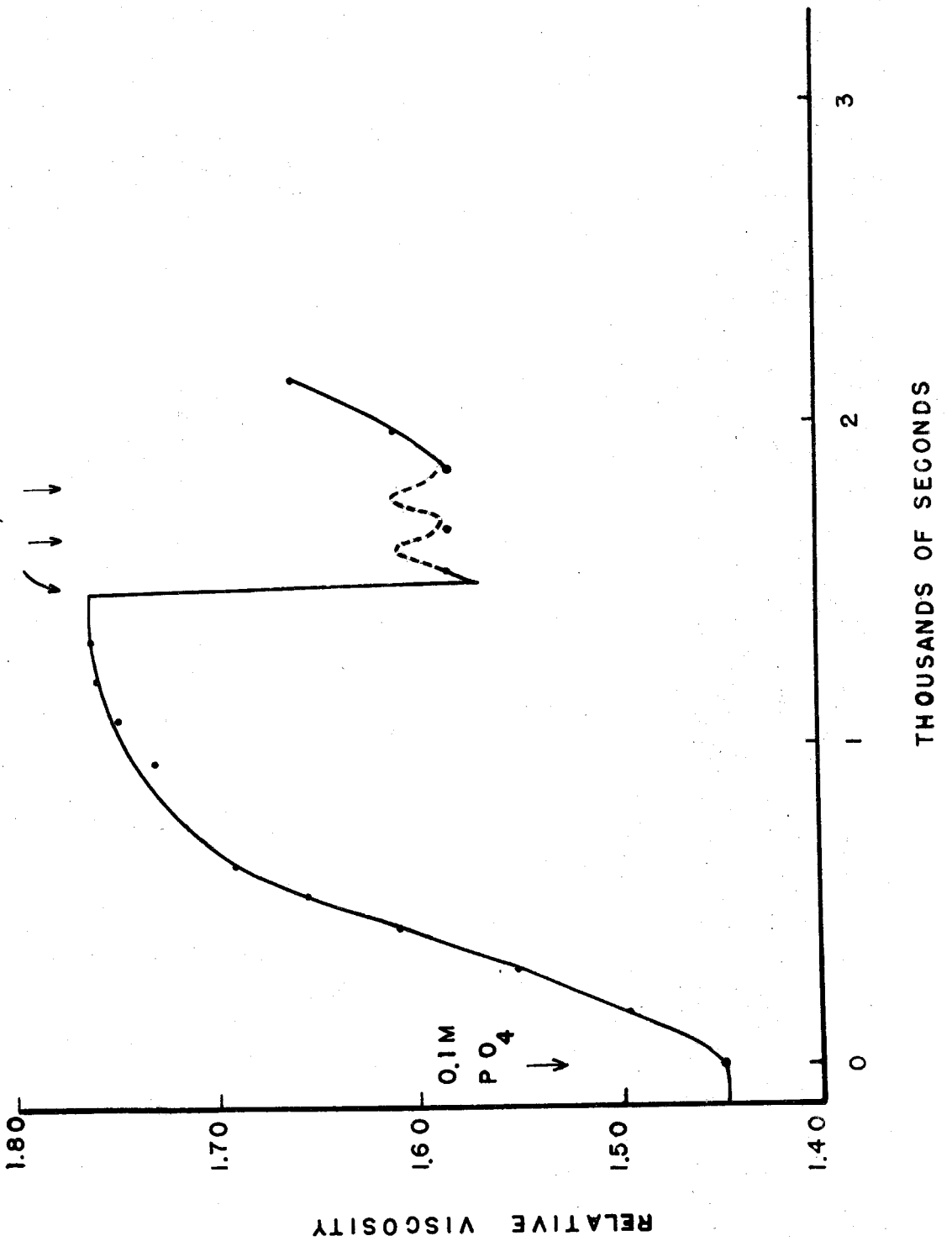
1.6μM ATP
0.1M PO4
RELATIVE VISCOSITY
1.80
1.70
1.60
1.50
1.40
0
1
2
3
THOUSANDS OF SECONDS

Unbuffered KCl extracts lose all of their ability to respond to phosphate, AMP or ATP if they are dialyzed against 1.4 M KCl or buffers overnight. Nearly all of the activity is lost if the preparations are stored at 0° for a similar period of time. Approximately half of the activity is lost if the material is frozen and stored at -10° C for a week.

Conclusion: The viscosity of the plasmodial extract of unbuffered 1.4 M KCl solution can be increased by either AMP or phosphate ions. Higher concentration is needed than of AMP, but phosphate treatment elicits a higher level of viscosity. Subsequent introduction of ATP into such a phosphate activated solution evokes a sharp decrease in viscosity followed by a rapid and complete recovery of the viscosity level. The system so constructed is thus completely reversible.

D. The Effect of ATP and Related Compounds on Salt Fractionated Plasmodial Extracts.

When the 1.4 M KCl extract is fractionated with ammonium sulphate at pH 7.0 and 0° C, the ability to change viscosity in response to ATP is found only in the fraction precipitated between 30% and 40% ammonium sulphate saturation. This active fraction is designated as the 30-40% SAS fraction. All fractions are readily soluble in KCl solution, and in the experiments described in this section, the

precipitates were dissolved in 1.4 M KCl unless otherwise indicated.

The initial viscosity of the 30-40% SAS fraction is high in comparison with that of either the crude KCl extract, the 0-30% SAS fraction or the supernatant which remains after 40% salt saturation. Addition of 0.2 to 0.4 μM ATP/ml causes a rapid, reversible decrease in the viscosity of the 30-40% SAS fraction (Fig. 8). The magnitude of the decrease in viscosity caused by an optimal amount of ATP is greater in partially purified preparations than in the crude KCl extracts. The recovery phase is, however, easily suppressed by an excess of ATP. A single addition of 3 μM of ATP per ml of solution is sufficient to keep a salt-fractionated preparation in a low viscosity state for hours. This amount of ATP has been used later as the standard amount for studying the effect of ATP in lowering the viscosity. Addition of phosphate ion, AMP and ADP to the 30-40% SAS fraction, has no effect on viscosity. It has not been possible to demonstrate any effect of magnesium or calcium ions on the viscosity of this fraction also.

The amount of total phosphorus (TP) and trichloroacetic acid precipitable phosphate (TCA-P) as well as the activity of ATPase and phosphatases present have been measured in each fraction of several preparations. Representative re-

Fig. 8. Relationship between the ATP-induced change in viscosity and rate of release of inorganic phosphate ion in 30-40% SAS fraction.

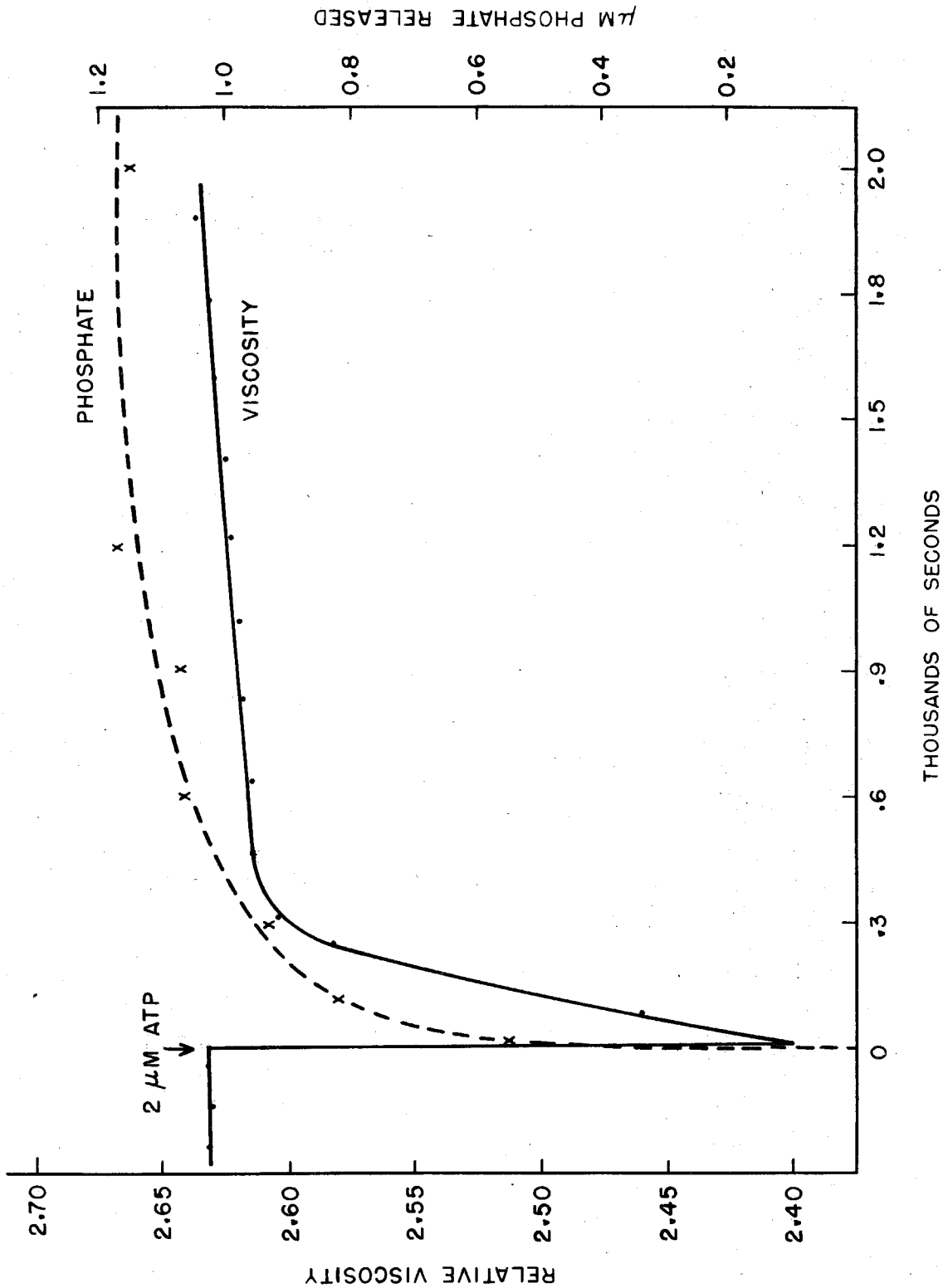
RELATIVE VISCOSITY
2.70
2.65
2.60
2.55
2.50
2.45
2.40
2 μM ATP
PHOSPHATE
VISCOSITY
μM PHOSPHATE RELEASED
1.2
1.0
0.8
0.6
0.4
0.2
0
.3
.6
.9
1.2
1.5
1.8
2.0
THOUSANDS OF SECONDS

sults are summarized in Table 1.* It is interesting to note that the active fraction contains a substantial portion of the TCA-P of the whole extract. There is 1.1 to 1.5% of phosphorus in the TCA precipitates, which, as indicated later, corresponds to 12 to 16% RNA. On the other hand, most of the phosphatase activity as well as conventional ATPase activity have been removed from the active fraction by the fractionation of salt. There is, however, associated with the purified fraction an ATPase activity which acts specifically in connection with viscosity changes induced by ATP. Increase in viscosity (the recovery phase) is accompanied by release of inorganic phosphate from ATP (Fig. 8). It should be noted, nevertheless, only one μM of phosphate has been liberated from the addition of 2 μM of ATP into a 4 cc protein solution after 10 minutes, but the viscosity of the solution has gone back to the original level already. It would imply that after the protein solution reacted with ATP, it would return to its original level in spite of the presence of a certain amount of excess ATP. This aspect has been further studied and will be discussed later on the purified myxomyosin.

The lowering of viscosity evoked by ATP decreases as the protein concentration is reduced. The reduced viscosities

---

* The experiment reported in Table 1 was performed in the writer's absence by Drs. L. Eggman and J. Bonner. It is included here for the sake of completeness. The author wishes to express his thanks for permission to reproduce these results.

Table 1

Summary of Properties of $(NH_4)_2SO_4$ Precipitated Fractions[1]

of 1.4 M KCl Extracts

Fraction	Relative viscosity of 1.5% protein solution	ATP Response	Protein %	Total Phosphorus %	TCA-P %	Relative Activity per mg. protein ATPase	Phosphatase
Initial extract	1.6 to 1.8	++	100	100	100	100	100
SAS ppt 0-32%	1.1 to 1.15	None	10-15	5	8	31	30
SAS ppt 32-40%	2.6 to 3.4	++++	25-30	42	57	16	33
40% SAS supernatant solution	1.1 to 1.2[2]	None[2]	55-60	50	18	95	179
Recovery			90-95	97	83		

[1] Precipitated fractions redissolved in 1.4 M KCl.

[2] Measured in 40% SAS. $(NH_4)_2SO_4$ *per se* does not affect ATP-response or viscosity of other fractions when present below concentrations which cause incipient precipitation.

of the protein in the presence and absence of ATP are given in Fig. 9. These data do not provide unambiguous information about the molecular dimension of the protein, because of the impurity of the system and the high shear gradient employed. The results do, however, indicate a relationship between protein concentration and response to ATP.

The 30-40% SAS protein solution at 1-2% concentration in high salt medium is thixotropic and the viscosity behavior depends on the thermal history of the sample. This is illustrated in Fig. 10. Curve A represents the viscosity of the freshly prepared protein solution. The effect of addition of 0.4 μM/ml ATP lowers the viscosity, followed in time by recovery. Addition of twice the amount of ATP, 0.8 μM/ml, then causes an almost doubled viscosity lowering, followed by a slight recovery. Curve B represents the behavior of an aliquot from same initial solution which has been stored for 12 hours at 0° C. The viscosity of this sample was measured in the viscometer without waiting of attainment of thermal equilibrium. As the solution warmed, the viscosity increased rapidly rather than dropping as might be expected. Addition of ATP to this solution (Curve B) in accordance with the treatment for the sample of curve A, produced a great lowering of viscosity which decreased almost to the level of sample A. Curve C represents results from the same protein solution as that of curve B, a sample stored at 0° C for 12 hours. When sample C was introduced

Fig. 9. The plot of reduced viscosity (cc/gm) vs. protein concentration of the 30-40% SAS fraction in the absence and in the presence of 3 μM/ml ATP.

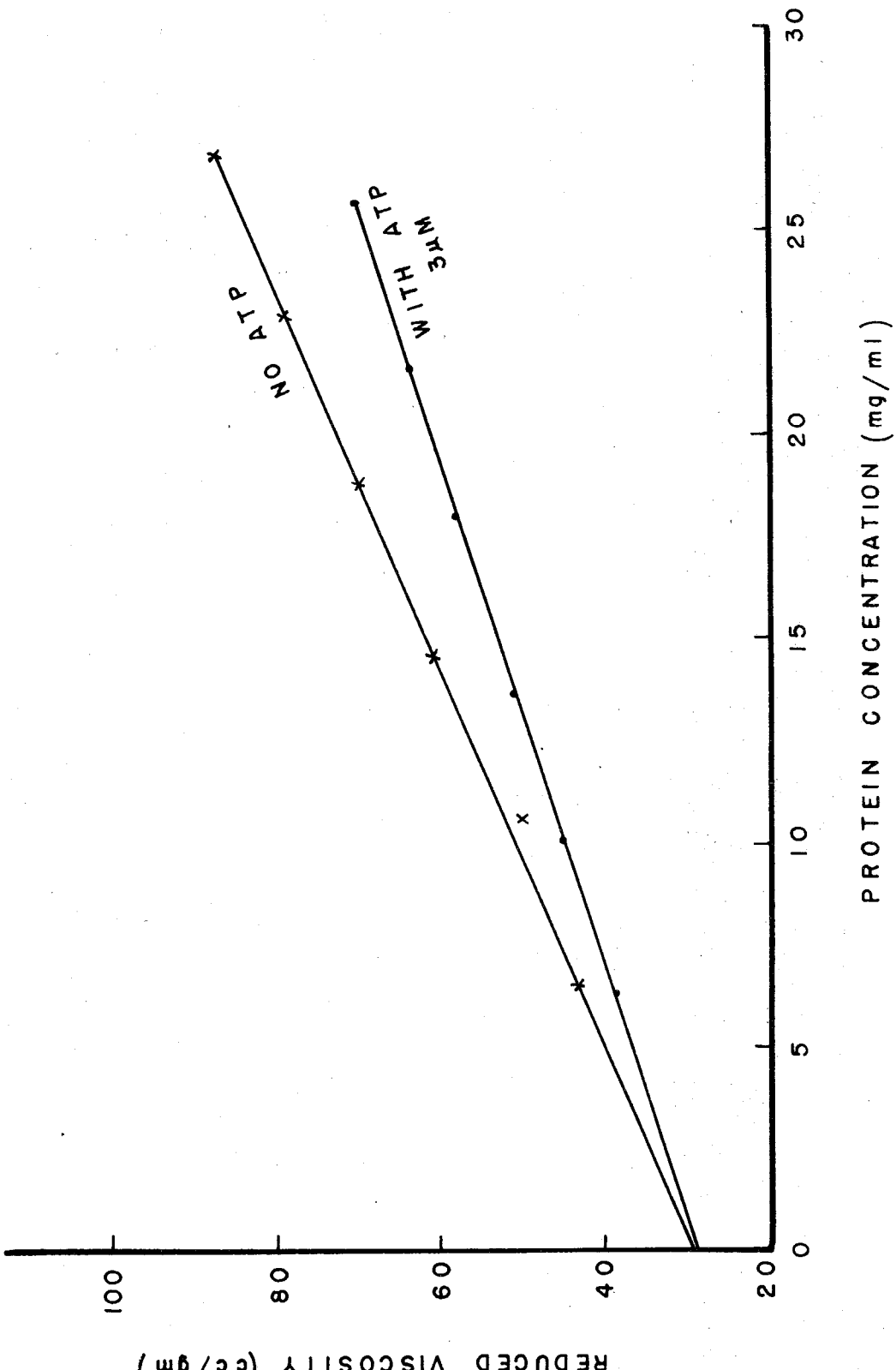
NO ATP
WITH ATP
3mM
REDUCED VISCOSITY (cc/gm)
PROTEIN CONCENTRATION (mg/ml)
100
80
60
40
20
0
5
10
15
20
25
30

Fig. 10. Work-softening and thermal history effects upon the viscosity of the 30-40% SAS fraction. See text for details. Protein concentration: 18 mg/ml.

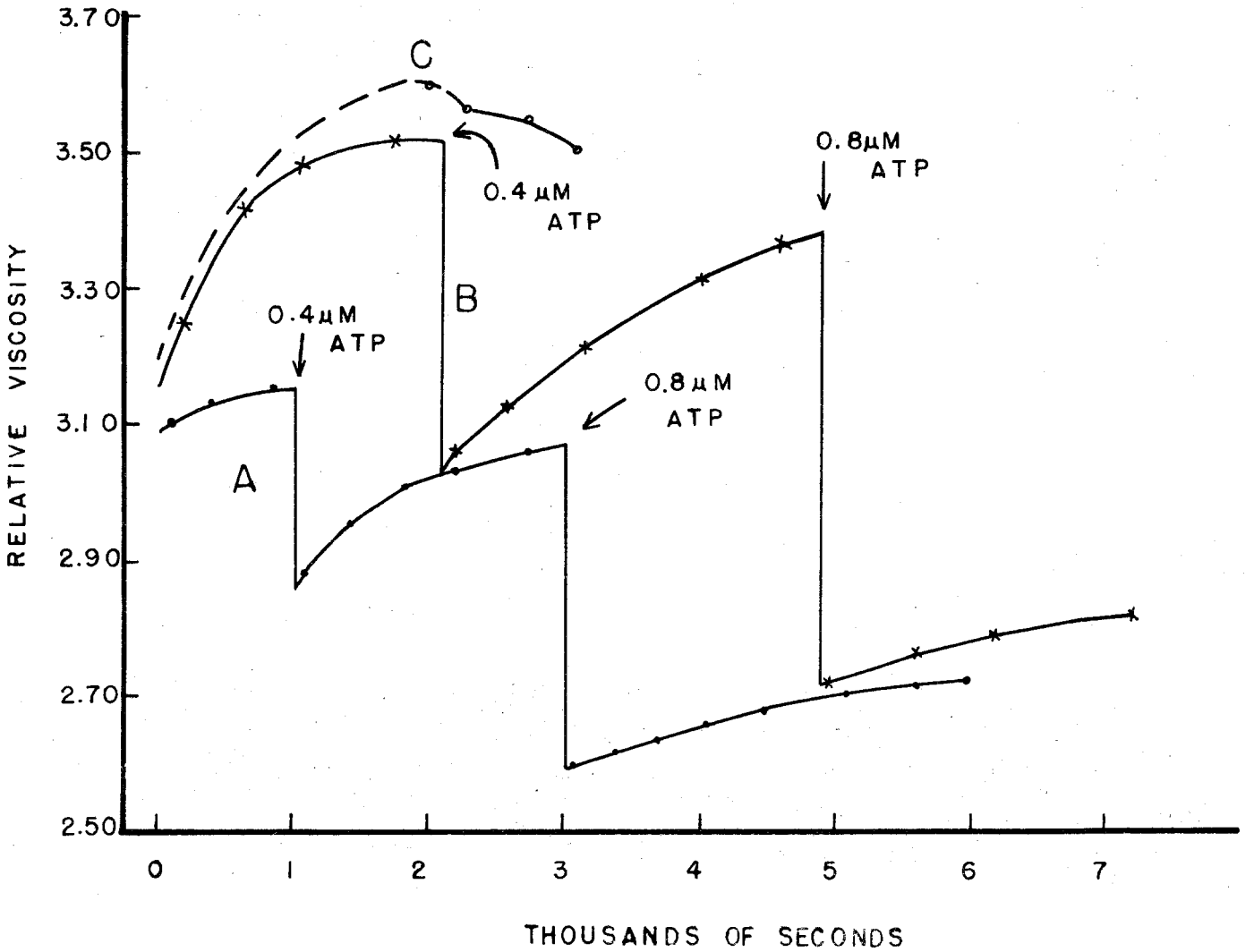
3.70
3.50
3.30
3.10
2.90
2.70
2.50
RELATIVE VISCOSITY
C
0.4 µM ATP
0.8µM ATP
0.4µM ATP
B
A
0.8 µM ATP
0
1
2
3
4
5
6
7
THOUSANDS OF SECONDS

into the viscometer, its viscosity was measured immediately and then not again until the thermal equilibrium had been reached. Curve C indicates that the increase of viscosity after low temperature treatment is a function of time and temperature and is not caused by work hardening, attending movement up and down through the capillary of the viscometer. Sample C, after it has reached its high viscosity state, shows thixtropic behavior. The viscosity goes down after each measurement. The level of curve C is higher than of curve B, because of the fact that the solution of curve B has been worked more times. The fact that the high viscosity generated after cold treatment is reduced by ATP, is clearly indicated by comparison of curves B and A. The thixotropic behavior of the high viscosity state suggests that it is an aggregation phenomenon, resulting from the formation of large structural elements that can be partially destroyed by flow through the viscometer.

The experiment, Fig. 11, shows that the storage of the protein solution at 0° C for two hours is sufficient to generate the high viscosity state when the solution is returned to 24.5° C after that period. Curve A of Fig. 11 represents the viscosity of the protein solution stored in the viscometer at 24.5° C for two hours. The viscosity of the sample is constant during this period. Curve B represents an aliquot of the same protein solution which has been held at 0° C for 2 hours. At the end of this cold

Fig. 11. Effect of storage at 0° C for 2 hours on the viscosity of the 30-40% SAS fraction. Protein concentration: 20 mg/ml.

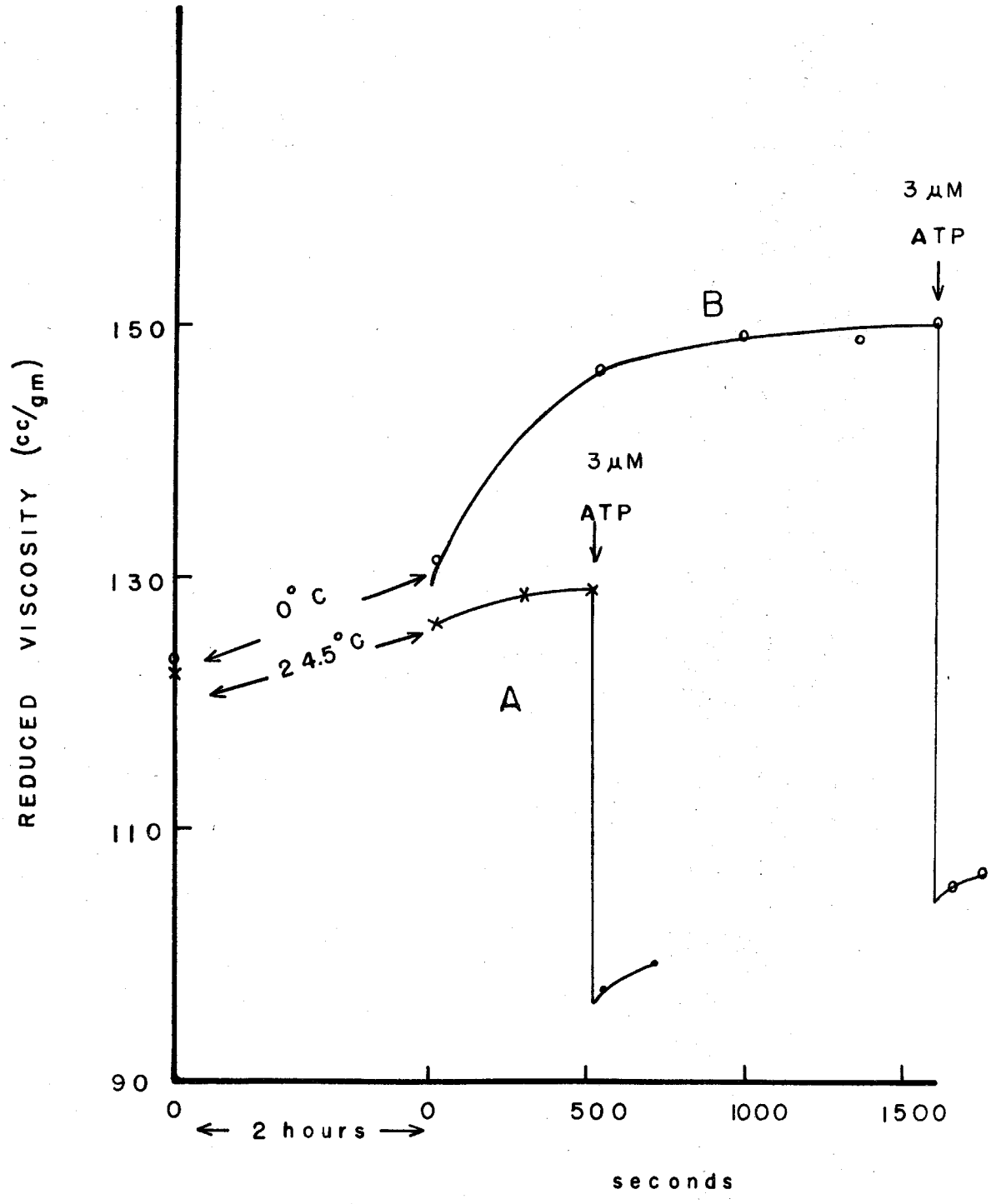
3 μM
ATP
B
150
3 μM
ATP
130
0° C
24.5° C
A
110
90
REDUCED VISCOSITY (cc/gm)
0
← 2 hours →
0
500
1000
1500
seconds

treatment, the sample of curve B was brought into the viscometer and its viscosity immediately measured. It is apparent that viscosity is rapidly increased after the cold treatment. The addition of ATP reduces most of the increased viscosity. It should be noted that the ordinate in Fig. 11 is reduced viscosity. When this stored protein solution is frozen at -10° C for 2 hours, an even greater subsequent increase in viscosities was apparent. The solution becomes highly thixotropic (each measurement causes the drop of 30 reduced viscosity cc/gm) and exhibits a large ATP effect (Table 2, exp. 1). It is clear that the protein system after storage at low temperature undergoes an aggregation process with a positive thermal coefficient. ATP substantially dissociates the aggregates so formed.

Dialysis of the protein overnight against 1.4 M KCl causes a large decrease in viscosity and lowers both the tendency to aggregate thermally and to respond to ATP. Addition of 0.25 - 0.5 μM/ml ATP into the dialyzing medium preserves roughly 40% of the reduced viscosity of the protein solution, but does not prevent the loss of ATP response. The viscosity of the 30-40% SAS protein solution in high salt medium is evidently not stable.

When the 30-40% SAS protein is dissolved in low ionic strength medium, such as 0.1 M KCl, 0.1 M K-maleate, or 0.1 M KCl + 0.1 M maleate, the reduced viscosity of the solution is comparable to that in 1.4 M KCl. The ATP re-

Table 2

The Effect of Salt Concentration and Temperature Treatment on the Viscosities of the 30-40% SAS Fraction Solutions

Expt. No.	Solvent	Temperature treatment	Reduced Viscosity (cc/gm)	Decrease of Reduced Viscosity by 3 μM/ml ATP
1	1.4 M KCl	initial	134.7	40
	1.4 M KCl	2 hours at - 10°C	282-221 Thixotropic	101
2	1.4 M KCl	initial	134.7	40.5
	0.1 M KCl	initial	126.1	32.5
	0.1 M K-maleate	initial	132.6	33.3
3	0.1 M KCl + 0.1 M K-maleate	initial	142.8	31.9
	0.1 M KCl + 0.1 M K-maleate	3 hours at 0°C	142.8	31.8
	0.1 M KCl + 0.1 M K-maleate	8 hours at 0°C	137.6	30.5
	0.1 M KCl + 0.1 M K-maleate	2 hours at - 10°C	142.1	31.8

sponse is somewhat lower but is substantial (Table 2, exp. 2). It was soon observed, however, that protein solutions in low ionic strength medium do not show the thermal aggregation effect and can be stored either at 0° C or frozen at -10° C for several hours without developing structural viscosity (Table 2, exp. 3). The protein solution can also be dialyzed overnight in low ionic strength media with little loss of reduced viscosity or ATP response. This finding opened the way for the physical-chemical analysis of the 30-40% SAS fraction and its further purification. A further technological matter observed at this stage facilitated experiments with the materials. The 30-40% SAS precipitates can be stored without change for at least four days at 0° C or -10° C. Purification of the protein may be interrupted, therefore, at the 30-40% SAS stage.

Conclusion: All of the ATP response activity can be fractionated from the 1.4 M KCl extract by salt precipitation. This protein fraction, which contains twenty percent of the total protein, need not be activated since it is already viscous and reacts with ATP reversibly with liberation of phosphate during the recovery phase. The protein system aggregates at room temperature after cold storage. In 0.1 μ KCl + 0.1 μ maleate, however, the protein can be stored or dialyzed at low temperature for 8-6 hours without inducing a tendency to aggregate at room

temperature. This fraction can be preserved for seven days in the form of the ammonium sulphate precipitate.

E. Properties of the Slime Material.

A mucous slime surrounds the protoplasmic strands of Physarum. The question may be raised as to whether the slime substance, mostly high molecular weight carbohydrates, influences the viscosity behavior of the 30-40% SAS protein prepared from the whole organism. It is known that material such as methyl cellulose have a positive temperature coefficient of viscosity as does the plasmodial extracts. A small amount of high molecular weight carbohydrate could conceivably accompany the protein through the present fractionation procedure and influence the temperature characteristics of the system. Quantitative analysis, using the anthrone reagent method (chapter II), of the active salt-fractionated material indicates that as much as 16 to 18% of the total soluble material and about 10% of the total TCA precipitable material is carbohydrate (calculated as glucose equivalent). A portion of the carbohydrate is probably due to the sugar component of the ribonucleic acid which is a constituent of myxomyosin complex as discussed below. Other carbohydrates are apparently also present however. An effort was then made to collect the slime as free as possible of the plasmodial strands and to study the slime under conditions similar to those used

with the protein. It was found that some slime material did go through the centrifugation and salt fractionation procedures and that the resultant preparation does have a rather high viscosity. This slime solution does not, however, react with ATP and does not exhibit any thermal history effects or aggregation phenomenon. The behavior of salt fractionated protein solution extracted from plasmodial strands free from slime substance is similar to those solutions containing small amounts of slime material. It appears then that the carbohydrates from the slime have no relation to the ATP-response and the thermal aggregation phenomenon of the protein solution, but merely contribute to the ground level of the viscosity of the solution.

Conclusion: The carbohydrate material from the slime has no relationship to the activity of the salt fractionated protein system.

IV. THE ISOLATION OF AN ACTIVE COMPONENT--MYXOMYOSIN

A. Electrophoretic Analysis of the 1.4 M KCl Plasmodial Extracts, and of the 30-40% SAS Fraction. Further Purification by Successive Salt Precipitation and Preliminary Centrifugation.

The behavior and viscosity response to ATP of the 1.4 M KCl plasmodial extract has been described in the previous chapter. Such extracts were inactivated by dialysis against either 1.4 M KCl or 0.1 M KCl at 0° C for 24 hours. The electrophoretic pattern of inactive preparation obtained by extraction with 1.4 M KCl and dialyzed in 0.1 M potassium maleate buffer at pH 7 is given in Fig. 12. There are two groups of boundaries in the pattern, a fast group which clearly consists of a variety of proteins and a slow group which do not resolve. The latter group must possess isoelectric points near pH 7, since they hardly move in the electrical field at this pH. It will be later shown that the large fraction of the total protein with low mobility at pH 7 is inactive and may be considered an impurity.

The 30-40% SAS fraction was found to retain its activity after a ten hour dialysis against 0.1 μ KCl + 0.1 μ K-maleate at 2° C. The dialysis carried out is complete in ten hours with stirring, as indicated by the agreement

Fig. 12. Electrophoresis patterns of the 1.4 M KCl crude extract

(Migration proceeds from right to left)

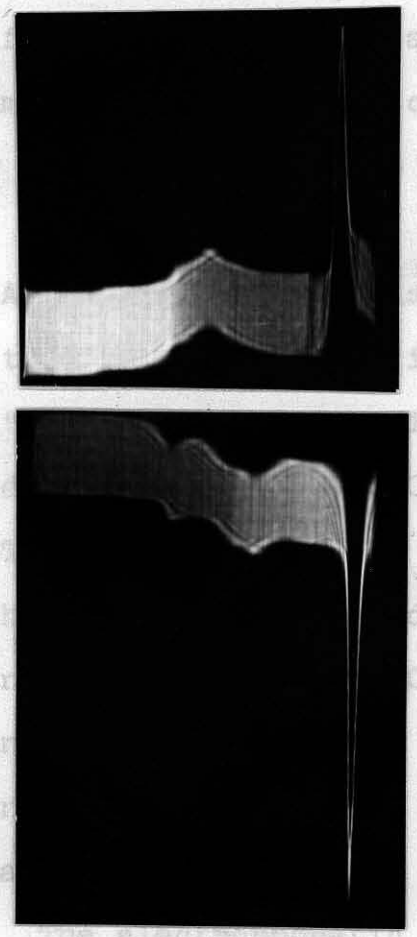

Asc.

Desc.

Buffer: 0.1 μ K-maleate

pH: 7.0

Current: 6 ma.

Time: 5500 seconds

within 1% of the conductance of the protein solution and of the buffer. The electrophoretic pattern of this material is shown in Fig. 13. The peaks in the electrophoretic patterns were arbitrarily identified as A, B, C, and D, in order of decreasing mobility. This pattern may be compared with that of the original 1.4 M KCl extract. It is apparent that the purification reduces the amount of slow moving boundary (D) component and that the component of moderately fast moving boundary, C, emerges as one of the major components.

When the 30-40% SAS protein solution is refractionated by ammonium sulphate, the active principle is precipitated by 25-36% SAS. The activity of the refractionated material is enhanced as compared with the original 30-40% SAS precipitates as shown in Table 3.

The activity of the salt refractionated materials is further enhanced by centrifugation at 42,000 x g (25,000 rpm) for one hour as indicated in Table 4. The supernatant from the centrifugation is clearer and more active than before. Heavy inert material has evidently been centrifuged from the system. The electrophoretic pattern of the centrifuged material (Fig. 14) shows in proportion that the area of slow moving peak D, has been greatly reduced and the area of the peak C substantially increased.

Fig. 13. Electrophoresis patterns of the 30-40% SAS fraction
(Migration proceeds from right to left)

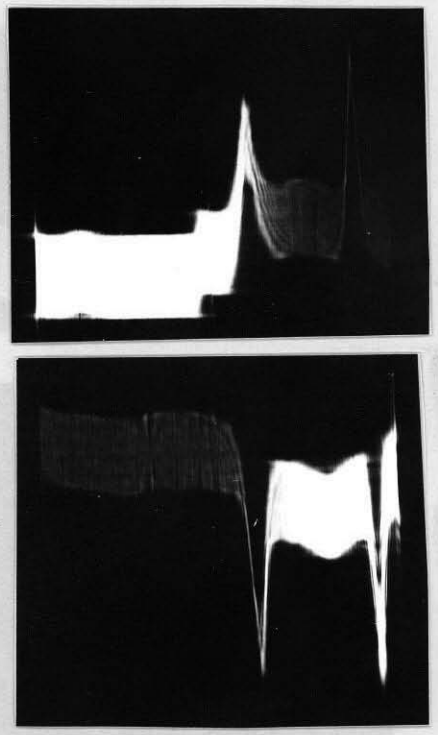

Asc.

Desc.

Buffer: 0.1 μ KCl + 0.1 μ K-maleate

pH: 7.0

Current: 9 ma.

Time: 9500 seconds

Concentration: 12.4 mg/ml

Fig. 14. Electrophoresis patterns of the 30-40% SAS fraction after a preliminary centrifugation (80,000×g 30 min)

(Migration proceeds from right to left)

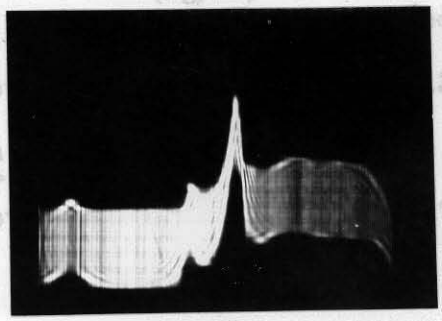

Asc.

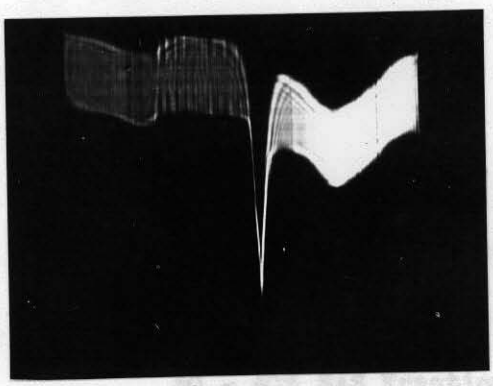

Desc.

Buffer: 0.1 μ KCl+0.1 μ K-maleate

pH: 7.0

Current: 9 ma.

Time: 9000 seconds

Concentration: 10.8 mg/ml

Table 3

The Effect of the Ammonium Sulphate Refractionation (25 - 36% SAS) on the Viscosity and the ATP Response of the 30 - 40% SAS Fraction

Material	Concentration (mg/ml)	Reduced Viscosity (cc/gm)	Decrease of Reduced Viscosity Caused by 3 µM/ml ATP
30-40% SAS Fraction	18.4	135.7	35.2
Refractionation (25-36% SAS) of the 30-40% SAS Fraction	18.2	171.5	53.8

Table 4

The Effect of Preliminary Centrifugation (42,000 x g 1 hour) on the Viscosity and the ATP Response of the 30 - 40% SAS Fraction

Material	Concentration (mg/ml)	Reduced Viscosity (cc/gm)	Decrease of Reduced Viscosity Caused by 3 µM/ml ATP
30-40% SAS Fraction	17.0	180.4	39.1
30-40% SAS Fraction purified by a preliminary centrifugation	14.6	174.8	47.4

B. The Identification of the Active Principle by Electrophoresis, Ultracentrifugation, and Viscosity Studies.

The protein preparation described in the preceding section is a mixture of components as evidenced by electrophoretic pattern. It is however, possible to ascertain which component is the active principle. The active material can be sedimented differentially in the preparative centrifuge. This procedure was combined with electrophoretic and viscosity measurement to identify the active material.

A protein solution purified by salt precipitation and preliminary centrifugation (at 80,000 x g 30 minutes) was centrifuged at 60,000 x g (30,000 rpm) for 3 hours in the angle preparative centrifuge. The top 2 cc and the bottom 2 cc of the supernatant were collected separatively. The pellet at the bottom of the tube was then redissolved in fresh KCl-buffer. The viscosity behavior of each solution is given in Table 5. The active principle has a high sedimentation constant since the pellet fraction was most active of the three solutions while the top fraction was inactive. The ultracentrifugal and electrophoretic patterns of these three fractions are shown in Fig. 15. The ultracentrifugal patterns suggest that the protein solution before centrifugation is composed of essentially two centrifugal components with a large difference in sedimentation constants. The fast moving fraction has a sedimentation constant above 24 S (Sverberg unit) while the slow moving

Fig. 15. Ultracentrifuge and electrophoretic patterns of partially purified 30-40% SAS fraction after centrifugation 3 hours at 100,000 x g

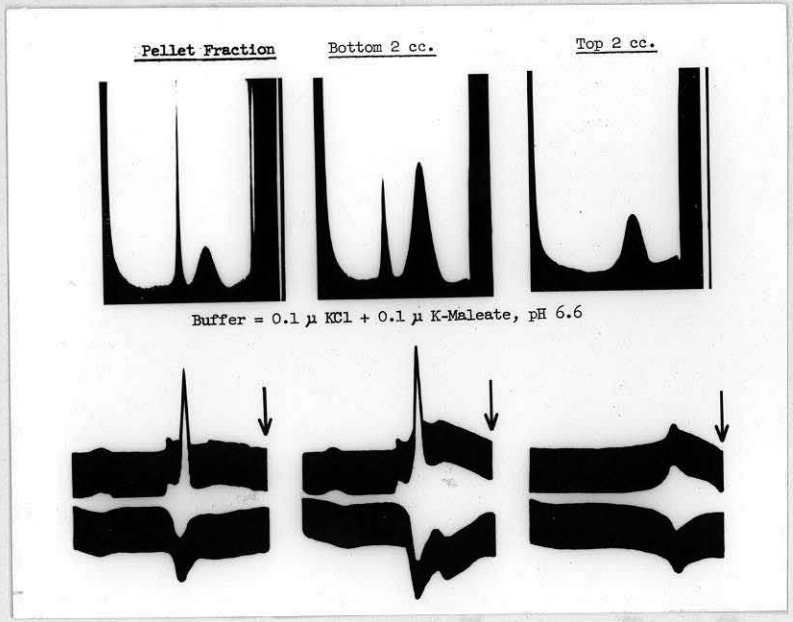

Concentration: (mg/ml)	4.0	8.6	3.5

Table 5

The Viscosity Data of Protein Solution Partially Purified After 3 hours Centrifugation at 60,000 x gm (40,000 rpm)

	Pellet Fraction	Bottom 2 cc	Top 2 cc
Concentration (mg/ml)	4.0	4.3	3.5
Reduced viscosity (cc/gm)	186.7	110.3	35.4
Decrease of Reduced Viscosity Caused by 3 μM/ml ATP	54.7	11.3	1.1

fraction has a sedimentation constant of 3 to 4 S. The top fraction of the centrifuge tube contained the protein components of low sedimentation constant and low electrophoretic mobility, and was inactive (Table 5 and Fig. 15). On the contrary, the pellet fraction of the tube contained a high concentration of fast sedimenting component, and electrophoretically three fast boundaries. The pellet fraction was the most active of all (Table 5 and Fig. 15). Since the amount of the high S component is so well related with the activity of the three fractions (Table 5, and Fig. 15), it may be concluded that the active principle is associated with the fast-sedimenting boundary.

The electrophoretic mobilities of various boundaries are given in Table 6. Peak A possesses the mobility of a nucleic acid or nucleotide (74,75), a mobility essentially equal to that of ATP (Table 6). There is 9% RNA in the highly purified active component (Chapter V) Peak A, which contributes ca. 5-10% of the preparation (concentration by area) at this stage, is identified as the RNA component. Two peaks, B and C, appear in the ascending pattern, but only one, B + C, in the corresponding position of the descending pattern. The peak, B + C, in the descending pattern moves with a mobility close to that of peak C in the ascending pattern (Table 6). The dn/dx area for peak, B + C, is equal to the sum of the areas from peaks B and C.

Table 6

The Electrophoretic Mobilities of the Boundaries of the Active Material (pH. 7.0, 0.2 μ ionic strength, KCl-maleate buffer or K-maleate buffer)

Limb.	Boundary	Mobility ($cm^2 volt^{-1} sec^{-1} \times 10^5$)
Ascending	A	14.3 - 14.6
	B	8.1 - 8.3
	C	6.5 - 7.0
Descending	A	13.3 - 13.8
	B+C	6.6 - 6.9
Ascending	ATP	15.3

The interaction of nucleic acids with various proteins in electrophoresis has been analyzed by Longsworth and MacInnes (74), by Goldwasser and Putman (75), and others (76). Under conditions in which the dissociation of the nucleic acid-protein complex is not complete, the descending and ascending patterns are not always enantiographic to each other. The ascending limb frequently exhibits more boundaries than does the descending limb. In a mixture of one protein and nucleic acid the number of boundaries is usually 3 and 2 respectively. In the present experiments, nucleic acid is present in the ascending protein solution, and moves into the buffer region. In the descending limb, nucleic acid leaves the protein boundary region and moves down through the original solution with a reduced mobility owing to chemical and physical interaction effects.

The present electrophoretic patterns may be explained if one assumes that the rate of equilibration of the nucleic acid-protein complex is comparable with the rate of electrophoretic separation of the two components. Thus the nucleoprotein complex is dissociated in the ascending limb to yield a free nucleic acid boundary A (5-10% in area) a protein boundary C (50-55%) and a nucleoprotein boundary (10-15%). In the descending limb, the nucleic acid rapidly moves away from the original boundary, leaving behind a substantially pure protein boundary, B + C (60-65%)(Fig. 16).

Fig. 16. Electrophoresis patterns of the starting material (31-40% SAS fraction) and of the fractions obtained by one cycle differential centrifugation at 100,000 x g for 2.5 hours (Migration proceeds from right to left)

Buffer: 0.2 μ K-maleate pH: 7.0 Current: 9 ma.

Starting Material | Supernatant Fraction | Pellet Fraction

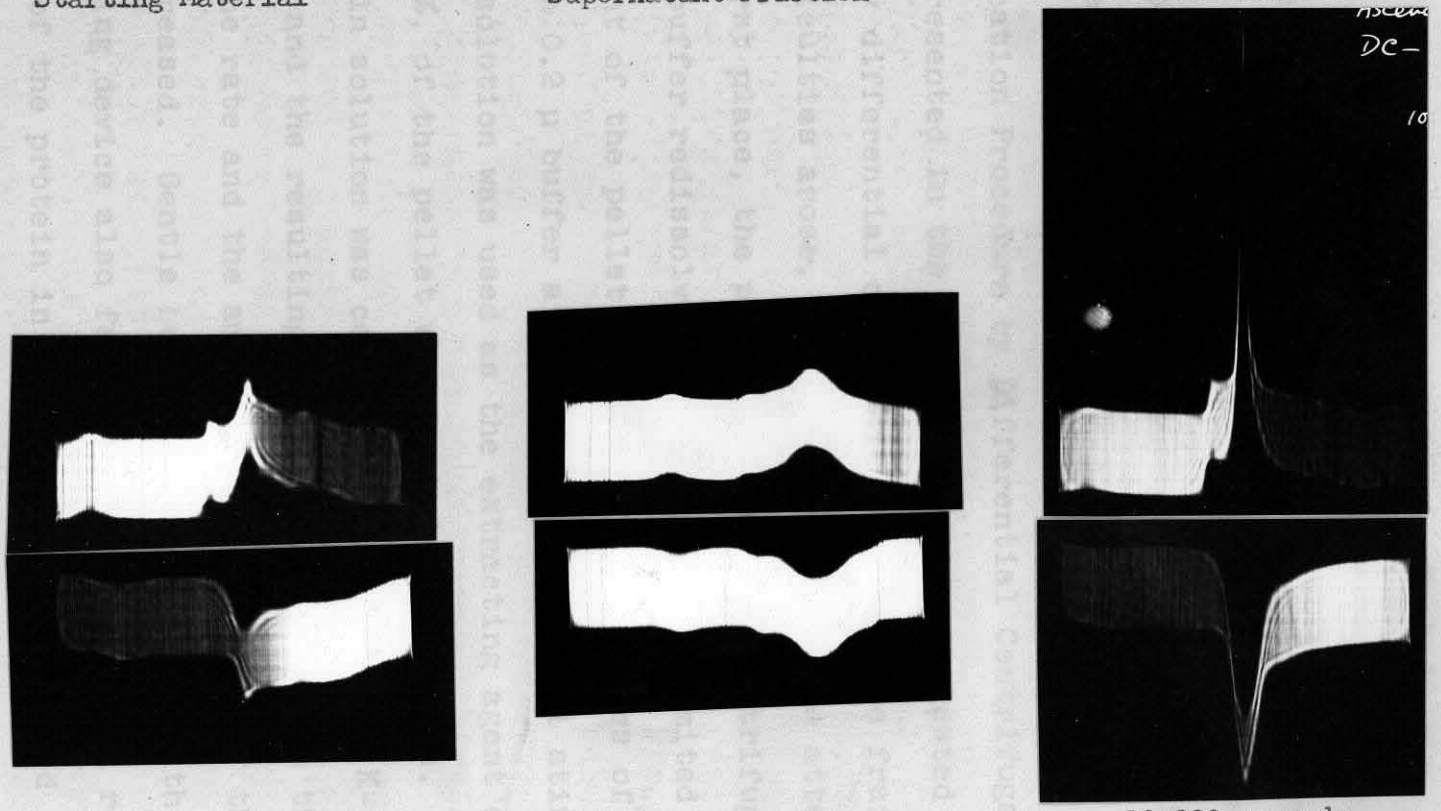

Time: 6000 seconds 6000 seconds 10,000 seconds
Concentration: (mg/ml) 5.9 3.1 9.7

It should be noted that the area percentages of peak A, B, and C, are different in the more purified preparation as shown in Table 7 of the following section. Peak A, the RNA component, is decreased and peak B and peak C increased.

It will be of interest in future work to analyze samples withdrawn from the trailing descending boundary for nucleic acid. Such experiments will serve to check the explanation presented above.

C. The Purification Procedure by Differential Centrifugation.

Results presented in the previous section suggested that purification by differential centrifugation might be fruitful. Two difficulties arose, however, when this was attempted.

In the first place, the pellet obtained by centrifugation in 0.2 μ buffer redissolved slowly and to a limited extent; 20 percent of the pellet dissolved in ten hours of extraction with 0.2 μ buffer at 2° C with occasional stirring. When 1 M salt solution was used as the extracting agent even less, about 10%, of the pellet went back into solution. When the protein solution was centrifuged in a 0.05 μ K-maleate buffer and the resulting pellet extracted with the same medium, the rate and the amount of dissolution of the pellet was increased. Gentle but constant stirring with a magnetic stirring device also facilitated solution. A recovery of 75% of the protein in the pellet was obtained when the protein solution was centrifuged and subsequently

redissolved in the 0.05 μ maleate buffer with stirring. The redissolved pellet was recentrifuged for a second cycle in the same buffer. 80-85% of the protein in the pellet from the second cycle centrifugation redissolved.

The second difficulty concerned the fact that the sedimentation constant of the active principle is highly concentration dependent while the sedimentation of the impurities is not. As the protein concentration is increased the sedimentation constant of the active principle is decreased and the effectiveness of the separation reduced. The differential centrifugation is therefore carried out with a dilute 0.5 - 0.45% protein solution. In this case, a shorter period is required.

A protein solution purified previously by salt precipitation and preliminary centrifugation, was diluted to 0.5% and was centrifuged at 100,000 x g (40,000 rpm) for 2 and one-half hours. The electrophoretic and ultracentrifugal patterns of the supernatant and the solution from the dissolved pellet are shown in Fig. 16 and Fig. 17. The single cycle pellet material was again centrifuged at 100,000 x g for two and a half hours and the pellet again redissolved. The electrophoretic and ultracentrifugal patterns of the doubly cycled product (Figs. 18 and 19) show that the ratio of the fast to slow components has been increased over that of the single cycled product. The improvement is, however, not as great as expected. A triply cycled material was also

Fig. 17. Ultracentrifuge patterns of the starting material (30-40% SAS fraction) and of the fractions obtained by one cycle centrifugation at 100,000×g for 2.5 hours

(Sedimentation proceeds from right to left)

Buffer: 0.2 μ K-maleate pH: 7.0

Starting Material	Supernatant	Pellet Fraction
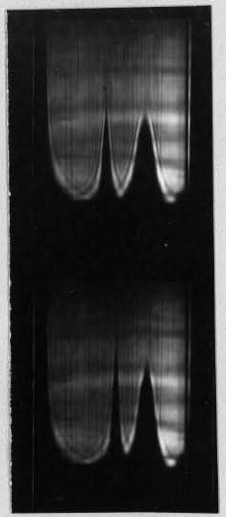	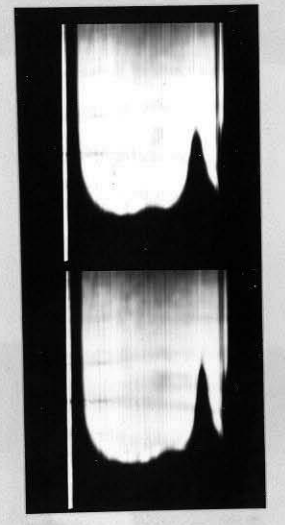	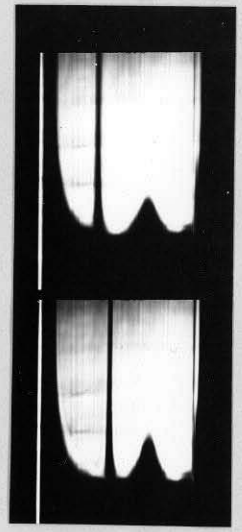
Rotor speed (rps) 850	860	850
Concentration (mg/ml) 5.9	3.1	9.7

Fig. 18. Electrophoresis patterns of the active principle (myxomyosin) after two and three cycles of differential centrifugation

(Migration proceeds from right to left)

Buffer: 0.2 μ K-maleate pH: 7.0

Second cycle product*

Third cycle product

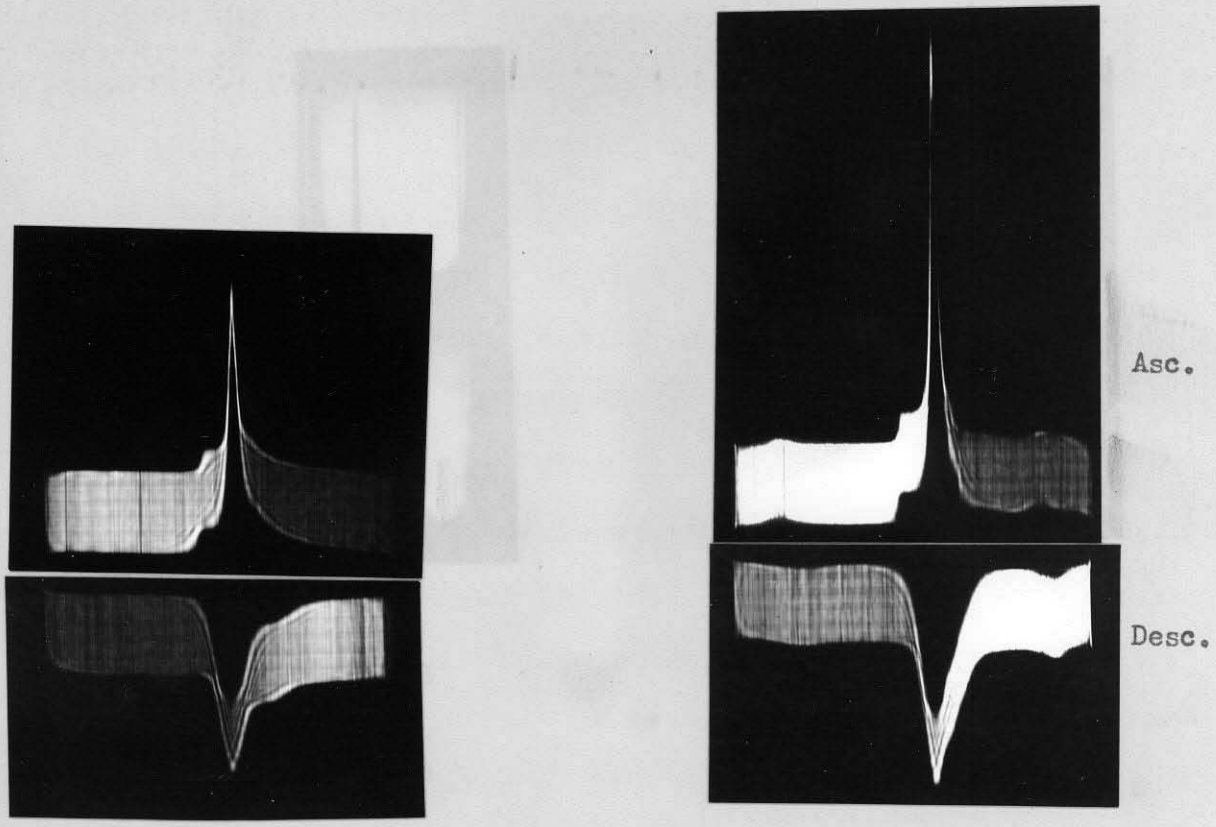

	Second cycle product*	Third cycle product
Current:	6 ma.	9 ma.
Time:	10,000 seconds	9,000 seconds
Concentration: (mg/ml)	5.5	11.8

* Boundary A has left the visible part of the cell

Fig. 19. Ultracentrifuge patterns of the active principle (myxomyosin) after two and three cycles of differential centrifugation

(Sedimentation proceeds from right to left)

Buffer: 0.2 μ K-maleate pH: 7.0

Second cycle product Third cycle product

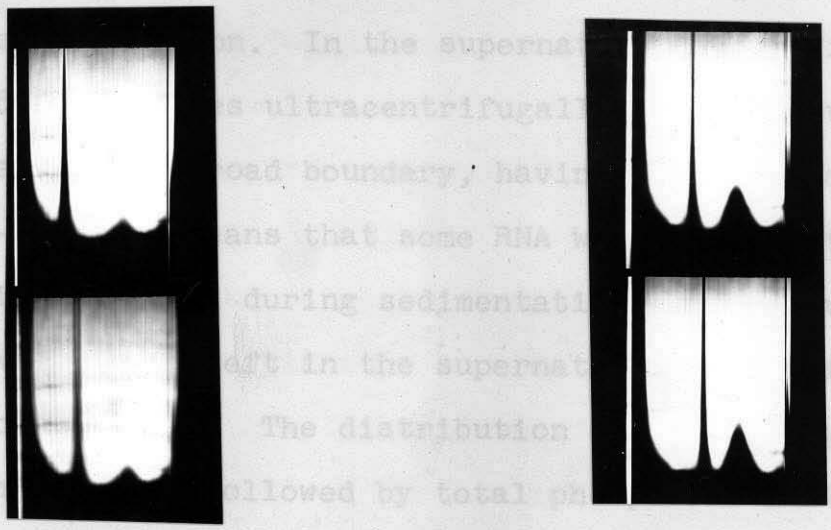

Rotor speed (rps)	848	850
Concentration (mg/ml)	5.5	11.8

obtained. Its pattern did not differ from that of the doubly cycled material and the slow-moving component was still present (Fig. 19).

Examination of the electrophoretic patterns shows that the RNA boundary is found in the supernatant fraction of the first cycle centrifugation, as well as in the pellet fractions of the first cycle, second cycle and even the third cycle centrifugation. In the supernatant of the first cycle (Fig. 16), RNA moves ultracentrifugally with the protein impurities as one broad boundary, having a sedimentation constant of 3-4 S. This means that some RNA was bound to the heavy and active material during sedimentation, for otherwise all RNA would have left in the supernatant after differential centrifugation. The distribution of RNA during centrifugation was also followed by total phosphorus analysis. The starting solution was the highly purified solution from the pellet of the first cycle centrifugation. The results are given in Table 9. The supernatant was enriched with RNA percentage wise after centrifugation. A large portion of RNA (55-60% of the total RNA) still adhered, however, to the fast sedimenting component. In other words, the fast sedimenting component appears to be a complex of nucleic acid-protein, and during centrifugation brings down with it a substantial amount of bound RNA, namely, 9% of its total weight.

Area measurements for the calculation of the concentra-

tion percentage of each fraction were carried out for the electrophoretic and ultracentrifugation patterns. The areas of peak B and peak C in the ascending pattern or peak B + C in the descending pattern of electrophoresis, correspond to 70-80%, ca. 75%, of the total concentration (Table 7). If peak A is also included as part of the active component, then the sum of the areas of peaks A, B, and C, makes 75-80% of the total, varying from one preparation to another (Table 7). Difficulties are encountered in exact separation of the areas of peak C and that of the trailing impurities (D). This is done by arbitrary extrapolation of a Gaussian curve to the base line.

The relative concentrations of the fast sedimenting peak, i.e., the active principle, as determined by area measurement, require corrections for radial dilution and for Johnston-Ogston effect. The correction for the Johnston-Ogston effect, calculated by the method of Trautman et al. is about 5-9% as shown in Table 8. The exact amount varies with concentration in the run and with position of the boundaries in the centrifuge cell. Estimation of the effect from the Johnston-Ogston equation and assuming that the sedimentation constant of the slow component sedimenting in the original solution, gives a value of 5-10%, depending on the assumed values of $S_{s,m}$ (Chapter II-J). The Johnston-Ogston correction is necessarily small since the ratio of the sedimentation constants of the fast and slow components

Table 7

The Percentage Area of Various Boundaries in the Electrophoretic Patterns of Myxomyosin Products of Two Cycle Centrifugation

Run No.	Patterns	Boundary A (RNA) %	Boundary B + Boundary C or Boundary B + C %	Boundary D (impurities) %
TPE-28	Ascending	4	76	20
	Descending	4	76	20
TPE-33	Ascending	3.5	72.5	24
	Descending	5	80	15
TPE-35	Ascending	5.5	71.5	23
	Descending	5	76	19

Table 8

The Percentage Area of the Two Boundaries in the Ultracentrifugal Patterns of Myxomyosin Products of Two Cycle Centrifugation

Run No.	Boundaries	Area	Radial Dilution Correction $(Xb/X_o)^2$	Johnston-Ogston Correction	Percentage Area
11-1-5	Fast	220	1.128	1.06	70.5
	Slow	100	1.026	1.06	29.5
9-1-5	Fast	180	1.121	1.054	68
	Slow	116	1.019	1.054	32
10-1-4	Fast	180	1.109	1.09	71
	Slow	104	1.024	1.09	29

is much larger than unity, in this case, about 6-7. After all the correction, the area of the fast sedimenting peak is ca. 70% as shown in Table 8. There are indications, at least in certain runs, that there is an elevated base line between the fast and the slow peak as well as in front of the fast peak. This phenomenon, which adds to the difficulty of correct area measurement, suggests some dissociation of the fast component during the run as well as the presence of a true heavy material. As will be shown later (Chapter VII), the active principle is a thin rod, ca. 50 Å in diameter and 3000-7000 Å in length. Both the electrophoresis and centrifugal patterns are consistent with such dimensions. In these circumstances neither analytical method can distinguish between a system containing a distribution of molecular sizes and a system containing molecules of a unique size. This situation is observed with samples of DNA, which give sharp centrifugal boundaries, but which can be shown, at very high dilution, to contain molecules of widely varying sedimentation constants (77).

The slow sedimenting component, with an S value 6-7 times lower than that of the active component, has not been removed by two or even three cycles of differential centrifugation as would be expected (Table 8 and Fig. 19). It is now clear that the slow component arises in part from the dissociation of RNA molecules from the nucleoprotein complex. There are several other factors which also tend

to reduce the efficiency of the differential centrifugation. Firstly, the failure of the fast sedimenting component to redissolve completely (Section B in this chapter). Secondly, the fast component tends to dissociate during the experiment. In later section it is shown that the slow component increases in concentration during storage. This process is accelerated as the ionic strength of the medium is reduced (cf. Chapter VII).

The best preparation of the active principle so far prepared is that obtained from the redissolved pellet after two cycles of centrifugation. It is estimated to be 75% pure. It exhibits a large viscosity change in response to ATP addition as is shown in Table 10. The active component has been named Myxomyosin, because of its origin and its similarity to actomyosin.

D. Summary of the Purification Procedure for Myxomyosin.

The procedure for the preparation of Myxomyosin is as follows:

1. 500 grams fresh weight of frozen plasmodia (stored at -10° C for less than two months) is crushed, and ground to a slurry at 0° C.
2. The ground plasmodia is extracted with 700 ml of 1.4 M KCl at 0° C for 1 hour. The extract is centrifuged in a Serval SS-1 centrifuge for 20 minutes at 16,000 x g. The supernatant is filtered through a

Table 9

Distribution of RNA in Fractions Obtained by Differential Centrifugation (100,000 x g 2.5 hours)

Fraction	Total Phosphorus	RNA Content Based on P Value	The Estimation of the Distribution of RNA
Original Solution (solution from pellet of one cycle centrifugation)	1.0%	10-11%	100%
Supernatant of the original solution after the second cycle centrifugation	1.4%	15%	45-40%
Redissolved Pellet Fraction of the original solution after the second cycle centrifugation	0.85%	9%	55-60%

Table 10

The Viscosity Data of Myxomyosin. (Products of Two Cycles Centrifugation)

Sample	Concentration (mg/ml)	Reduced Viscosity (cc/gm)	Reduced Viscosity Decreased by 3 μM/ml ATP
Fresh	5.5	330.5	113.5
Under storage at 0°C for one week	5.5	305.5	90.0

glass wool pad; the sedimented debris and particles discarded.

3. The extract is next fractionated with ammonium sulphate, the fraction which precipitates between 32 and 40 percent saturation (0° C and pH 7) is retained. The precipitate is usually frozen in the freezer at -10° C overnight at this stage.

4. The material is refractionated by ammonium sulphate between 25-36 percent saturation. The precipitate is washed with a solution 36% saturated in ammonium sulphate.

5. The washed precipitate is redissolved in sufficient 0.05 μ K-maleate buffer to make up a solution approximately 1% in protein. The solution is centrifuged at 80,000 x g (35,000 rpm) for 35 minutes in the Spinco preparative centrifuge. The pellet is discarded.

6. The supernatant from 5 is dialyzed against 0.05 μ maleate buffer for 6-7 hours.

7. The dialyzed supernatant is diluted to approximate concentration of 0.5% and centrifuged at 100,000 x g (40,000 rpm) for 2.5 hours. The supernatant is discarded.

8. The pellet is extracted with 0.05 μ maleate at 0° C with stirring for ten hours. The solution is then centrifuged at 30,000 rpm for 12 minutes to remove

the undissolved pellet. The supernatant is adjusted to contain ca. 0.5% of protein.

9. The solution is again centrifuged at 100,000 x g for 2.5 hours. The supernatant is discarded.
10. The pellet is extracted with 0.05 μ maleate at 0° C with stirring for eight hours. The solution is then dialyzed against 0.2 μ K-maleate for ten to twelve hours.
11. The dialyzed solution is centrifuged at 30,000 rpm for 12 minutes to remove undissolved particles. The final yellow solution contains 200-240 mg of highly purified myxomyosin.
12. The myxomyosin solution may be stored at 0° C and should be studied within 3-4 days.

E. Storage Behavior of the Purified Myxomyosin.

This problem has not been investigated in detail. The present culture methods for slime mold and the preparative procedure for myxomyosin both have such a limited productive capacities that serious storage problems never arise. A myxomyosin solution is usually studied and used up within 3-4 days. The preparation has been usually kept in a refrigerator at ca. 2° C until just before use.

Aliquots of the same preparation (the doubly cycled material) used for the electrophoretic and ultracentrifugal patterns of Figs. 18 and 19, and the viscosity data of Table 10, were stored at 0° C and at -10° C for one week.

The electrophoretic and ultracentrifugal patterns of these aliquots are given in Fig. 20 and Fig. 21, and a portion of the related viscosity data . One week storage at 0° C, lowers the viscosity and the ATP response of the preparation (Table 10) and increases the amount of the slowly sedimenting component. Some convection and anomalies in electrophoretic patterns also have developed. The ultracentrifugal and electrophoretic patterns of the aliquot frozen at -20° C for one week did not, on the other hand, show any differences from the original. The viscosity of the material under storage at -10° C has not been quantitatively studied. There are indications that the viscosity and the activity may be lower. The behavior of myxomyosin under storage at 0° C suggests a slow decomposition of the molecule under this condition.

Fig. 20. Electrophoretic patterns of myxomyosin stored for one week at two temperatures

(Migration proceeds from right to left)

Buffer: 0.2 μ K-maleate pH: 7.0

Current: 6 ma. Time: 10,000 seconds

At 0° C* At -10° C*

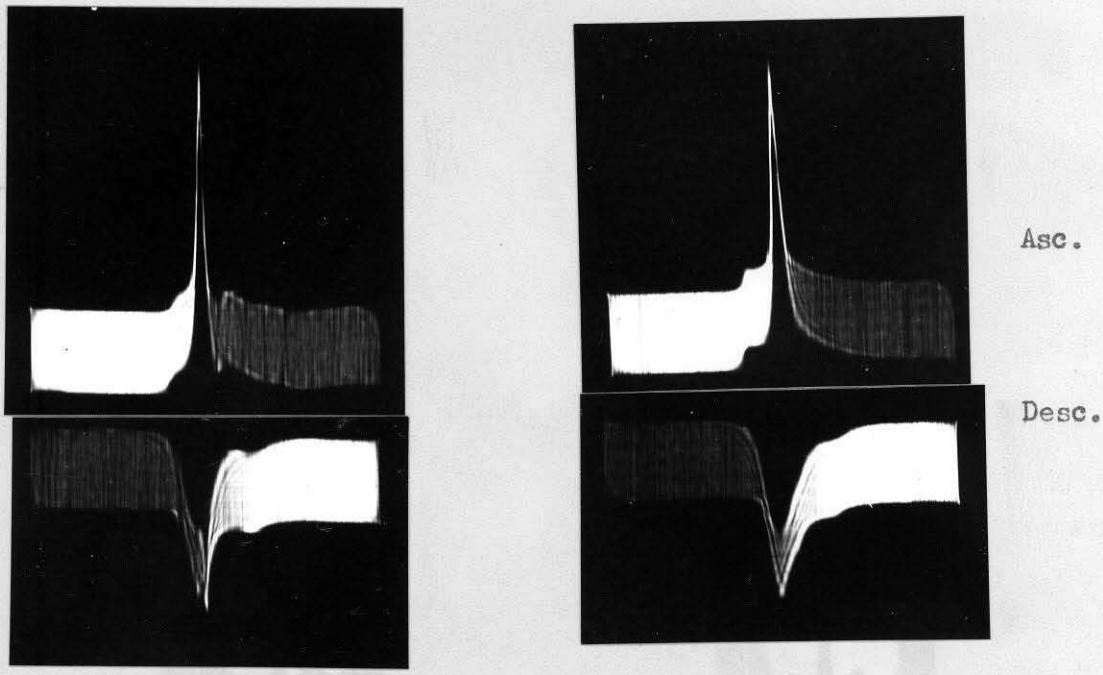

Asc.

Desc.

Concentration: 5.5 mg/ml

* Boundary A has left the visible part of the cell

Fig. 21. Ultracentrifuge patterns of myxomyosin stored for one week at two temperatures

(Sedimentation proceeds from right to left)

Buffer: 0.2 μ K-maleate pH: 7.0

Concentration: 5.5 mg/ml

At 0° C

At -10° C*

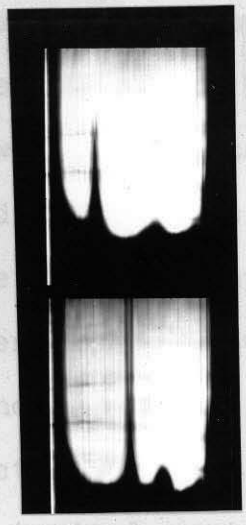

rotor speed (rps) 850 853

* rotor vibration

V. THE CHEMICAL NATURE OF MYXOMYOSIN

The ultraviolet absorption spectrum of myxomyosin in 0.01 M KCl at pH 6.3 is given in Fig. 22. For the reasons stated below, it appears that this absorption spectrum represents contributions of a protein moiety, ribonucleic acid, one or more yellow pigments and possibly some tightly bound maleate ions introduced during the preparative procedure.

Protein is the major constituent of myxomyosin as indicated in the data of Table 11 in which it is shown that the protein weight percent of a myxomyosin solution by the biuret method agrees substantially with that obtained by the TCA precipitation method. The discrepancies are consistent with the fact that the biuret measurement is based on the number of peptide bonds present, and, as will be shown below, approximately 10% of the precipitable mass is non-proteinaceous. The x-ray diffraction pattern of myxomyosin (Appendix I) is similar to a typical protein powder pattern and particularly resembles that of the keratin-epidermis-myosin type.

The presence of RNA in myxomyosin which was suspected from the UV spectrum, was confirmed by paper chromatography. The hydrolysis and chromatographic procedures employed are fully described in Chapter II-E. Four ultraviolet-absorbing

Fig. 22. Ultraviolet absorption spectrum of myxomyosin and the yellow pigment. See text for detail.

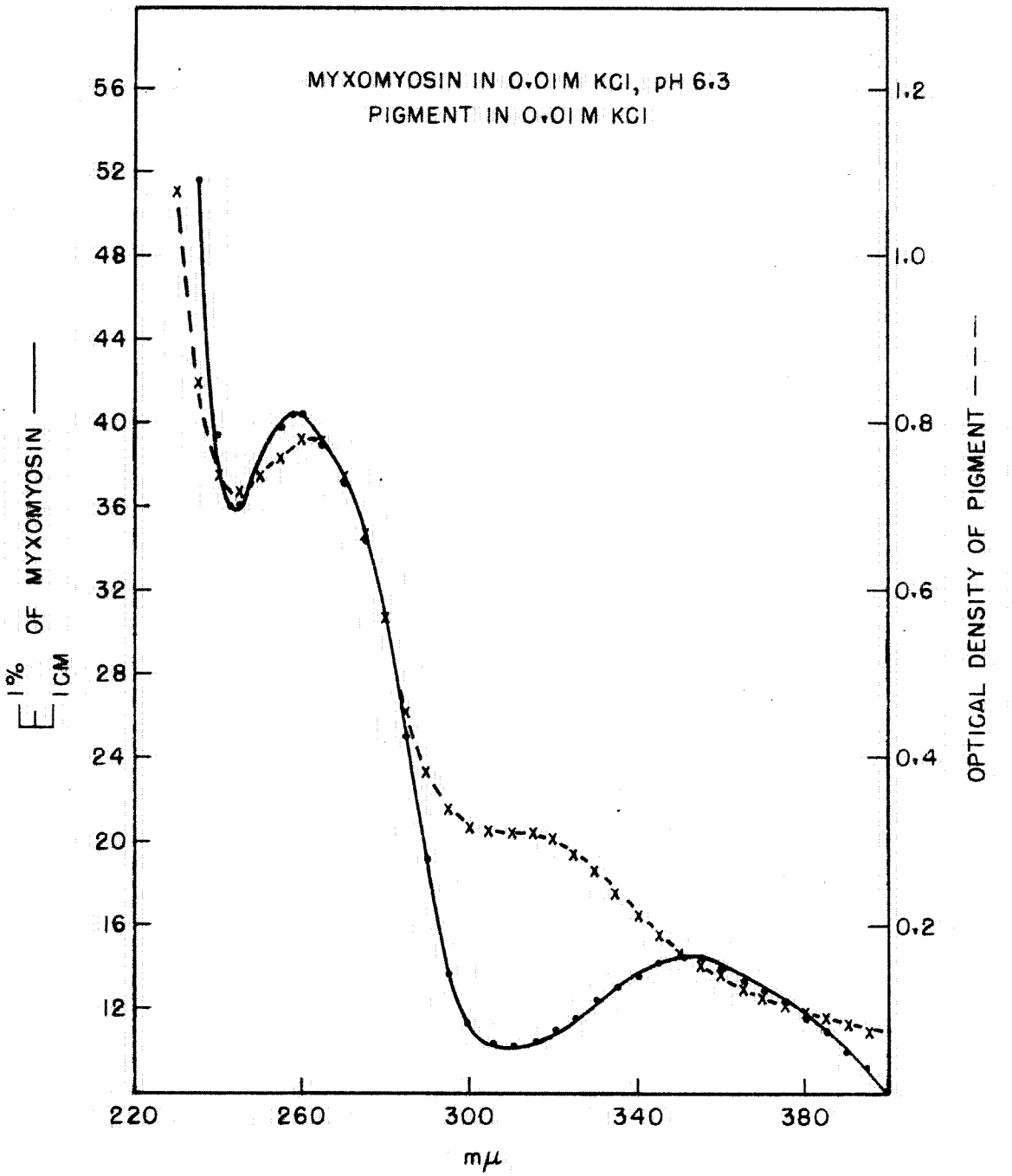
MYXOMYOSIN IN 0.01M KCl, pH 6.3
PIGMENT IN 0.01M KCl
$E^{1\%}_{1cm}$ OF MYXOMYOSIN ——
OPTICAL DENSITY OF PIGMENT – – –
56
52
48
44
40
36
32
28
24
20
16
12
1.2
1.0
0.8
0.6
0.4
0.2
220
260
300
340
380
mμ

Table 11

Comparison of the TCA Precipitation Method and the Biuret Method for the Determination of Protein Concentration of Myxomyosin Solutions

	Protein Concentration (weight per cent)	
	TCA Precipitation	Biuret Determination*
Samples		
1	1.04 ± .01	.96 ± .05
2	.94 ± .01	.84 ± .05
3	.77 ± .01	.60 ± .05

* Based on Bovine serum albumin color standard

spots are found on a myxomyosin hydrolysate. Based on their R_f values and on co-chromatography with similar hydrolysates of yeast RNA, these spots are identified as uracil, cytidine, adenine and guanine. If 8 and 270 are taken as the values of E (extinction coefficient of 1 cm 1% solution) for the protein and ribonucleic acid respectively, the nucleic acid content of myxomyosin may be computed from its extinction coefficient. This calculation, based on an extinction coefficient of 40, gives 13% as the nucleic acid content of myxomyosin. Since the yellow pigment also absorbs in the 260 region, this result may be too high. Calculated on a total phosphorus content of 0.8% (Chapter IV), 9% RNA is present. The fastest moving peak, A, in the electrophoretic pattern of myxomyosin, which moves with the mobility of free nucleic acid, has an area corresponding to a concentration of 3.5 - 5% RNA (Chapter IV). The value of 9% for the amount of RNA is tentatively adopted because there is less ambiguity in the estimation of RNA based on the phosphorus content than in the other estimations. It should be noted, however, that RNA content of myxomyosin may vary to some extent in different preparations, as has been reported for other cytoplasmic nucleoproteins (80). This aspect has not yet been examined systematically. It has, however, been noted that the area of the fast moving peak in the electrophoretic pattern varies in different preparations.

Myxomyosin solutions are always slightly yellowish and

are fluorescent. The yellow color cannot be removed from the protein by exhaustive dialysis, nor by extraction with benzene, ligroin, ether, or carbon tetrachloride. It also cannot be removed by the precipitation of the protein from solution with salt, TCA or by centrifugation. The yellow pigment, however, can be liberated substantially by precipitation of the protein with aqueous acetone, or by ammoniacal aqueous acetone (3% ammonia - 90% acetone) solution.

A myxomyosin solution freed from maleate ion by dialysis was extracted with ammoniacal acetone. All proteins were precipitated and removed. Both ammonia and acetone were then evaporated at 50° C with successive additions of small quantities of distilled water to prevent complete drying of the residue. Finally, the residue was taken up in 0.01 M KCl. The clear yellow solution gives a yellow fluorescence when irradiated at 360 mμ. The ultraviolet absorption spectrum possesses a minimum at 245 mμ, a maximum at 265 mμ, and a plateau at 300 to 320 mμ, as indicated in Fig. 22. Since neither the protein nor the nucleic acid absorb at 350 mμ, it seems reasonable to assume that the myxomyosin absorption maximum at 350 mμ is caused by one or more of these pigments. It would also appear that not all of the myxomyosin absorption at 260 mμ is due to RNA since the yellow compound also absorbs in this region. Whether one or several compounds are present in the yellow solution is not yet known, but it is unlikely to be seriously contaminated by nucleotides because of the mild treatment. The

pigment is probably not the same as that described by Seifriz and Zetzmann (78), since it does not change color from yellow to red with a pH change from 7 to 1 as reported by Seifriz. Filtrol, an activated clay, completely absorbs the yellow color and the fluorescence from a perchloric acid hydrolysate of myxomyosin. A large part of the yellow color and fluorescence is recovered by elution of the filtrol with ammoniacal acetone. When the hydrolysate is chromatogramed in an isopropanol-HCl system, most of the yellow color and the fluorescence stays at the origin although a portion travels diffusely. The chemical nature of this yellow pigment is unknown. Since the yellow pigment is not concentrated in myxomyosin but is also present in the other nonactive fractions, it is unlikely that this pigment plays any significant role in myxomyosin.

It should be noted that the absorption spectrum of myxomyosin is very similar to that of the cold acid extracts of Fraction I nucleoprotein of green leaves (79). This extract containing nucleic acids and yellowish-brown pigments also has an absorption maximum near 340 mμ.

It has been mentioned above that maleate ions, which absorb in the far violet region, might possibly be bound to myxomyosin and remain even after exhaustive dialysis. It is therefore, necessary to obtain the spectrum of maleate ion at a known concentration in order to determine the magnitude of any necessary correction. The optical density of

2×10^{-3} M maleate at 260 mμ is 0.2. Taking the molecular weight of myxomyosin as six millions, as reported later, it may be calculated that if one molecule of myxomyosin absorbs one million maleate ions, the contribution of maleate ion to the absorption of myxomyosin will be 0.5%. This calculation indicates that the contribution of maleate to the myxomyosin spectrum should be small, since it is unlikely from our general knowledge of ion binding that myxomyosin would bind so many maleate ions.

Conclusion: Myxomyosin is a nucleoprotein complex, containing approximately 9% RNA and one or several yellow and fluorescent pigments.

VI. THE KINETIC ASPECT OF ATP-MYXOMYOSIN INTERACTION

It was indicated in Chapter III that the active principle in the 30-40% SAS fraction changes in viscosity in response to ATP and that the ATP is hydrolyzed concurrently with these changes. A preliminary investigation of these reactions has been carried out with myxomyosin.

A. The ATPase Activity of Myxomyosin.

The fate of ATP during the enzymatic process is not known. The end product could be either AMP and pyrophosphate, or ADP and orthophosphate. By analogy with the muscle system, ATP is probably hydrolyzed to ADP and orthophosphate. The method for determination of orthophosphate described by Lowry and Lopez (Chapter II) is claimed to be a very mild one which does not hydrolyze labile phosphate ester such as creatine-phosphate. Therefore, the analytical method employed should not hydrolyze ADP and pyrophosphate. Thus, the orthophosphate measured is that liberated by the enzymatic activity of myxomyosin.

Fig. 23 shows the activity of myxomyosin as an ATPase under conditions of substrate saturation. These data, together with knowledge of the molecular weight of myxomyosin (ca. 6×10^6 reported in Chapter VII) and the purity of the preparation, enable the turnover rate of the enzyme to be calculated in terms of moles of substrate hydrolyzed per

Fig. 23. The dephosphorylation of ATP by myxomyosin in 0.2 μ K-maleate buffer, pH 7 and at 24.45° C.

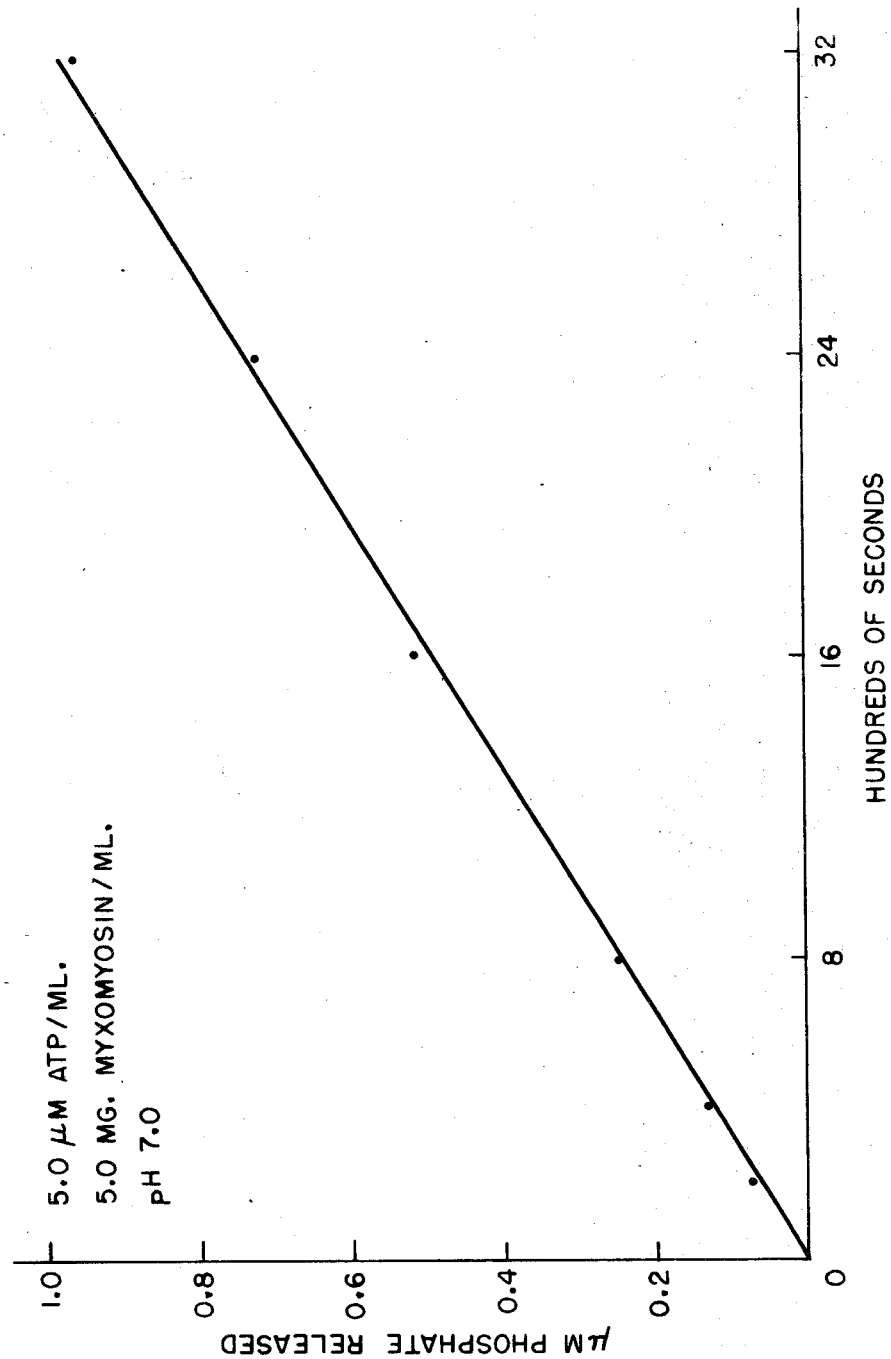
5.0 μM ATP/ML.
5.0 MG. MYXOMYOSIN/ML.
pH 7.0
μM PHOSPHATE RELEASED
1.0
0.8
0.6
0.4
0.2
0
8
16
24
32
HUNDREDS OF SECONDS

mole of enzyme per minute. This turnover rate of myxomyosin at 24.5° C and pH 7 is about 30. This turnover number may be compared with 6000 for actomyosin* and with 100 to 300,000 (81) for enzymatic reactions in general. The low ATPase activity of myxomyosin raises the question that the activity measured may be caused by a small ATPase contaminant and is not due to the myxomyosin moiety. No attempt has been made to resolve this question here. However, since myxomyosin changes its physical state reversibly in reponse to ATP, the ATPase must be intimately related to the system. It should be mentioned that the same question exists in the case of actomyosin.

B. The Change of Physical State of Myxomyosin Following Interaction with ATP.

The changes in viscosity of myxomyosin as a function of ATP concentration is plotted in Fig. 24 and Fig. 25. These data were obtained with a single preparation of myxomyosin, at a concentration of 0.5%, and with a shear gradient of 600 sec^{-1}. The ATP employed was estimated from free inorganic phosphate measurements to be 90% pure on molar basis. Data are expressed as reduced viscosity so as to compensate, to a large extent, for the effects of

---

* Calculation of the ATP turnover number is based on the data of Oullet, et al. (82). (Maximum reaction velocity 0.5 uM $liter^{-1}$ sec^{-1} for 0.1 gm $liter^{-1}$ of enzyme; molecular weight of enzyme, 2 x 10^7).

Fig. 24. Changes in viscosity of myxomyosin as a function of ATP concentration. Concentration of added ATP is as indicated adjacent to curves.

Portion of curve shown in detail in Fig. 25 (5.9 μ M ATP/ml) has been superimposed for reference. Myxomyosin concentration: 5.0 mg/ml. Shear gradient: 600 sec^{-1}.

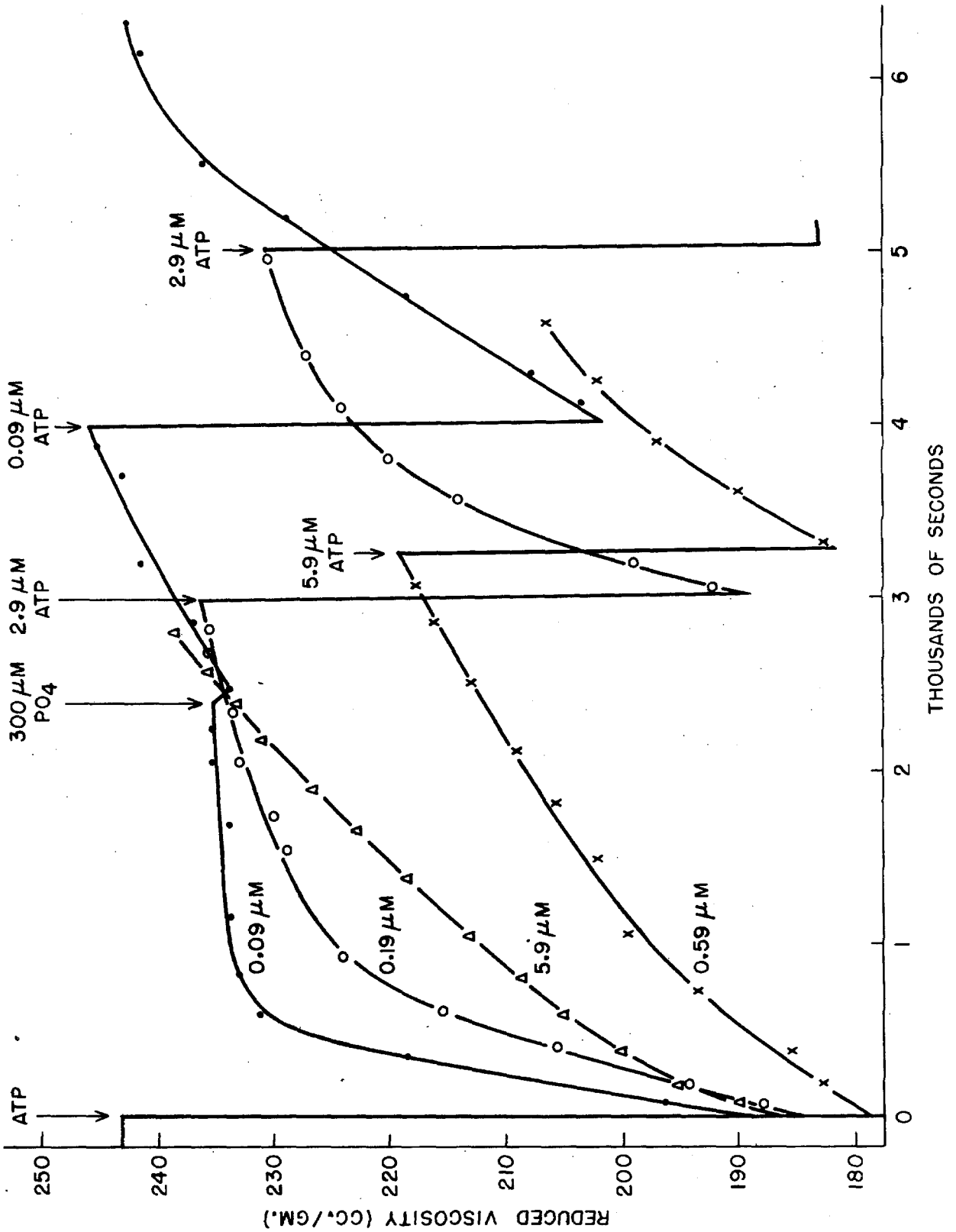
REDUCED VISCOSITY (CC./GM.)
250
240
230
220
210
200
190
180
THOUSANDS OF SECONDS
0
1
2
3
4
5
6
ATP
300 μM PO4
2.9 μM ATP
0.09 μM ATP
5.9 μM ATP
2.9 μM ATP
0.09 μM
0.19 μM
5.9 μM
0.59 μM

Fig. 25. Changes in viscosity of myxomyosin in large excess of ATP (5.9 μM/ml). Myxomyosin concentration: 5.0 mg/ml. Shear gradient: 600 sec^{-1}.

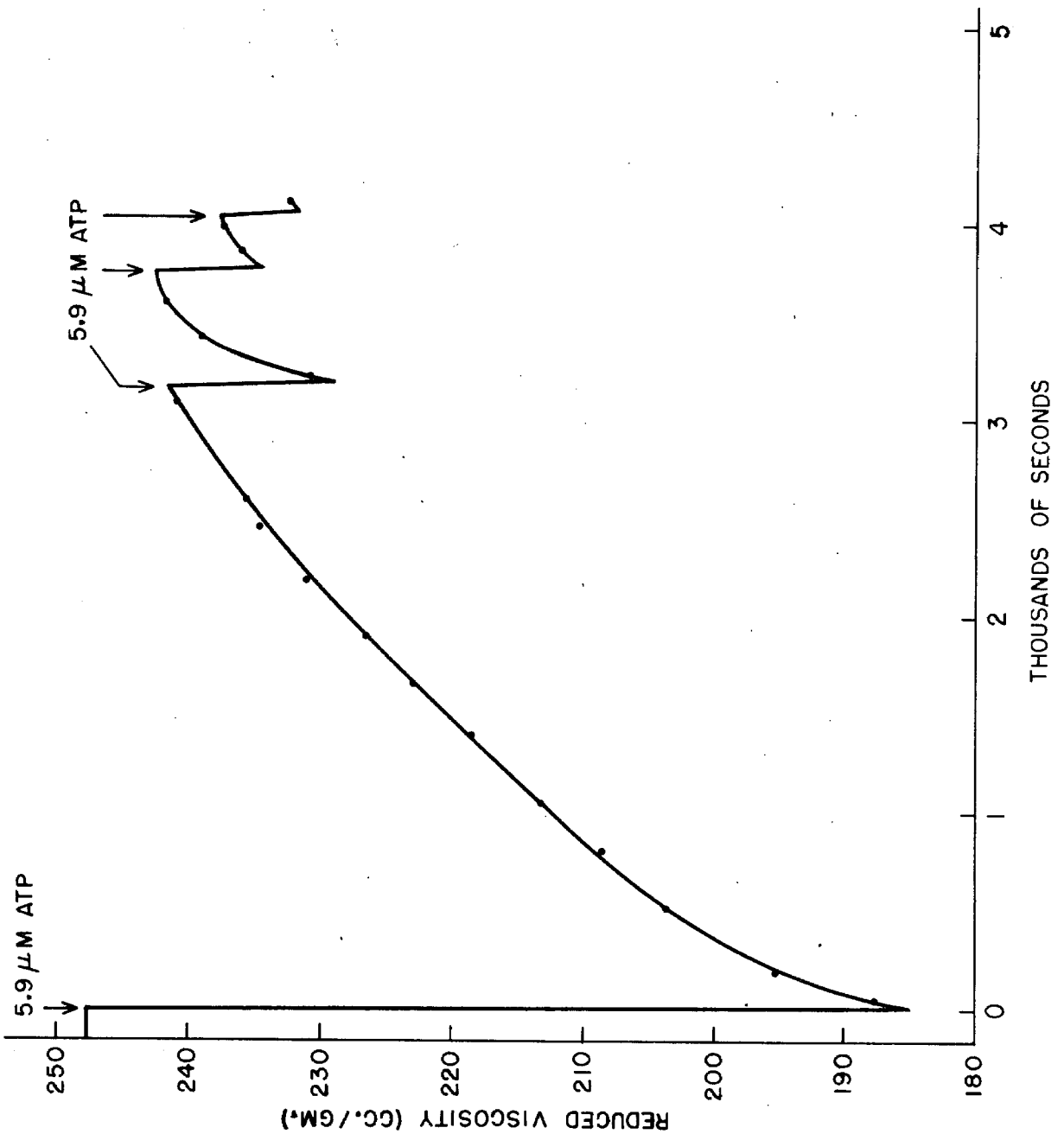
5.9 μM ATP
5.9 μM ATP
REDUCED VISCOSITY (CC./GM.)
250
240
230
220
210
200
190
180
0
1
2
3
4
5
THOUSANDS OF SECONDS

dilution due to addition of reagents into the system.

The results indicate that the same decrease in viscosity can be brought about by 0.09 μM, 0.19 μM, 0.59 μM or 5.9 μM per ml of ATP. This means that at a concentration of 0.09 μM/ml of ATP, the system is already ATP saturated so far as the reaction which results in a decrease in viscosity is concerned. It can be calculated, from data concerning the purity of the preparation and the molecular weight of myxomyosin, that less than 130 to 140 ATP molecules are required to saturate one molecule of myxomyosin in solution. This amount of ATP is about 1.5% of the total weight of myxomyosin in solution. However, as the concentration of ATP added increases, the rate of recovery of viscosity decreases. The shape of the curves in Fig. 24, describing the changes of viscosity, is similar to those observed for the actomyosin-ATP interaction as measured by light scattering (83) or viscosity (84, 85). Subsequent addition of 2.9 - 5.9 μM/ml ATP to the recovered solution, brought the viscosity level down again to the low level evoked by first addition of ATP.

The addition of a large excess of ATP, 5.9 μM/ml, corresponding to 8400-8500 ATP molecules per molecule of myxomyosin in solution, alters the relation between ATP concentration and the rate of viscosity recovery (Fig. 25). Recovery of viscosity of such a solution is linear with

time even after 2800 seconds in contrast to the hyperbolic recovery curves of the solution containing many times less ATP. Furthermore the rate of recovery is larger and to a higher level. The system so obtained is refractory to ATP. Addition of ATP in large quantities after 3000 seconds has little effect on the viscosity of this system. The refractory behavior of myxomyosin during recovery in the presence of high concentration of ATP is not observed in the case of myxomyosin solutions reacted with 10, 30, or 60 times less ATP. That myxomyosin should exhibit a refractory period during recovery of viscosity after addition of ATP, might be detected from enzymatic studies. Following addition of 0.9 μM/ml of ATP to the solution, there is still at least 4 μM/ml of ATP left in the solution after 3000 seconds. If the viscosity of the solution can recover and rise in the presence of 4 μM/ml of ATP, further addition of ATP to the system should have no effect. This is found to be the case.

Two significant deductions can now be made.

First, the rate of ATP destruction must be close to the rate of formation of orthophosphate as measured. This is shown by the following arguments. If the bulk of the ATP were hydrolyzed into AMP and pyrophosphate at the usual rate for this reaction, and if the orthophosphate found is the result of the activity of contaminating ATPase, then at the end of 3000 seconds, there should be no ATP

left in solution. Further addition of ATP should produce a second effect. Since further addition of ATP at 3000 seconds does not have any effect, the system must still be saturated with ATP. ATP must, therefore, be slowly transformed to ADP at the approximate rate observed for the liberation of orthophosphate

Second, the existence of a new state for myxomyosin is indicated. This state is one which has a high viscosity but refractory to ATP. This refractory state cannot be explained on the basis of competition for multiple-points attachment in the presence of excess substrate. If this were the case, one would not expect to get the observed initial decrease in viscosity in the presence of a large excess of substrate.

Somewhat similar results have been observed with actomyosin. For example, Watanabe, et al. (86) has reported that beyond a certain optimal ATP concentration, there is a strong substrate inhibition effect in the ATPase activity. Inhibition of ATPase activity by ADP has also been reported (87). Intermediate complexes of suitable half life such as actomyosin-P (88) or actomyosin-ADP (87) which are incapable of reacting with ATP have been postulated. Based on our observation and by analogy with these proposals for actomyosin, the following scheme for the reaction between ATP and Myxomyosin is proposed.

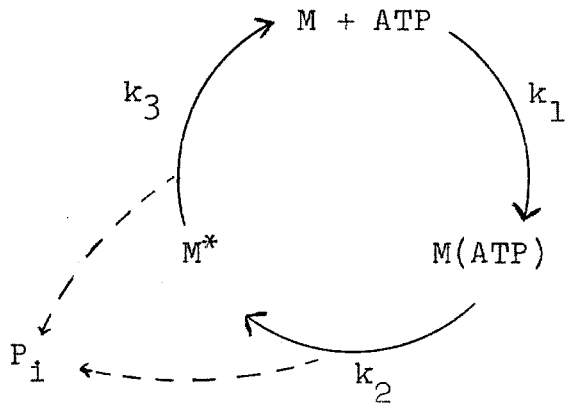

Tentative scheme of ATP and Myxomyosin interaction

M represents myxomyosin as it exists in the initial high viscosity state. M(ATP) represents the low viscosity state of the myxomyosin-ATP complex. The rate, k_1, of the transformation between the two states is very large as indicated by the rapid decrease of viscosity after introduction of ATP into the system. Less than 130 molecules of ATP per molecule of myxomyosin is sufficient to convert all the available myxomyosin from state M to state M(ATP). M(ATP) is next transformed to state M^* at a moderate rate k_2. M^* is the high viscosity state which is refractory to ATP. Whether M^* consists of M-P, or M-ADP, or whether it represents a particular configuration incapable of reacting with ATP, cannot be determined from the data at hand. M^* decays to M at a rate k_3 to complete the

cycle. The rate constant k_3 of this transformation is presumably much smaller than k_1 or k_2. This must be so if myxomyosin is accumulated in state M^* in the presence of excess ATP. Orthophosphate is liberated either in the transformation of M(ATP) to M^* or of M^* to M. In excess ATP, the rate of cycling will be constant. Therefore, the rate of liberation of orthophosphate should be constant. This is found experimentally (Fig. 23). Addition of a large amount of orthophosphate has no effect on the viscosity (Fig. 24). No quantitative treatment of the kinetics of viscosity recovery can be given here because of the scantiness of the present data. Thus, by varying the magnitude of rate constants ($k_1 \gg k_2 > k_3$) and assuming the viscosity level of M, M(ATP) and M^* (M^* is required to have higher viscosity than M), the viscosity behavior of the myxomyosin system in response to various concentration of ATP may be explained.

The effect of shear gradient on the viscosity recovery has also been studied to some extent. The apparent viscosity and the decrease in viscosity caused by ATP, but not the rate of recovery, is strongly affected by shear gradient (Fig. 26). Shear gradient might be expected to influence the rate of recovery of concentrated (2%), and viscous (relative viscosity over 3) solutions. At low protein concentrations (0.3%), however, no effect of the shear gradient on the rate of recovery has been detected (Fig. 26).

Fig. 26. The effect of shear gradient (G) on the viscosity of myxomyosin solution. Myxomyosin concentration: 3 mg/ml.

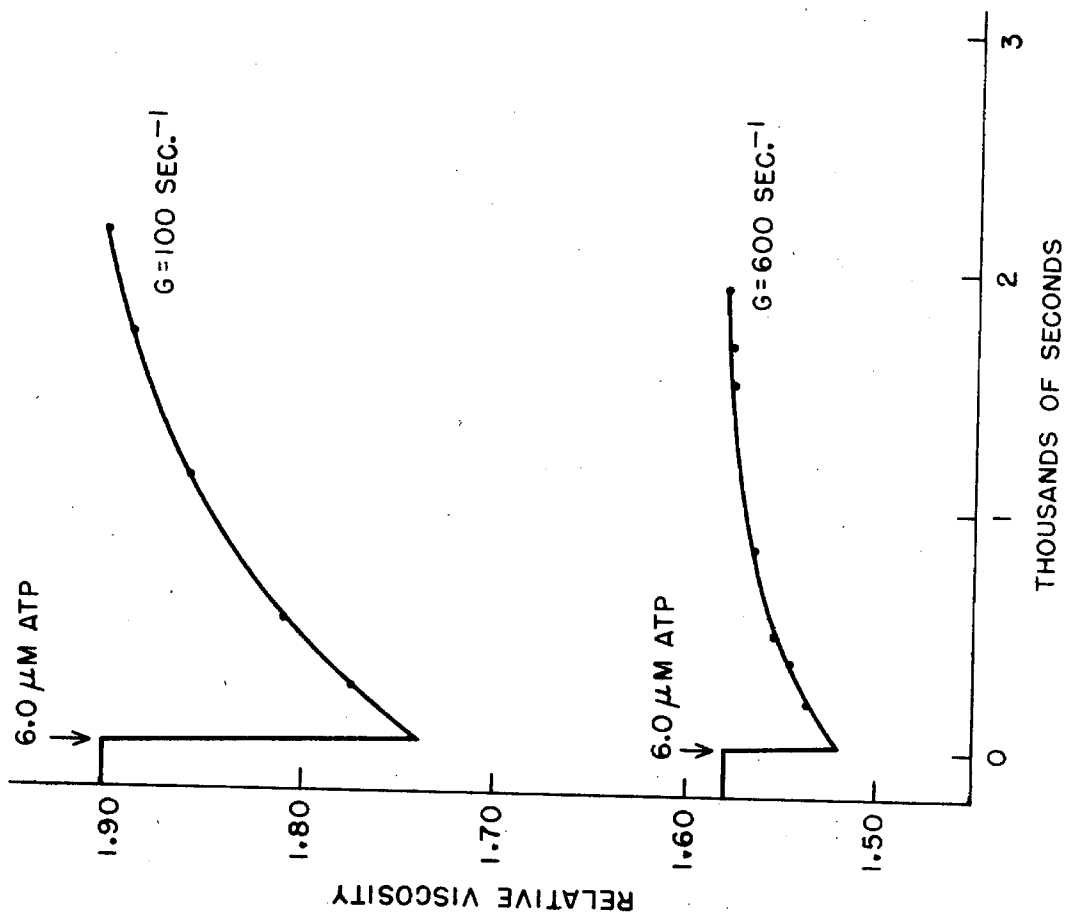
6.0 μM ATP
G=100 SEC.⁻¹
6.0 μM ATP
G=600 SEC.⁻¹
RELATIVE VISCOSITY
1.90
1.80
1.70
1.60
1.50
0
1
2
3
THOUSANDS OF SECONDS

It may be noted that the 2% protein solution of 30-40% SAS fraction (before purification by differential centrifugation) can be held for hours in the low viscosity state with 3 μM/ml of ATP in contrast to the above described behavior of the purer material. The reason for this is not yet known. It is possible that the protein-ATP ratios employed in these experiments with the 30-40% SAS preparations were those which give rise to a low recovery rate. On the other hand, other chemical factors may have been operative. Addition of large excess of ATP to 30-40% SAS fraction has not been investigated.

C. The Action of RNAase on Myxomyosin.

Since RNA has been found to complex with the protein in solution, the effect of RNAase on the ATP response of myxomyosin was studied. RNAase was introduced into a 0.5% myxomyosin solution to a final concentration of 0.03%. This myxomyosin solution was an aliquot of that used for activity measurements described in the foregoing section. All solutions were treated identically and their behavior can be directly compared. RNAase is a small symmetrical molecule. The amount added is 6% by weight of the myxomyosin. Therefore, the contribution of the RNAase to the reduced viscosity will be small. If RNA is depolymerized to small polynucleotides by the enzyme, the reduced viscosity should be lowered to some extent. The result found is, however, quite different, as shown in Fig. 27. Curve B represents the

Fig. 27. The effect of RNAase (0.25 mg/ml) on the viscosity of Myxomyosin. Myxomyosin concentration: 5 mg/ml. Shear gradient: 600 sec^{-1}.

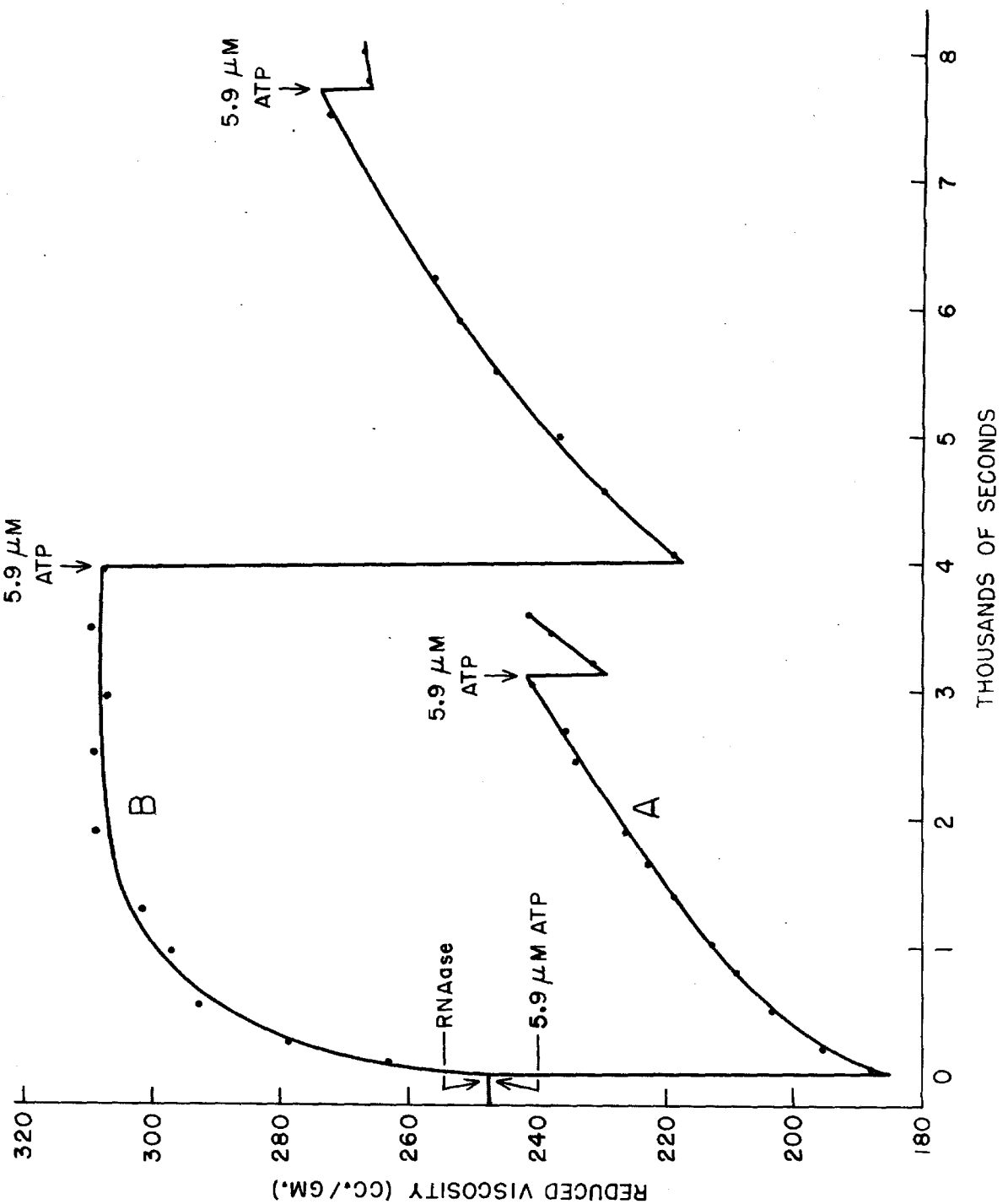
REDUCED VISCOSITY (CC./GM.)
320
300
280
260
240
220
200
180
0
1
2
3
4
5
6
7
8
THOUSANDS OF SECONDS
5.9 μM ATP
5.9 μM ATP
5.9 μM ATP
5.9 μM ATP
RNAase
5.9 μM ATP
A
B

RNAase treated solution. The reduced viscosity of the solution rose very rapidly after addition of RNAase, increasing ca. 30% in half an hour. The viscosity increase generated by the action of RNAase may be reversed by ATP as indicated by the addition of 5.9 μM/ml ATP and as in the case of the untreated aliquot (Fig. 27, curve A), a refractory state is found in the presence of this large excess of ATP.

There are several plausible explanations for the effect of RNAase. First, RNAase may non-specifically aggregate with myxomyosin and increase the asymmetry or hydration of the myxomyosin molecules in the process. This would be an artifact. This hypothesis would lead to the further conclusion that the nonspecific RNA-myxomyosin aggregate is broken up by ATP and that the residues reversibly aggregate even in the presence of ATP. The highly specific ATP response does not, however, seem likely to be involved in a non-specific aggregation process. In addition, the RNAase and the myxomyosin are both negatively charged at the pH of these experiments and hence could hardly be expected to aggregate strongly.

Secondly, the myxomyosin may be unfolded when RNA is removed. This explanation is not convincing, because one would have to postulate that ATP can refold the myxomyosin polypeptide chains, which reversibly unfolds itself again and becomes refractory to ATP.

As proposed in Chapter VII, the effect of ATP on the physical state of myxomyosin can be best explained on the basis that ATP dissociates asymmetric or hydrated aggregates to the monomer. The monomer is about 4000 Å in length and 50 Å in diameter with a molecular weight of roughly 6 millions. The effect of RNA can be reasonably explained on the basis that the nucleic acid keeps the protein moiety from aggregation by forming a complex which will be strongly negatively charged and therefore tend to aggregate to a lesser extent than the protein alone. When RNA is removed, the myxomyosin can aggregate to a large extent. This aggregation can be, however, broken by ATP. The explanation assumes that the mechanism whereby the viscosity level generated by RNAase is decreased by ATP is the same mechanism whereby the viscosity is decreased by ATP in the absence of RNAase. Such a similarity is indeed indicated from the experiment. Nucleic acid, therefore, acts in a manner essentially similar to that of ATP in keeping the myxomyosin from aggregation. RNA is, however, less effective and is not destroyed by myxomyosin. It is tentatively concluded that nucleic acid may not be an indispensable part of the system, but its presence in complex form with the protein, does exert an influence on the physical state of myxomyosin in solution.

Conclusion: The ATPase activity of myxomyosin has been found to be about 200 times less than that of actomyosin, with a turnover rate of 30. Approximately 130 molecules of

ATP per molecule of myxomyosin are enough to evoke the maximum effect of ATP on the viscosity of myxomyosin solution in these experiments. Higher concentrations of ATP decrease the rate of recovery, and in very large excess of ATP, upon recovery, a refractory state of high viscosity is found. RNAase increases the reduced viscosity of myxomyosin to ca. 30% within 30 minutes and this increase in viscosity is reversibly decreased by ATP. It is tentatively concluded that myxomyosin aggregates more strongly when RNA is removed from the complex. This aggregation in the absence of RNA can be reversed by ATP as it is in the presence of RNA.

VII. CHARACTERIZATION OF THE PHYSICAL-CHEMICAL STATE OF MYXOMYOSIN: CHANGES INDUCED IN MYXOMYOSIN BY ADDITION OF ATP OR REDUCTION OF THE IONIC STRENGTH OF THE MEDIUM

The molecular weight and dimensions of the myxomyosin molecule have been studied by a variety of physical-chemical methods. The effects of ATP and of changes in ionic strength of the medium on these measurements have also been observed.

A. Viscosity.

The effect of shear gradient on viscosity and the ATP response of myxomyosin have been illustrated in Fig. 26 of the previous chapter. In order to obtain information concerning the dimensions of the myxomyosin molecules, viscosity measurements were made at a series of shear gradients and extrapolated to zero gradient as shown in Fig. 28 and Fig. 29. Some uncertainty is introduced through this operation because of the non-linear character of the extrapolation, but this uncertainty may be minimized by the use of dilute solutions. A plot of reduced viscosity vs. concentration can be made to obtain the intrinsic viscosity of randomly oriented molecules in solution.

The relative viscosity of the more concentrated myxomyosin solutions plotted as a function of shear gradient in

Fig. 28. The relative viscosity of concentrated myxomyosin solutions (0.2 to 0.8% as indicated at the end of each curve) vs. shear gradient.

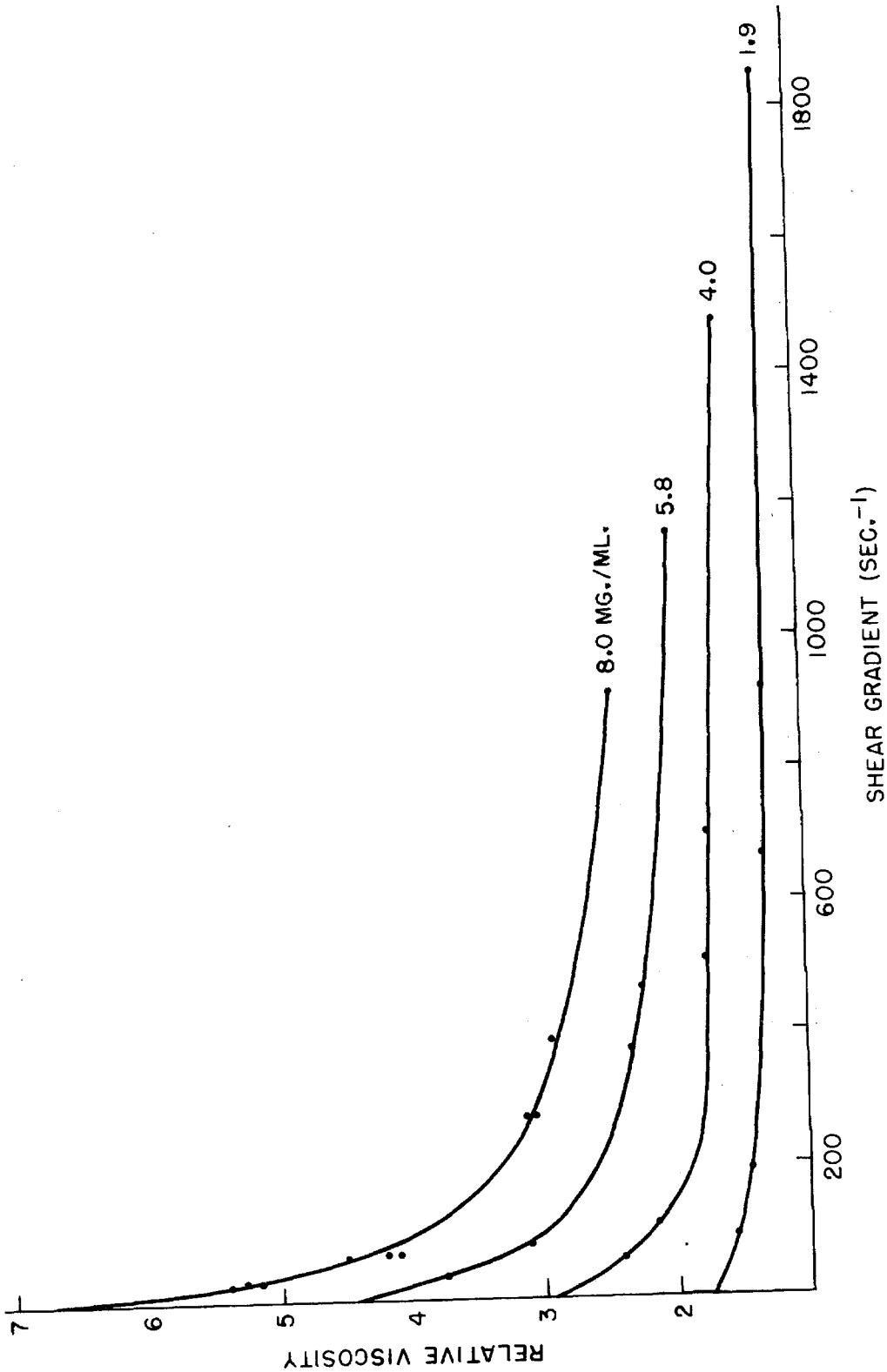
8.0 MG./ML.
5.8
4.0
1.9
RELATIVE VISCOSITY
SHEAR GRADIENT (SEC.$^{-1}$)
7
6
5
4
3
2
200
600
1000
1400
1800

Fig. 29. The relative viscosity of dilute myxomyosin solutions (0.1 to 0.3% as indicated at the end of each curve) vs. shear gradient.

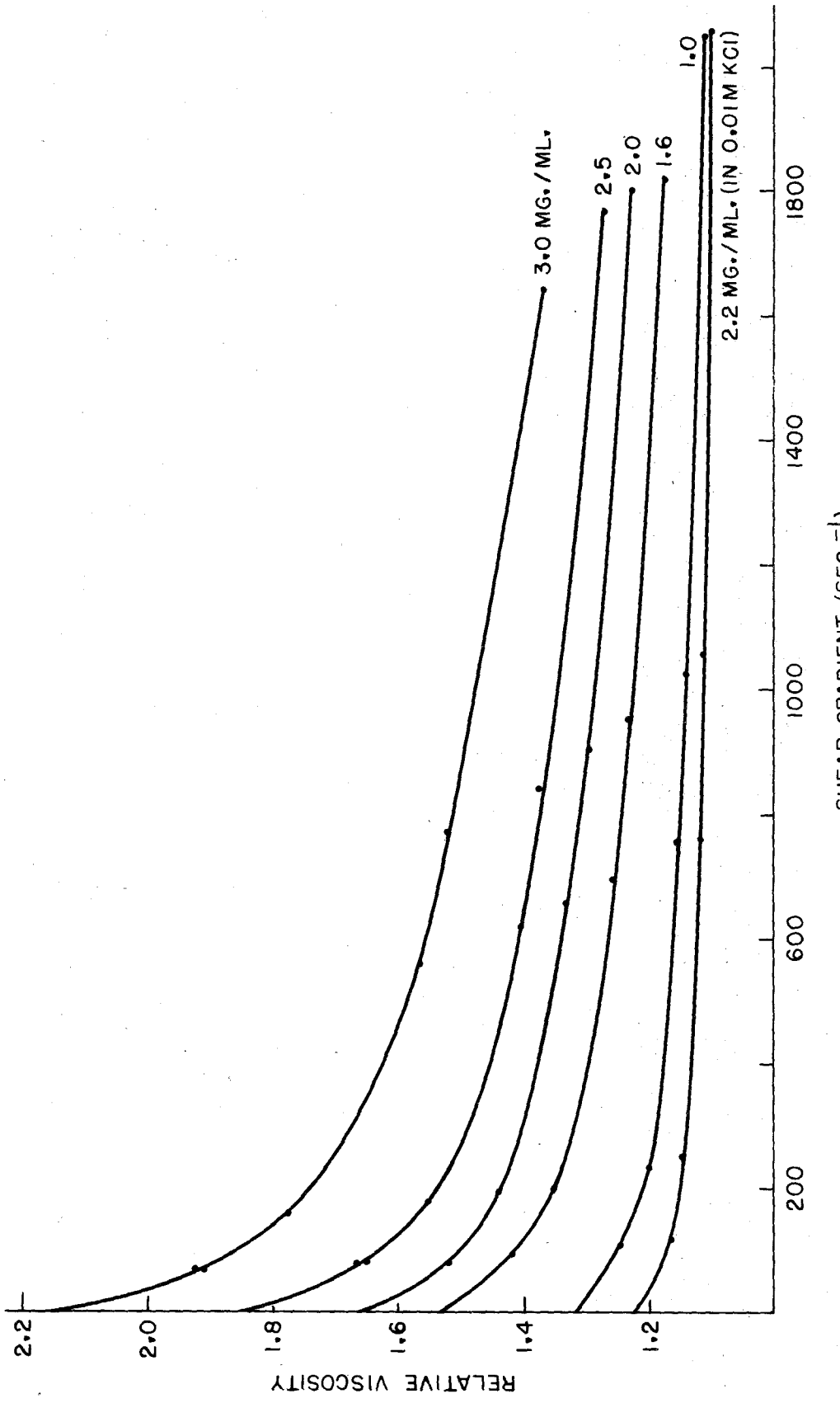
RELATIVE VISCOSITY
2.2
2.0
1.8
1.6
1.4
1.2
200
600
1000
1400
1800
SHEAR GRADIENT (SEC.$^{-1}$)
3.0 MG./ML.
2.5
2.0
1.6
1.0
2.2 MG./ML. (IN 0.01M KCl)

Fig. 28. From the information of Fig. 28, the upper plot in Fig. 30 has been constructed. At zero gradient, an intrinsic viscosity of 300 cc/gm is obtained. Certain anomalies in the viscosity, such as work hardening and work softening, have been noted. For example, the spread of points on the 0.8% concentration curve at 50 sec^{-1} gradient in Fig. 28, is due to work hardening. These anomalies disappear when solutions less concentrated than 0.3% are investigated.

In Fig. 29 relative viscosity is plotted as a function of shear gradient for dilute solutions (0.1 - 0.3%). The extrapolations of Fig. 29 are fairly reliable, because of the small slopes of these curves. The lowest curve of Fig. 29 shows that if myxomyosin is dialyzed against 0.01 M KCl rather than 0.2 M neutral buffer, the viscosity is considerably reduced and is independent of shear gradient. Addition of KCl to a final concentration of 0.2 to 0.5 M and incubation at 0^{o} C or at room temperature for two hours does not reverse the effect of low ionic strength treatment on the viscosity.

The study of the effect of ATP on the viscosity at zero shear gradient is difficult, because the effect changes with time (Chapter VI). A set of measurements were made, however, at low shear gradients within 300 seconds after addition of 5.0 μM ATP/ml. During this 300 second interval, the recovery is expected to be less than 10% Extrapolation to zero gradient of the data obtained at two shear gradients was carried

Fig. 30. The reduced viscosity of myxomyosin solutions vs. concentration. The shear gradients are indicated at the end of each curve.

Upper plot: concentrated myxomyosin solutions (0.2 to 0.8%).

Lower plot: dilute myxomyosin solutions (0.1 to 0.3%) with and without ATP. See text for detail.

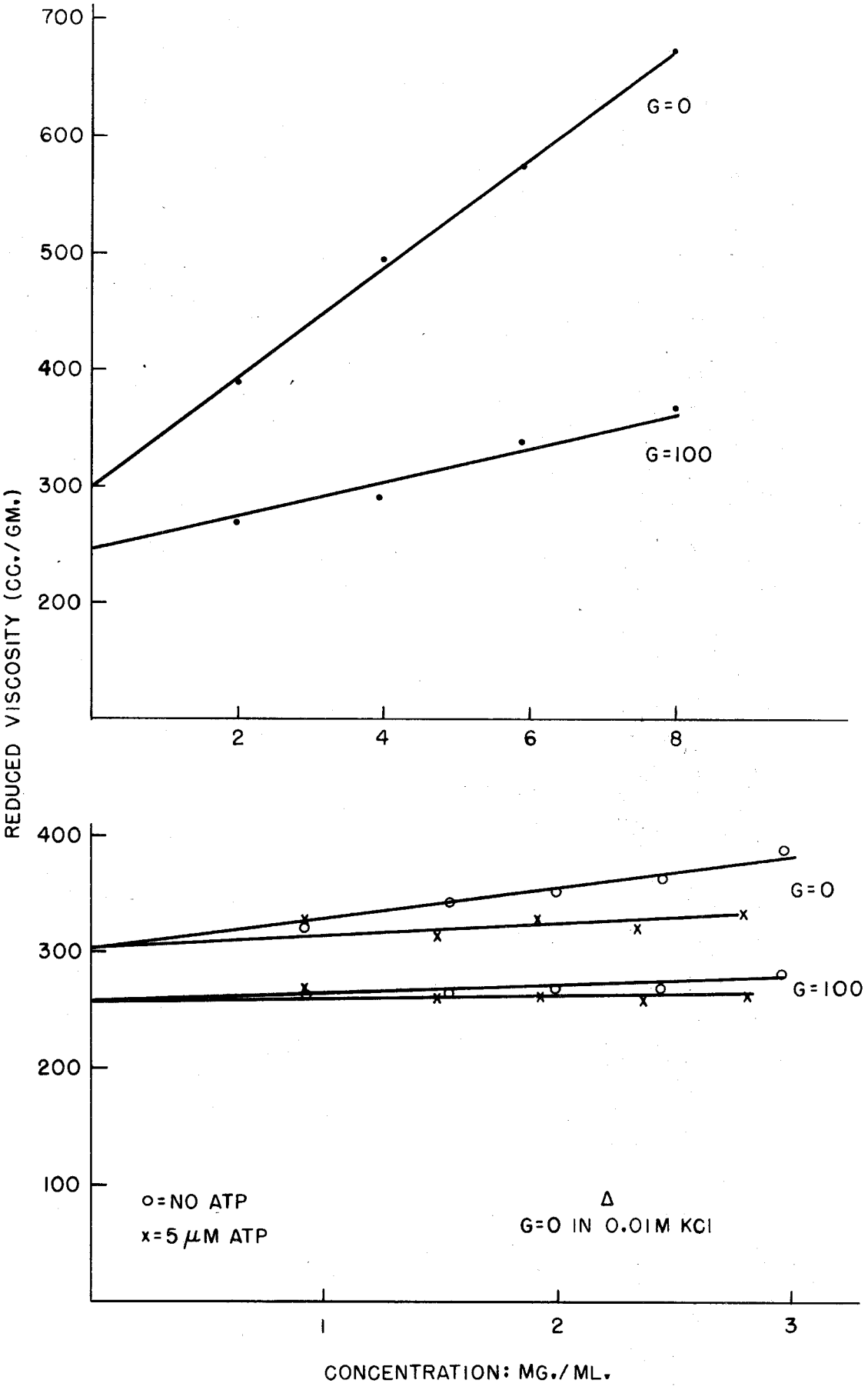
700
600
500
400
300
200
G=0
G=100
2
4
6
8
REDUCED VISCOSITY (CC./GM.)
400
300
200
100
G=0
G=100
o=NO ATP
x=5 μM ATP
Δ
G=0 IN 0.01M KCl
1
2
3
CONCENTRATION: MG./ML.

out, bearing in mind the slopes of the curves obtained in the absence of ATP (Fig. 31). The lower plot of Fig. 30 is constructed from data obtained by interpolation to 100 sec^{-1} or extrapolation to 0 sec^{-1} of the results presented in Fig. 29 and Fig. 31. It is apparent that at 100 sec^{-1} and at these low concentrations there is substantially no effect of ATP on the viscosity. At zero gradient, on the other hand, ATP significantly reduces the viscosity. This effect disappears gradually with increasing dilution. Thus ATP reduces the slope of the line, but does not change the intercept. This intercept again gives an intrinsic viscosity value of 300 cc/gm. The uncertainty of the intercept is estimated to be $\pm$ 15 cc/gm. The reduced viscosity of myxomyosin at one concentration and in 0.01 M KCl is also given in Fig. 29. The single point indicates an intrinsic viscosity not higher than 85 cc/gm.

The presence of slowly sedimenting impurities, estimated to be 25% by weight, (Chapter IV), introduces an error in the above evaluation of the intrinsic viscosity of myxomyosin. To correct this error, the viscosity of the supernatant solution from the first cycle centrifugation was measured at 600 sec^{-1} gradient (Table 12). The reduced viscosity of this solution is independent of concentration and therefore may be assumed to be independent of shear gradient. A value of 63 cc/gm for the intrinsic viscosity of the impurities has been adopted. The appro-

Fig. 31. The relative viscosity of myxomyosin solutions with 5 μM/ml ATP vs. shear gradient. Measurements were obtained within 300 seconds after addition of ATP. Protein concentrations are indicated at the end of each curve.

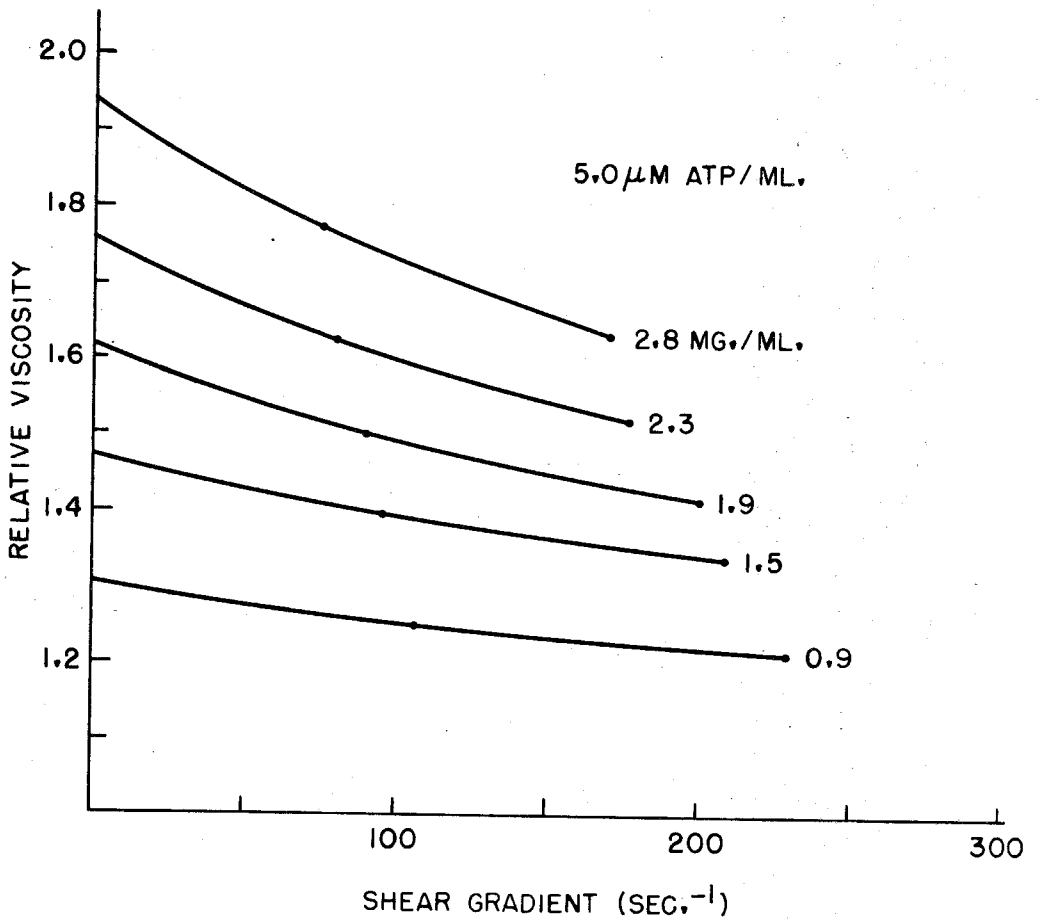
2.0
1.8
1.6
1.4
1.2
RELATIVE VISCOSITY
5.0μM ATP/ML.
2.8 MG./ML.
2.3
1.9
1.5
0.9
100
200
300
SHEAR GRADIENT (SEC.-1)

Table 12

The Reduced Viscosities of the Supernatant Solutions from the First Cycle Centrifugation Measured at Shear Gradient 600 sec^{-1}

Concentration (mg/ml)	Reduced viscosity (cc/gm)
6.5	64.2
4.5	63.8
3.0	63.6
1.5	63.5

priate calculations are made with the equation of Chapter II, p. 35. The corrected intrinsic viscosity of myxomyosin is found to be 380 cc/gm. With the partial specific volume (0.72) determined in this work, the viscosity increment of the unhydrated protein is 530. If the protein is assumed to be 25% hydrated, the viscosity increment of the hydrated protein is 395. From the table given by Mehl, Oncley and Simha (65) which is based on the rigid prolate ellipsoid model, a value 80 is obtained for the axial ratio of myxomyosin. The total uncertainty in the viscosity increment, compounded from uncertainties in the extrapolation of data, the errors in partial specific volume, and the purity of the preparation is estimated to be $\pm$ 25. This corresponds to a range of axial ratios of 84-76. It should be noted that the range of error in concluding that ATP does not affect the axis ratio at infinite dilution is smaller, since a single preparation was involved. For these experiments, it is estimated that a change in axial ratio outside of the range of 82-78 would have been detected.

Perrin's equation (p.34) relating frictional coefficient and axial ratio gives a value of 3.63 for the frictional coefficient of a prolate ellipsoid with an axial ratio of 80. The hydration (assumed to be 25%) will contribute another f/f_o factor of 1.10 according to the table of Oncley (89). Therefore, the total frictional coefficient, f/f_o, of myxomyosin is 4.0.

B. Flow Birefringence.

Measurement of the extinction angle, χ , of myxomyosin were carried out to obtain information about the length and the shape of the molecule. In Fig. 32, χ is plotted as a function of the shear gradient, G, for various concentrations of myxomyosin. Table 13 gives the calculated rotary diffusion, Θ, and the apparent length of the molecule based on the tabulated χ values and corresponding shear gradients. An axial ratio of 80, a relative viscosity of the medium of 1.02, and the experimental temperature 25° C were employed in the calculations involving the equation of Chapter II, p. 28. The results indicate that the length of myxomyosin varies from 5,800-10,000 Å, depending on the shear gradient employed for the measurement. The reproducibility among three separate preparations is in the range of 5%, or 300-500 Å.

The length of myxomyosin in 0.01 M KCl was found to be approximately 4000 Å, substantially shorter than that of myxomyosin in 0.2 μ (Table 13). The cross of isocline is diffuse and the birefringence is considerably weakened in these preparations.

In taking the birefringence measurement at various gradients of 50-1500 sec^{-1}, the solution suffers a certain amount of shearing action. When such a solution is measured a second time, the χ was found to have increased 0.5° to 1.0°. This phenomenon is more pronounced in the case of

Fig. 32. The extinction angle χ of myxomyosin solutions vs. shear gradient.

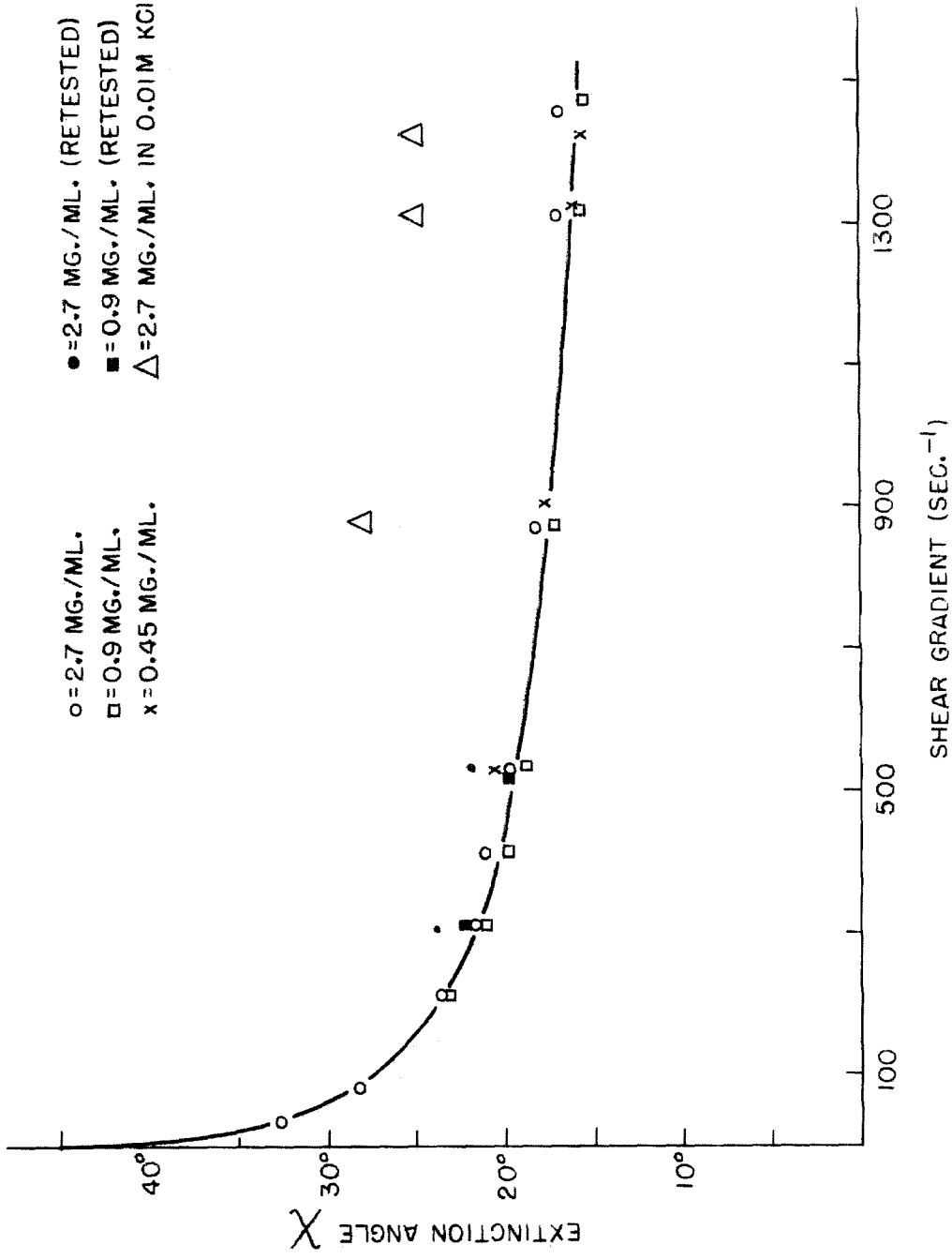
o=2.7 MG./ML.
□=0.9 MG./ML.
x=0.45 MG./ML.
●=2.7 MG./ML. (RETESTED)
■=0.9 MG./ML. (RETESTED)
△=2.7 MG./ML. IN 0.01M KCl
EXTINCTION ANGLE χ
40°
30°
20°
10°
100
500
900
1300
SHEAR GRADIENT (SEC.⁻¹)

Table 13.

The Rotary Diffusion Coefficients and the Apparent Lengths of Myxomyosin Calculated From the Flow Birefringence Data

Concentration of protein (mg/ml)	Shear Gradient (sec^{-1})	Extinction Angle (degree)	Rotary Diffusion Constant (sec^{-1})	Apparent Length (1000 Å)
2.7	38	32.6	12.9	11.42
	82	28.2	18.8	10.04
	205	23.9	31.6	8.46
	308	21.8	39.0	7.92
	411	21.0	48.0	7.36
	523	19.9	54.8	7.06
	878	18.3	77.4	6.28
	1315	17.0	99.2	5.78
*remeasurement	302	24.0	46.8	7.44
	530	22.1	68.8	6.52
0.9	205	23.6	30.7	8.56
	303	21.0	35.5	8.14
	415	19.9	43.5	7.62
	538	19.1	51.7	7.18
	858	17.0	64.5	6.68
	1323	15.9	85.9	6.06
remeasurement	304	22.0	39.3	7.88
	530	19.9	55.2	7.02
0.45	535	20.6	59.8	6.86
	915	18.0	77.9	6.26
	1323	16.0	87.1	6.04
2.9(in 0.01 M KCl)	861	28.0	193.5	4.60
	1318	25.0	223.4	4.40

* See text on the effect of shearing force.

more concentrated solutions (0.3 - 0.4%) and results in a shortening of 500 Å of apparent length (Table 13). The effect is smaller in the same solution in the presence of ATP, or in the less concentrated solution (0.09 - 0.05%) in the absence of ATP (Table 13). This phenomenon is not well understood, but appears to be related to the work softening effects found in the viscosity determinations. It is interpreted as resulting from mechanical breakdown of the molecular aggregates which tend to dissociate at high dilution or in the presence of ATP.

The value of χ has also been measured at several concentrations of myxomyosin (0.045, 0.09, 0.2, 0.3, and 0.4%), each solution being a fresh one. It has been found that the χ values agree with each other within the experimental error at all of these concentrations. This is in agreement with the results of the viscosity studies (Fig. 32). It will be recalled that the reduced viscosity of myxomyosin is independent of concentration below 0.3% and at shear gradients above 100 sec^{-1}. Under these conditions, the molecules are free to assume any spatial orientation without interfering with each other.

The values of χ for solutions containing excess ATP (10 μM/ml) are given in Fig. 32-A for varying shear gradients. The calculations of Θ and of the length of molecule are given in Table 14. The apparent length of myxomyosin in an excess of ATP is 6,000 - 12,000 Å. ATP does not increase

Fig. 32-A. The effect of ATP (10 μM/ml) on the extinction angle χ of myxomyosin solutions.

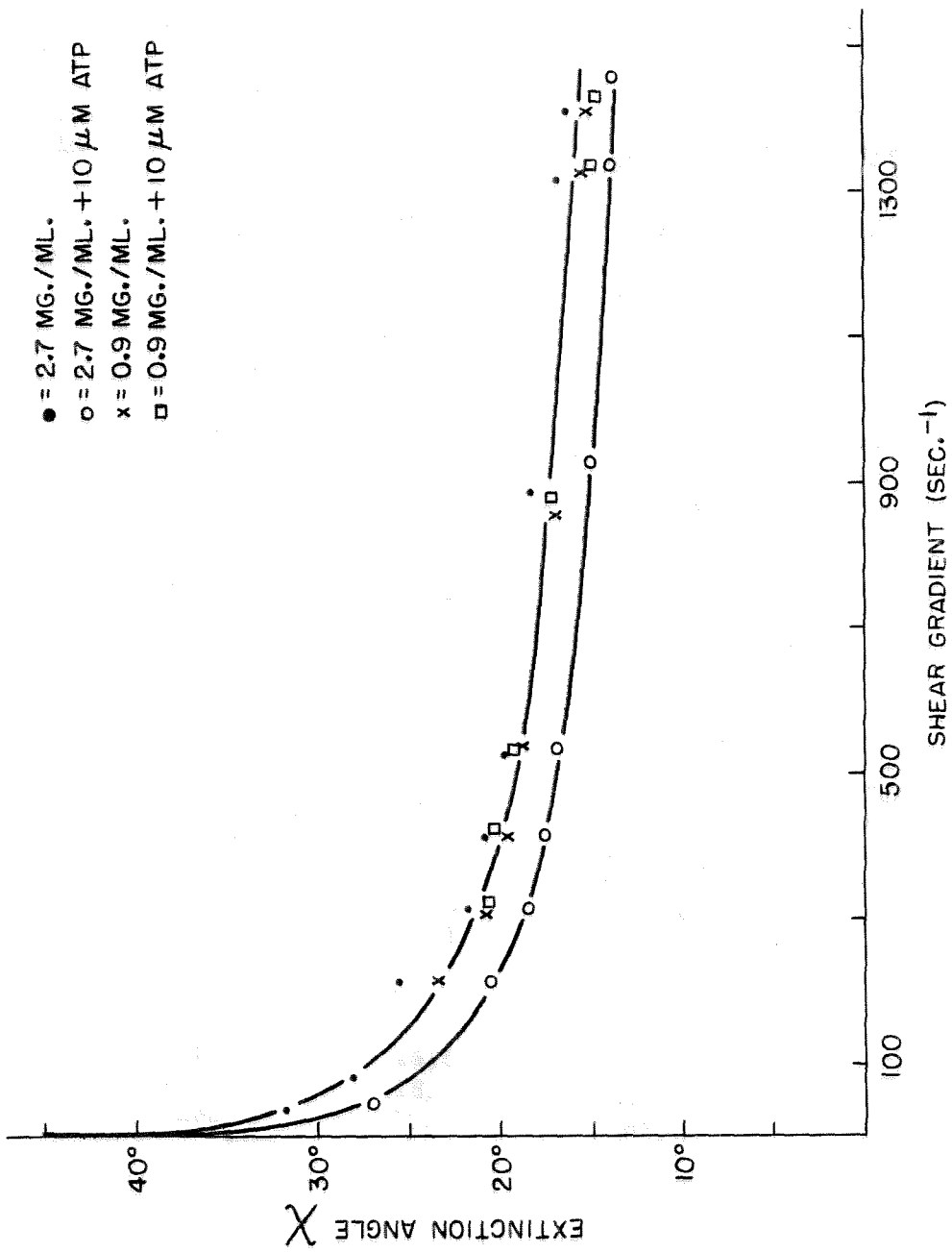
● = 2.7 MG./ML.
o = 2.7 MG./ML. + 10 μM ATP
x = 0.9 MG./ML.
□ = 0.9 MG./ML. + 10 μM ATP
EXTINCTION ANGLE χ
40°
30°
20°
10°
100
500
900
1300
SHEAR GRADIENT (SEC.⁻¹)

Table 14.

The Effect of ATP (10 μM/ml) on the Rotary Diffusion Coefficients and the Apparent Lengths of Myxomyosin Calculated From the Flow Birefringence Data

Concentration of protein (mg/ml)	Shear Gradient (sec^{-1})	Extinction Angle (degree)	Rotary Diffusion Constant (sec^{-1})	Apparent Length (1000 Å)
2.7	46	27.0	9.8	12.48
	213	20.6	23.8	9.28
	309	18.5	27.8	8.84
	409	17.8	34.1	8.26
	537	16.9	39.9	7.82
	927	14.8	51.5	7.18
	1343	14.1	68.2	6.54
remeasurement	306	19.2	29.7	8.64
	546	17.2	42.2	7.68
0.9	321	21.2	38.3	7.94
	401	20.6	44.8	7.54
	534	18.5	48.1	7.36
	886	17.5	70.9	6.46
	1338	15.5	82.1	6.16
remeasurement	318	20.5	35.3	8.16
	528	19.1	50.8	7.24
0.45	533	19.5	53.4	7.10
	888	16.5	62.5	6.74
	1336	15.5	82.0	6.16

the χ values for solutions of 0.05 - 0.09% concentration. The apparent length of myxomyosin is therefore not changed by more than 5% by ATP. χ values for solutions at 0.2 - 0.4% concentration were increased slightly by ATP indicating an increase of rotary diffusion coefficient, and an increase of apparent length of 5-8%. This effect is not well understood. However, the measurements on the solutions containing ATP at a level of 10.0 μM/ml, required a period of an hour. In the presence of such concentrations of ATP, the myxomyosin will be converted to the refractory high viscosity, state M^*. This will be further discussed in the last section in this chapter.

C. Electron Microscopy.

Preparations of myxomyosin with and without ATP have been examined under the electron microscope. The samples were sprayed and air dried (Chapter II-K). Excess ATP was added to the sample 5 minutes before spraying. Since myxomyosin is unstable in 0.01 M KCl, and since higher concentrations of salt interfere with electron microscopy, the dilution of myxomyosin with respect to salt was also carried 5 minutes before spraying. The photographs (Figs. 33, 34), reveal rod-like molecules of 3000-7000 Å, mostly within the range of 3500-4500, in length and 50 Å in diameter. The accuracy of the diameter measurement is estimated at $\pm$ 5Å. The shape of the rod in cross section cannot

Fig. 33. Electron micrographs of myxomyosin molecules in high concentration (Chromium shadowing; x 25,000)

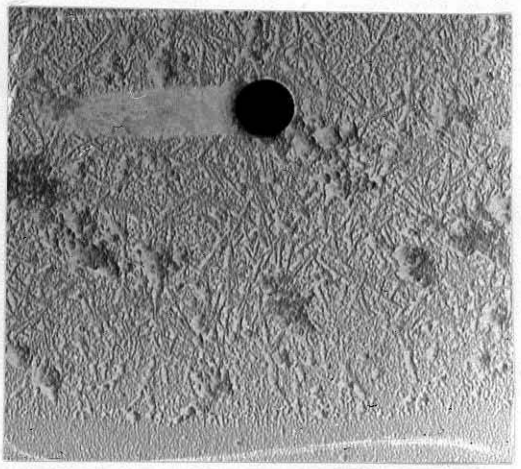

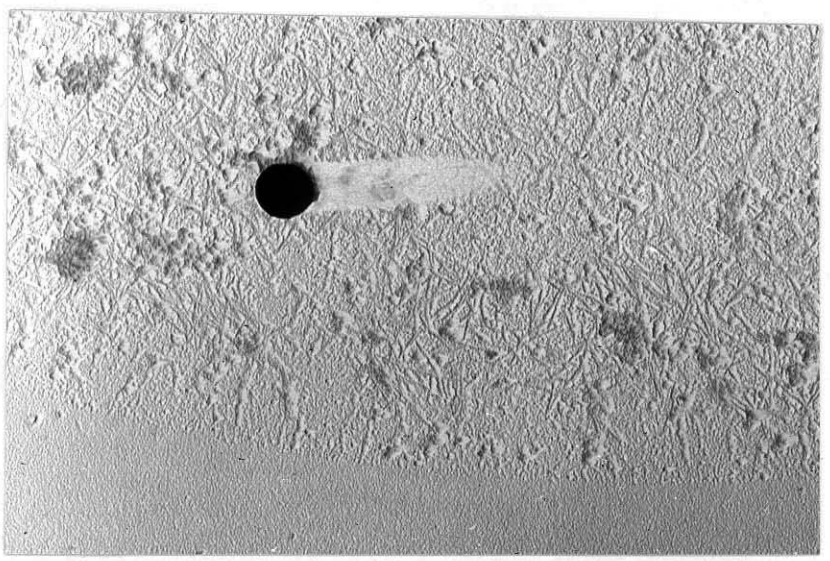

Fig. 34. Electron micrographs of myxomyosin molecules in low concentration

(Chromium shadowing; x 25,000)

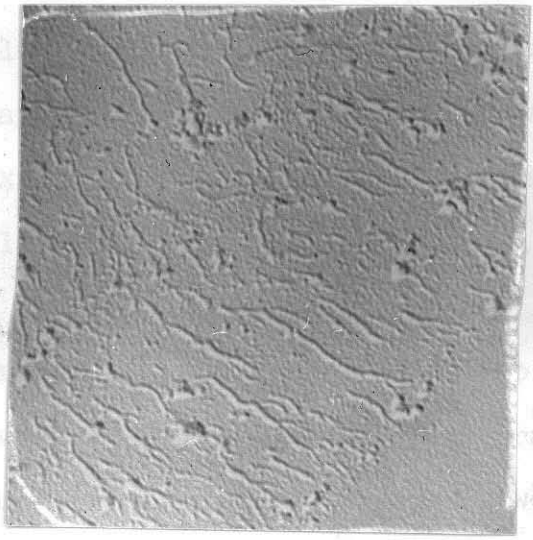

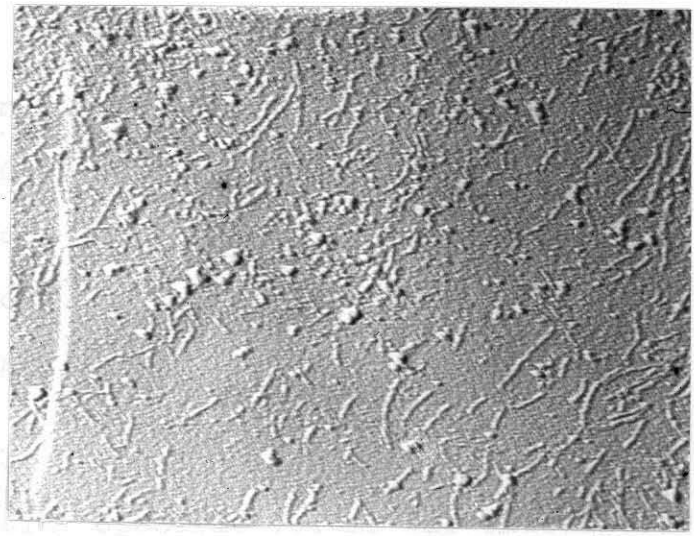

be determined. Many of the rods are somewhat deformed. Some globular material is also visible.

The myxomyosin rods appear to be qualitatively the same in the presence and in the absence of ATP (Fig. 35, and Fig. 36).

With the value of partial specific volume, 0.72, the diameter, 50 Å, and the length 4000 Å, and with the assumption that the myxomyosin is a cylindrical rod, the molecular weight may be calculated to be 6.6 millions. The average length of 4000 Å is arbitrarily chosen on the basis of the result of the viscosity study (axial ratio of 80) and because of the presence in the electron micrographs of a large proportion of molecules of this length. However, molecules, 5000 Å in length (molecular weight 8.3 millions) and molecules, 3000 Å in length (molecular weight, 4.9 millions) are also present in substantial numbers.

Electron micrographs of myxomyosin which has been stored in 0.01 M KCl for ca. 24 hours (Fig. 37) show that the molecules have been considerably shortened. The lengths of some molecules remain in the range 2000-3000 Å but most are less than 1000 Å.

D. Partial Specific Volume.

The partial specific volume was calculated from density and concentration determinations. The concentrations were measured with the differential refractometer and with the

Fig. 35. Electron micrograph of myxomyosin molecules in 0.01 M ATP solution

(Thorium shadowing; x 25,000)

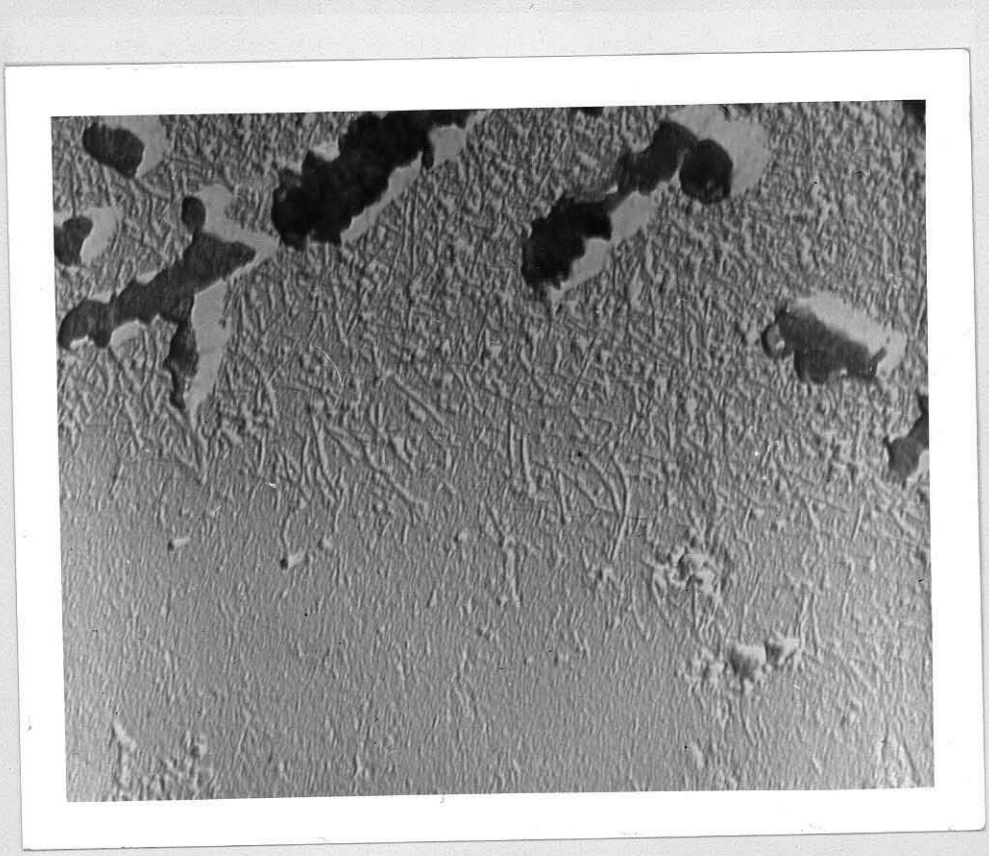

Fig. 36. Electron micrograph of myxomyosin molecules in 0.01 M ATP solution (Chromium shadowing; x 25,000)

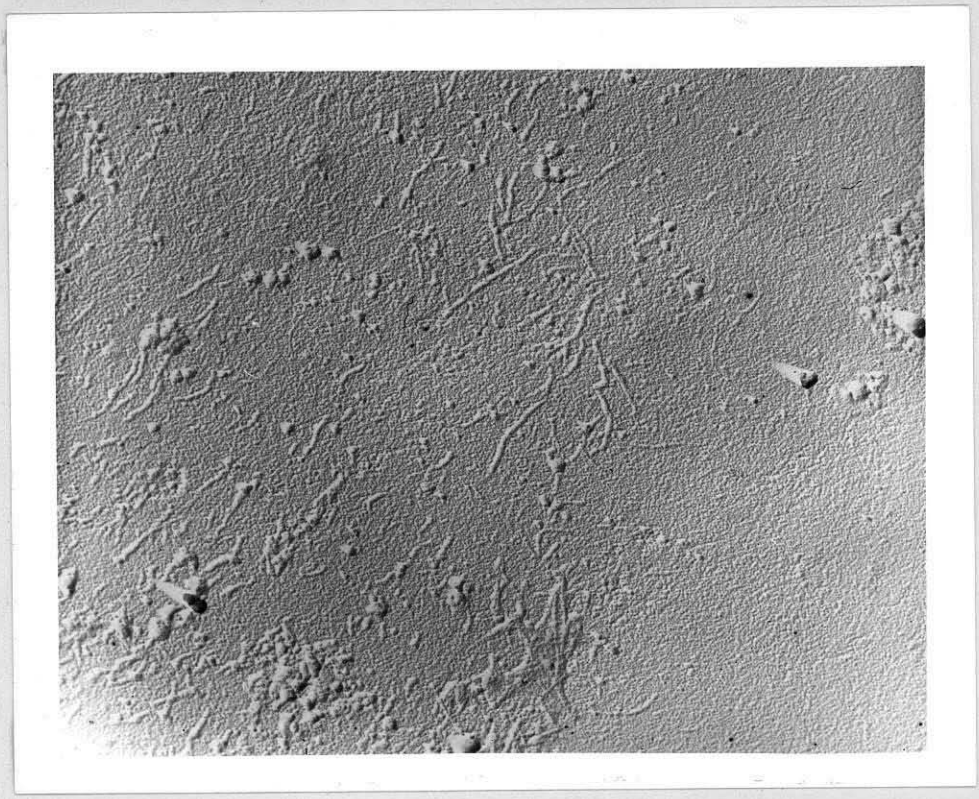

Fig. 37. Electron micrograph of myxomyosin molecules dialyzed in 0.01 M KCl overnight (Thorium shadowing; x 25,000)

assumption that the refractive index increment of myxomyosin is 0.185 cc/gm. The partial specific volume obtained for one preparation was 0.723, and for a second preparation, 0.715. An average value of 0.72 is taken as the partial specific volume. This value, because of the uncertainty in the assumed refractive index increment, is considered reliable to about 5%.

E. Sedimentation.

Detailed sedimentation studies of myxomyosin for the purpose of evaluating the sedimentation constant and its change in the presence of ATP were carried out at varying protein concentration. A plot of $1/S_{20,w}$ vs. concentration is present in Fig. 38. The extrapolated value of $S_{20,w}$ at zero concentration, evaluated from the plot, is 30 $\pm$ 0.5 S. Using this value of S, the frictional coefficient of 4.0 derived from viscosity studies, and a partial specific volume of 0.72, a molecular weight of 6.1 millions may be calculated from the equation given in Chapter II, p. 42.

Because of the uncertainty in the partial specific volume, this value of 6.1 millions for the molecular weight of myxomyosin must be regarded as uncertainty $\pm$ 6%. This uncertainty, together with uncertainties of the values of S and f/f_o, contributes a total maximum uncertainty ca. $\pm$ 10%.

Fig. 38. The $1/S_{20,w}$ of myxomyosin vs. concentration.

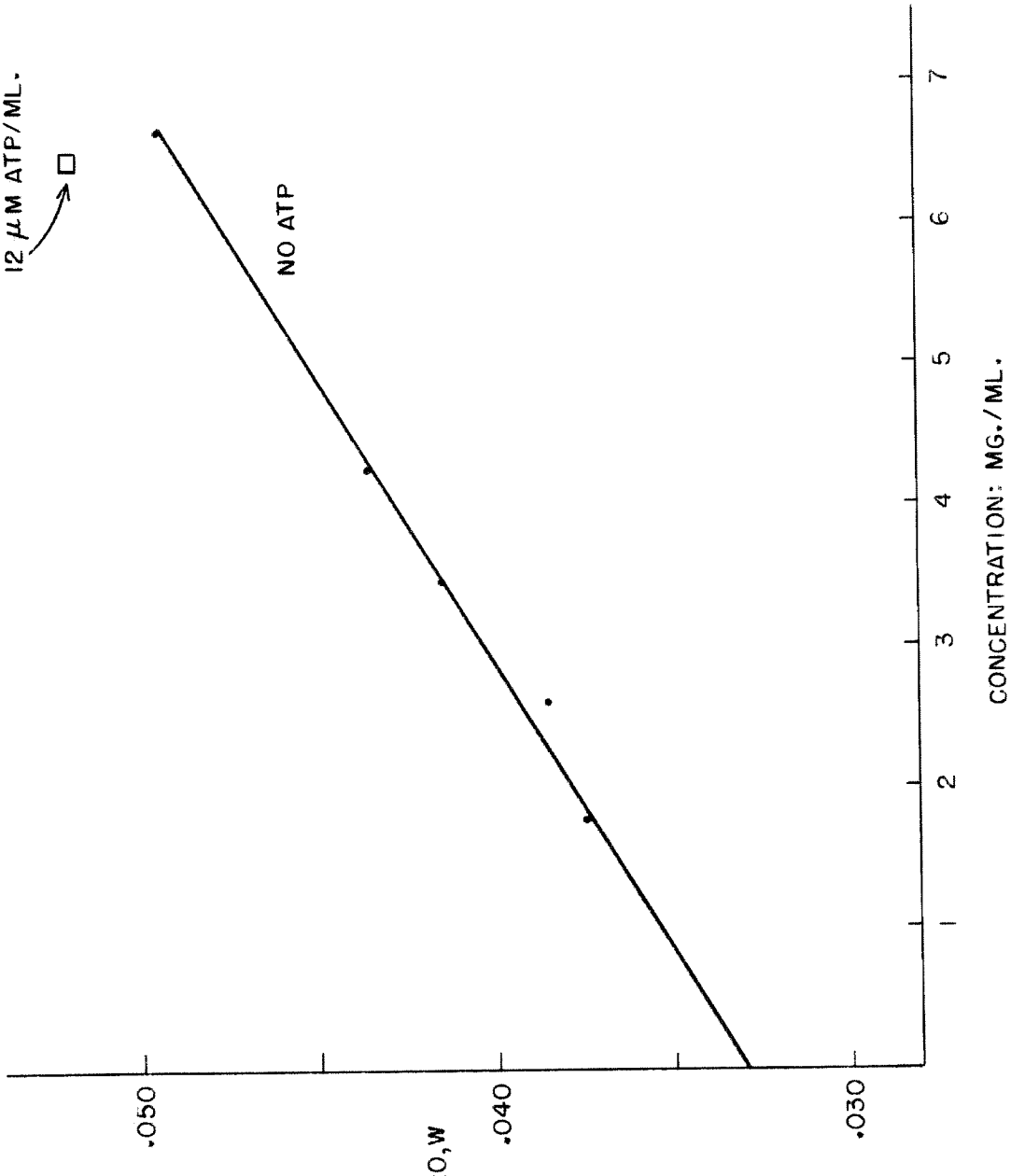
12 μM ATP/ML.
NO ATP
.050
.040
.030
$1/S_{20,w}$
1
2
3
4
5
6
7
CONCENTRATION: MG./ML.

The slowly sedimenting material, which consists of protein impurities and some RNA (Chapter V), has a sedimentation constant of about 3 to 5 S, with an average of 3.8 S. This value appears to be independent of concentration. The uncertainty of the S value of the slow boundary is due to boundary spreading which results from polydispersity.

Sedimentation studies of myxomyosin in the presence of an excess of ATP have been carried out with 3 different preparations. None of the experiments were performed, however, in such a way that the S value in an excess of ATP could be extrapolated to infinite dilution. Three pertinent conclusions can, nevertheless, be made on the basis of these studies. First, within the experimental error of estimation, the area under the myxomyosin boundaries is not decreased or transformed into other components by ATP. Second, ATP sharpens the boundary of myxomyosin to a moderate extent. This sharpening effect is shown in Fig. 39. The effect is pronounced in concentrated solution but less evident in dilute solution. Third, in addition to the sharpening effect, a decrease of 5 to 10% in the sedimentation constant is caused by ATP. For example, at a protein concentration of 0.75%, myxomyosin has a $S_{20,w}$ value of 20.2 in the absence of ATP and of 19.1 in the presence of ATP. (Correction for the contributions of ATP to the viscosity and density of the medium have been included in the calculation of the corrected sedimentation constants.)

Fig. 39. Ultracentrifuge patterns of myxomyosin in the presence and in the absence of ATP (12 μM/ml)

(Sedimentation proceeds from right to left)

Buffer: 0.2 μ K-maleate pH: 7.0

Rotor speed (rpm); 47,660 Concentration (mg/ml): 7.5

In the Absence of ATP

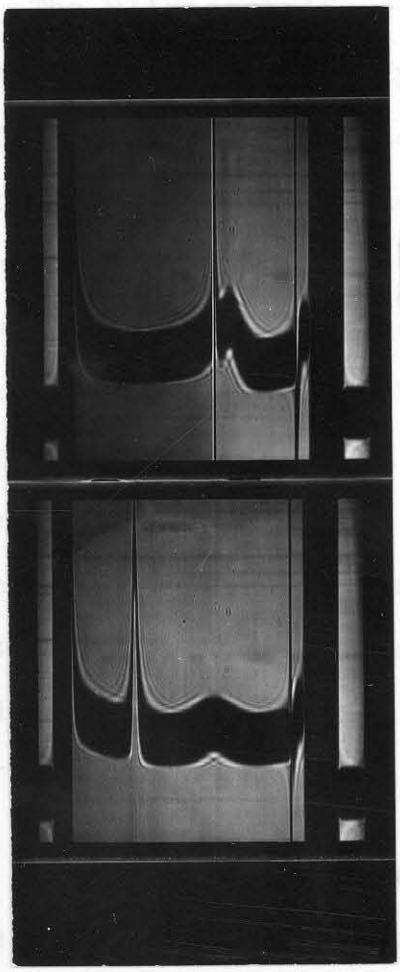

In the Presence of ATP

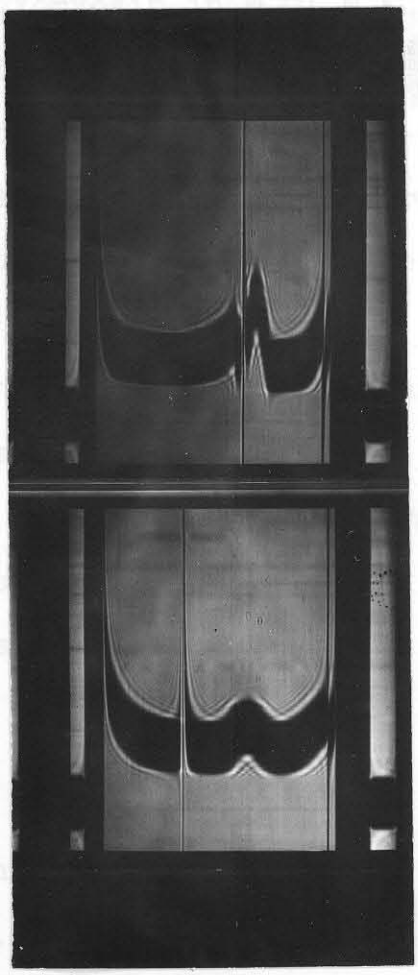

These experiments were performed with samples which were in contact with excess ATP (5 to 10 μM/ml) for periods of about 30 minutes before sedimentation began and for one hour during sedimentation. Therefore, the myxomyosin studied was probably in the state M^* as discussed in Chapter VI.

The above observations lead to the conclusion that the bulk of the myxomyosin is not drastically affected by ATP. Myxomyosin does not break up into small units or suffer an extensive change in shape. The small decrease in sedimentation constant is probably due to an increase in the frictional ratio, as suggested by boundary sharpening.

The ultracentrifuge pattern of myxomyosin in 0.01 M KCl (Fig. 40) differs greatly from that of myxomyosin in 0.2 μ beffer. In the low ionic strength medium, the pattern consists of a very broad and comparatively slow moving boundary which spreads and almost disappears during the run. An even slower boundary, corresponding to the impurity initially present, is also observable. Spreading of the major boundary suggests the presence of a polydisperse system rather than a relatively homogeneous one as found in high salt concentration. These observations suggest that in 0.01 M KCl myxomyosin undergoes a degradation process to give a series of products of smaller size.

F. Electrophoresis.

This section will consider the influence of ATP on the electrophoretic pattern of myxomyosin. The electrophoretic

Fig. 40. The ultracentrifuge patterns of myxomyosin dialyzed in 0.01 M KCl overnight

(Sedimentation proceeds from right to left)

Medium: 0.01 M KCl pH: 6.3

Rotor speed (rpm): 47,660 Concentration (mg/ml): 5.8

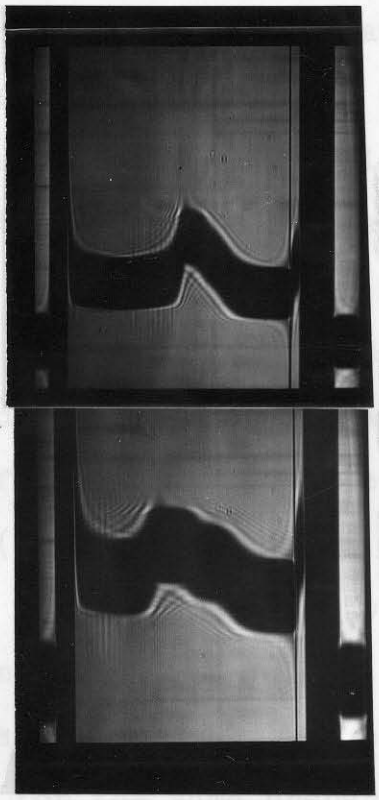

behavior of purified myxomyosin has been described in Chapter IV. In the present work, myxomyosin purified by one cycle or by two cycles of centrifugation was used.

In the study of the material purified by one cycle centrifugation, ATP (3 μM/ml) was added to the protein solution before the run. The electrophoretic scanning patterns of the same preparation with and without ATP are given in Fig. 41. The boundary A is increased in area in the ATP treated sample because ATP moves with the mobility of RNA as shown in Chapter IV. In the presence of ATP, the B boundary of the ascending limb is substantially increased in area at the expense of the boundary, C, which is the major boundary in the original preparation. The major boundary, B + C, in the descending pattern is not affected. At this boundary ATP is absent since it migrates away from the boundary region. A minor boundary disturbance in the region of the descending starting boundary is noted.

For the study of myxomyosin purified by two-cycle centrifugation, ATP (3 μM/ml) was added not only to the protein solution but also to the whole buffer system. This reduces starting boundary anamolies and, of course, now causes all components to move in the presence of ATP at all times. The patterns for the same preparation with and without ATP, are given in Fig. 42. Four observations can be made from these patterns. First, the disturbance near the descending starting boundary disappears. Second, the

Fig. 41. Electrophoretic patterns of myxomyosin with and without ATP in the solution

(Migration proceeds from right to left)

Current: 9 ma. Time: 9000 seconds

Concentration (mg/ml): 6.0

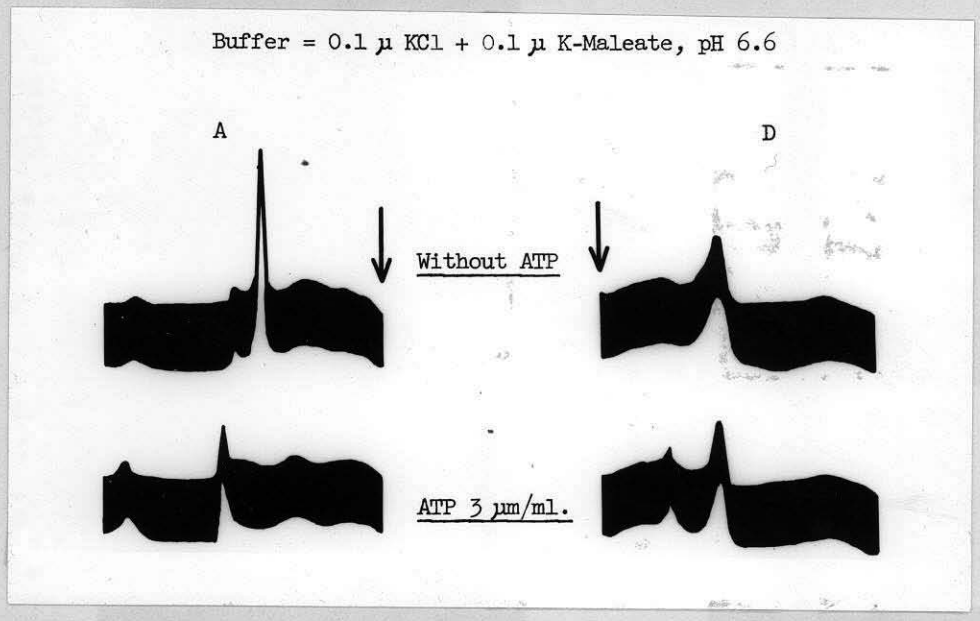

Fig. 42. Electrophoretic patterns of myxomyosin with and without ATP in the solution as well as in the buffer

Buffer: 0.2 μ K-maleate pH: 7.0

Current: 6 ma. Time: 9300 seconds

Concentration (mg/ml): 6.0 mg

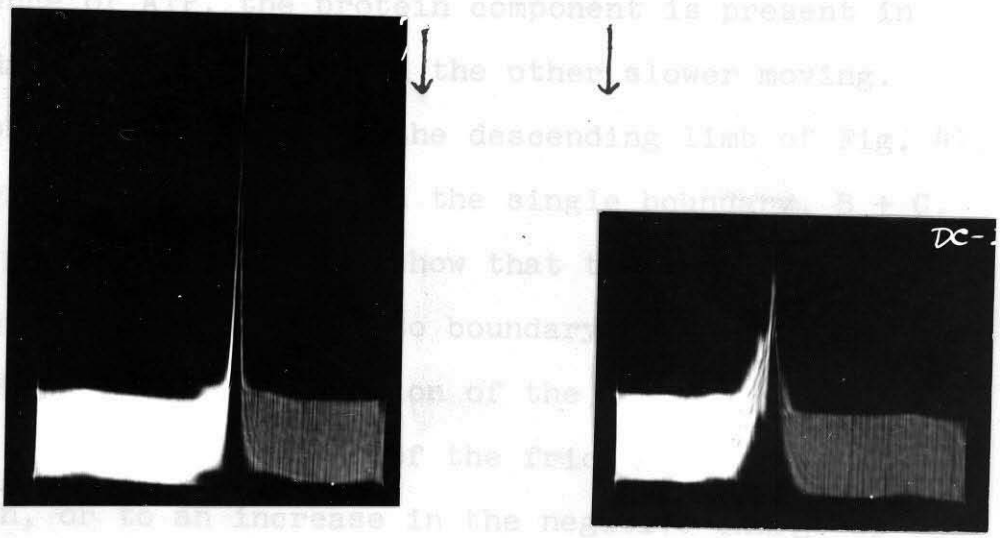

boundary A does not increase in area, confirming the hypothesis that the previous increase was the result of the addition of an ATP boundary to the pattern. Third, the boundary B in the ascending pattern is again substantially increased while the boundary C correspondingly decreased. The descending boundary, B + C, is split into two boundaries for the first time. This last finding supports the notion that in the presence of ATP, the protein component is present in two boundaries, one faster and the other slower moving. In the absence of ATP, as in the descending limb of Fig. 41, the protein component moves in the single boundary, B + C.

The patterns in Fig. 42 show that the major effect of ATP is to convert boundary C to boundary B which has a higher mobility in the direction of the anode. This might be due either to a reduction of the frictional resistance of myxomyosin, or to an increase in the negative charge of the myxomyosin. Since no great change in the molecular dimensions of myxomyosin due to ATP can be detected by other methods, the explanation based on a charge effect is regarded as more applicable. An enhancement of the negative charge here implies that negatively charged ATP is bound to the protein to form a myxomyosin-ATP complex. It should be noted that the electrophoretic studies of myxomyosin-ATP interaction were carried out at 1.5° C in which the enzymatic

activity is ordinarily largely suppressed. Interaction of myxomyosin with ATP at this temperature has not been studied by other physical methods.

G. Swelling of Extruded Fiber of Myxomyosin.

The myxomyosin fiber formed by extrusion of myxomyosin solution into an ammonium sulphate solution as described in Chapter II, is estimated to contain 50% by weight of protein. The fiber exhibits some birefringence. When the fiber is placed in buffer solution, it swells but does not dissolve even after several days at room temperature. The rate of increase in volume of the fiber in buffer, and the effect of ATP on the swelling rate have been studied. An apparently uniform fiber was chosen, rinsed briefly in water to remove most of the ammonium sulphate and broken in half. One half was placed in buffer alone, the other half in buffer with ATP (0.02 M). The increase in volume of the fibers under these two conditions at a period of 50 hours is shown in Fig. 43. Similar results have been obtained in a second experiment.

The data of Fig. 43 show that a greater increase in volume of myxomyosin fiber occurs in the presence of ATP than in its absence. This is evident after 2 hours and the effect persists for 24 hours when the fiber volume has increased in ATP by 120% compared to 30% in the absence of ATP. The volume increase is primarily due to diameter changes. The sudden increase in the volume of the control

Fig. 43. The percent increase in volume of the myxomyosin fibers suspended in 0.2 μ maleate buffer in the presence and the absence of ATP.

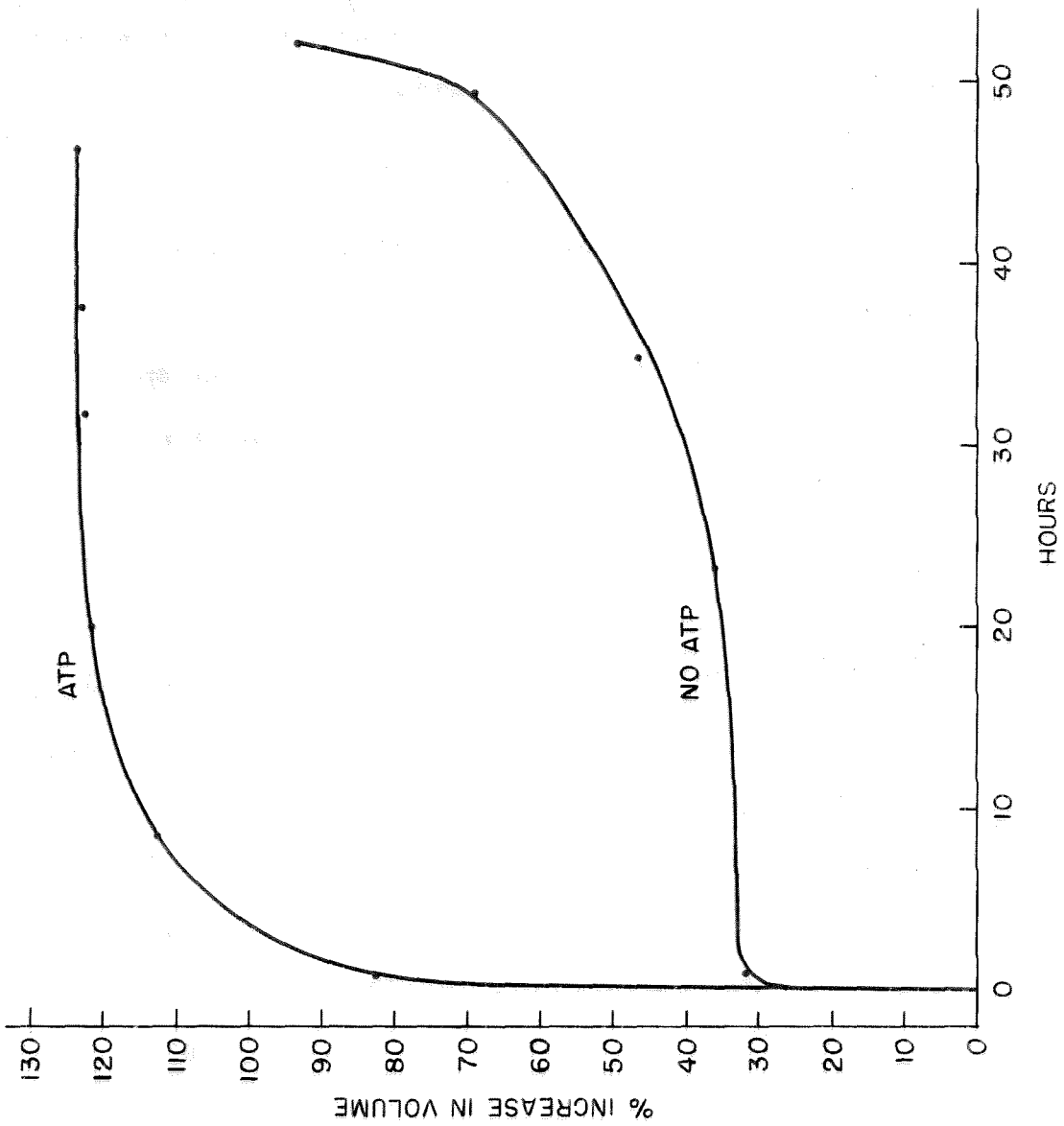
% INCREASE IN VOLUME
0
10
20
30
40
50
60
70
80
90
100
110
120
130
HOURS
0
10
20
30
40
50
ATP
NO ATP

fiber after 24 hours is believed to be the result of the formation of large fissures in the fiber.

The enhanced swelling of myxomyosin in the presence of ATP is associated with a binding of ATP as indicated by the electrophoresis study. An increase in net negative charge would be expected to result in an increase in swelling because of the Donnan effect.

H. Discussion and Conclusion.

The molecular weight and dimensions of myxomyosin preparations containing 25 percent of low molecular weight impurities have been studied by viscosity, sedimentation, electron microscopy, and flow birefringence procedures. These studies have revealed that myxomyosin is a highly asymmetrical, fairly stiff molecule, which may possibly exist in a distribution of lengths.

Sedimentation and viscosity studies indicate a weight-average molecular weight of myxomyosin of 6 millions $\pm$ 10% and an axial ratio of 80 $\pm$ 5% based on the assumption that the shape of the molecule may be approximated by a rigid prolate ellipsoid model. The errors introduced by the presence of the impurities have been substantially eliminated in these calculations.

The electron micrographs confirm the above assumption that myxomyosin is a rod-shaped molecule, and show that it has a diameter of 50 Å $\pm$ 5 Å, and a range of lengths of 3000 to 6000 Å, the most frequent length being 4000 Å. The

The corresponding molecular weight range for a cylindrical rod, 50 Å in diameter, is 4.9 to 9.9 millions. The molecular weight for the most frequent length of 4000 Å is 6.5 millions.

Measurements of the extinction angle from flow birefringence support the above findings and give a distribution of apparent lengths of 5,800 - 10,000 Å. The values so obtained are greater than those estimated from viscosity and electron microscopy. A few molecules 7000 Å or longer in length can however be seen in the electron micrographs. The reasons for the greater apparent length from flow birefringence data have not been known. The discrepancy may be due to the fact that birefringence of flow heavily weights the longest molecules, as explained in Chapter II, p. 30. In the case of DNA, there is a similar disagreement in estimated length of the molecule as between light scattering and birefringence data. This has not yet been explained (63).

ATP has a striking effect on the physical properties of concentrated myxomyosin solutions as shown by the viscosity studies of previous chapters. As the concentration of myxomyosin in the solution decreases, however, the ATP effect becomes less pronounced. Viscosity studies show that the immediate reaction product of highly dilute myxomyosin and excess ATP is not different in molecular dimension (f/f_o) from the starting material. Nevertheless, the

slope of the line which relates reduced viscosity to protein concentration is lowered by ATP. This suggests that ATP does not change the molecular dimensions of myxomyosin (dimensions of state M are similar to dimension of state M(ATP)), but that ATP reduces the aggregation of myxomyosin monomers with each other. Dilute preparations of myxomyosin show no qualitative difference traceable to ATP which can be detected by electron microscopy. Flow birefringence measurements on dilute myxomyosin (0.09-0.5%) show no changes in apparent length of myxomyosin molecule after reaction with an excess of ATP for 30 to 60 minutes. The myxomyosin thus observed is probably in the M^* state rather than in the M(ATP) state as suggested in Chapter IV.

Sedimentation studies and birefringence measurements at moderate concentration (0.2 - 0.4%) of myxomyosin reveal some new aspects of ATP-myxomyosin interaction. In these studies, an apparent slight increase in the frictional coefficient of myxomyosin has been observed. This corresponds to an approximate 5 to 10% decrease in S value and 6-8% increase in apparent length from flow birefringence. The tentative interpretation of these data is that the myxomyosin in the M^* state is associated in end-on complexes.

The electrophoretic studies of myxomyosin in the presence of ATP show that a substantial portion of the myxomyosin acquires an increased mobility towards the anode. This is interpreted as indicating that myxomyosin molecules

have increased in negative charge owing to the binding of ATP.

Concentrated myxomyosin fibers (50% by weight) suspended in buffer solutions swell more rapidly and to a greater extent in the presence of ATP than in the absence of ATP. This is further evidence that ATP increases the net negative charge on myxomyosin.

In low ionic strength media (0.01 M KCl), myxomyosin undergoes degradation to form a series of much smaller products. This has been shown by sedimentation, viscosity, flow birefringence and by electron microscopy studies. The degradation is apparently not reversible.

VIII. DISCUSSION

A. Problems Related to Extraction and Purification.

One would like to know the amount of myxomyosin present in the plasmodium of the slime mold. This question cannot yet be answered without ambiguity, because the extractability of myxomyosin by the method employed in this research has not been determined. However, of the total non-dialyzable material in the 1.4 M KCl crude extract 3-5% is myxomyosin. If one assumes that all of the myxomyosin can be extracted by the present procedure, then this material makes up at least 1% of the total dry weight of the plasmodium. This impressive figure suggests that myxomyosin is an important constituent of the plasmodium on a weight basis.

It has been pointed out in Chapter III, that only when the plasmodium is extracted with a concentrated salt solution (1.4 M KCl), does the resulting crude extract exhibit an ATP response. This interesting fact may be considered in the light of our knowledge concerning the influence of RNA on the behavior of myxomyosin. The findings of Chapter VI indicate that myxomyosin aggregates more strongly and exhibits a larger viscosity response to added ATP, after RNA has been removed from the protein moiety. It is well known that nucleoproteins dissociate in medium of high salt

concentration (1-2 M). It may be that when the plasmodium is extracted with a dilute salt solution, the soluble myxomyosin becomes bound by cytoplasmic RNA which is also extracted during the process. The formation of a RNA-protein complex of myxomyosin (about 15% RNA is present in the 30-40% SAS fraction of the 1.4 M KCl extract) would tend to reduce the aggregation of myxomyosin and to suppress the response of myxomyosin to ATP. When the extraction of the plasmodia is carried out in strong salt medium, any excess RNA will not become bound to the protein to such a large extent. The myxomyosin molecules are then free to aggregate with each other to yield a high viscosity level and a large response to ATP. On the other hand, the possibility cannot be dismissed that a certain amount of RNA is originally and specifically bound to the myxomyosin protein moiety for some purposesunknown. It is clearly desirable that a detailed study of the properties of myxomyosin freed of RNA, be made.

The present preparation of myxomyosin prepared by differential centrifugation still contains about 25% by weight of small molecules. Whether this is due to the break down of myxomyosin during the preparation, or whether it is at least in part due to the inherent characteristics of the convective centrifugation of the angle rotor, has not been determined. If differential centrifugation can be performed by non-convective centrifugation with a swinging

bucket type of rotor, then the movement of the boundaries and therefore the efficiency of centrifugation can be quantitatively calculated and observed. The stability of myxomyosin during storage as affected by various factors, such as ionic strength, pH, temperature, suppression of possible contaminating proteolytic enzymes should also be investigated.

Whether or not myxomyosin molecules with the dimensions observed in this research exist as a unique molecular species in the plasmodium, has not been directly determined. In the present preparation a range of various lengths of molecules has been found (Chapter VII). This may be due to the breaking of the long molecules during the extraction and purification processes. It is also possible that a distribution of sizes of myxomyosin molecules does exist in the plasmodium. It should be noted, however, that after degradation in low ionic strength medium, the original myxomyosin molecule cannot be reassembled and its response to ATP is not restored when it is put back into high salt medium. Therefore, in order for the myxomyosin to respond to ATP, it must possess a certain minimum size and a specific configuration.

B. Problems Related to Kinetics of ATP-myxomyosin Interaction and the Physical-chemical States of Myxomyosin.

The kinetics of the ATP effect on the physical-chemical states of myxomyosin is an interesting problem which requires more investigation. The state M(ATP) can be studied by some

rapid methods, presumably by light scattering. The state M^* has been investigated only indirectly by sedimentation and flow birefringence methods. Presumably, light scattering and intrinsic viscosity measurements on material in the M^* state should provide information concerning its nature. Care should be taken in setting up experiments for the study of the two states, M(ATP) and M^*, since both are transitional in the hypothetical cycle.

Experiments other than electrophoresis should be performed to study the binding of ATP to myxomyosin. The binding of ATP can perhaps be quantitatively followed analytically. This, together with information on the charge of myxomyosin should yield some insight into the mechanism of the reaction of ATP on myxomyosin.

Myxomyosin fibers of better orientation should be prepared. The effects of ionic strength, pH, temperature and other reagents on the physical dimensions and mechanical properties of the fiber may reveal further facts concerning the behavior of myxomyosin in a structure.

C. Studies of the Structure of Plasmodial Strand of Slime Mold.

The tendency of myxomyosin to aggregate <u>in vitro</u> suggests that it probably exists <u>in vivo</u> in a structural form rather than in a soluble form. Therefore, attempts have been made to look for the oriented microscopic structures of myxomyosin in the plasmodium, structures similar to those

of the striation of muscle. In order to avoid the change of structure caused by chemical fixatives, the mild freeze-dry technique was adopted for fixation. The detailed results are reported in Appendix II. No evidence of oriented striations were seen under magnifications up to 1000 x either in the longitudinal or cross sectional views. There are areas of the plasmodium which suggest that they possess a gel structure such as that reported by Howard (36) on the basis of histological studies and by others (39, 40) on the basis of observation of the living specimens. (Appendix II). Striations of the myxomyosin structure are, however, either so minute or so small in amount as to be invisible under the present conditions. It is also possible that the myxomyosin structure may take the form of a net work rather than a side by side aggregation. The hypothesis that myxomyosin assumes a net structure is favored by the present author.

D. A Brief Comparison of Actomyosin and Myxomyosin.

It is of interest to compare certain properties of actomyosin and myxomyosin.

Four similarities of the two proteins may first be noted.

The molecular weight and the molecular dimension of actomyosin vary widely according to the method of preparation and even from one preparation to the next. The Weber-Edsall "natural" actomyosin has been reported to possess a

molecular weight of from 4-20 millions or more, and the molecules to be 60 Å in diameter by 4-10,000 Å in length (14, 83, 90, 91). Their width appears under the electron microscope to be from 50-250 Å and their length up to 15,000 Å (92). Actomyosin and myxomyosin appear to be the longest and most asymmetric undenatured protein molecules so far isolated.

Solutions of the two proteins react similarly to ATP, the solution viscosity first decreasing and then recovering. Studies of the nature of the ATP protein interaction by electron microscopy and sedimentation methods cannot be yet directly compared.

ATPase activity has been shown to be present in preparations of actomyosin and myxomyosin. The enzymatic activities in both cases are much lower than that of conventional ATPase (14).

Actomyosin is believed to be closely associated with the activity of muscle contraction. Myxomyosin is believed to be closely related to the phenomenon of protoplasmic streaming.

Three differences between two proteins may also be noted.

Actomyosin is an interaction product of two distinct proteins, actin and myoxin. Myxomyosin has not thus far been observed to consist of two proteins. It appears rather to be a complex with RNA as is nucleotropomyosin (14).

The effect of ATP on actomyosin is sensitive to Ca and Mg ions (14, 15, 89). The ATP response of myxomyosin does not seem to be affected by these two ions. The effect of Ca and Mg ions on the ATPase activity of myxomyosin has not been determined.

The solubility of the two proteins is apparently different. Actomyosin, behaves like a true globulin and precipitates in the absence of salt. Myxomyosin is soluble in water, but undergoes a breakdown.

E. The Significance of the Findings Concerning Myxomyosin.

It has been mentioned in the introduction, that both actomyosin and myxomyosin are believed to be the essential parts of the machinery for the transformation of chemical energy into mechanical work in biological systems. Myxomyosin appears to be the simpler system. Whether or not work on myxomyosin will reveal basic information on the transformation of chemical to mechanical energy, information not readily obtained in muscle research, cannot be decided. Two contributions to the understanding of biological energy transformation might result from work on myxomyosin, contributions which are difficult to make with the muscle system.

Firstly, organized protoplasmic movement as it exists in the living cells of green plants, slime molds, amoebae, leucocytes, and fibroblasts, is more likely to be explained

with the basic principles revealed by work on myxomyosin systems than by analogy from work on muscle which is highly specialized.

Secondly, the myxomyosin system operates in a single cell in contrast to the muscle tissue which is a more complicated system. Therefore, the control and the operation mechanism of myxomyosin-like systems, might be more easily understood. Such an understanding will contribute to the knowledge of the physiology and the organization of the living cells.

IX. MECHANISM FOR PROTOPLASMIC STREAMING

It is of interest to examine the results of this study of myxomyosin from the standpoint of what they may contribute to our understanding of the mechanism of protoplasmic streaming. The results, presented in this thesis, suggest an hypothesis concerning protoplasmic streaming which is consistent with known facts. It is necessary to this hypothesis, however, to impute to the plasmagel layer certain properties which have not yet been established. Experimental tests of the basic ideas of the present hypothesis require further work.

The experimental facts on which the present proposal is based on are reviewed briefly below:

A. Results from microscopic examination of the streaming strand.

1. The whole plasmodial strand is under pressure. If one end of the strand is cut abruptly, plasmasol spurts out (Howard (36)).

2. Protoplasmic streaming can be accelerated, stopped or reversed by applying an appropriate pressure differenced across a plane normal to the longitudinal axis of the strand (Kamiya (45)). The pressure difference needed is usually about 15 cm of water. Kamiya has also shown that the velocity distribution in the moving protoplasmic front

is parabolic, being fastest in the middle of the strand and slowest along the sides as expected in laminar flow. These facts taken together led him to conclude that the protoplasmic flow is caused by differences in pressure in different zones of the plasmodium (Chapter I-A).

3. The direction of protoplasmic flow reverses during each cycle of contraction and relaxation (Seifriz (42)). Seifriz has concluded that the mechanism of protoplasmic movement of the slime mold is one of the rhythmic contraction and relaxation of protoplasm, reminiscent of the action of a heart (Chapter I-A).

4. A plasmodial strand, in the course of normal growth can penetrate a pore with an average size of 1 micron. It cannot, however, survive ejection through a pore 0.2 mm in diameter. Moore (93) has concluded on the basis of these observations that the plasmodium requires an intact structure of large size, namely the walls of the strand, in order to survive. Nevertheless, protoplasm contains available pre-structural elements of molecular magnitude which can be mobilized to form the walls of freshly formed strands.

5. ATP has a liquefying effect on the gel structure of the plasmodium (Chapter III-A). This is attended by a flow of protoplasm in the direction of the liquefied portion.

B. Results from the study of the myxomyosin system.

1. It is known that actomyosin forms the structure of muscle and serves as the mechanical basis for contraction. Because of the similarities between actomyosin and myxomyosin in physical dimensions and in other unique characteristics, myxomyosin is here regarded as a structural protein. It apparently constitutes a major portion of the plasmagel (cf. 5 above).

2. ATP reduces the aggregation of myxomyosin in solution and increases the rate and the extent of swelling of the artificial myxomyosin fiber. Myxomyosin increases its negative charge by binding ATP.

3. Myxomyosin hydrolyzes ATP.

C. Results on the chemo-mechanical behavior of cross-linked polyelectrolyte gels.

Lightly cross-linked polymers which contain charged groups, such as cross-linked polyacrylic acids, expand when their polar groups are charged. Such systems contract when the charged groups are neutralized. These effects are large, sometimes several hundred percent, and are indefinitely reversible (92).

A mechanism of protoplasmic streaming of slime mold based on the foregoing results is presented as follows:

Surrounding the channels inside the plasmodial strand in which the plasmasol flows, is a gelatinous layer which serves as a sheath for the strand and elastically resists the

pressure developed in the protoplasm by the osmotic uptake of water (A-1). The frame of the gel is composed of myxomyosin (A-4, A-5, and B-1) partially cross-linked, and sensitive to ATP (A-5, B-2). When ATP is made available at a particular area, it is bound to the myxomyosin frame-work and enhances the negative charge on the myxomyosin (B-2). The gelatinous layer swells by virtue of the Donnan effect (B-2, C), the frame work tends to dissociate (B-2), and the whole structure becomes less able to resist the internal pressure. In consequence, the gel layer yields and protoplasmic flows occur, relieving the pressure in other portions of the strand. A contraction of the frame-work then occurs simultaneously in other active portions of the strand in response to the tension exerted by the frame-work. Enzymatic removal of ATP (B-3) in the expanding area causes the process to come to a halt. Accumulation of ATP at the other end of the strand sets off a reverse flow. The reversibility of this system can be viewed as resulting from the relationships between the rates of supply and removal of ATP in various parts of the frame work of the plasmagel. The mechanism for control of the ATP level in the rhythmic manner postulated, cannot yet be explained.

APPENDIX I

THE X-RAY DIFFRACTION PATTERN OF MYXOMYOSIN*

The myxomyosin fibers prepared by extrusion into ammonium sulphate have been described in Chapters II and III of this dissertation. These fibers show very weak birefringence indicating that only partial orientation has been achieved. The orientation must be very limited since the x-ray diffraction corresponds to that of a powder rather than of a fiber. The x-ray pattern obtained with copper $K\alpha$ radiation ($\lambda = 1.54$ Å) and with a sample to film distance of 5 cm, shows three rings on a 7 hour exposure. The spacings for the rings, determined from Bragg's equation, $d = \frac{\lambda}{2 \sin\theta}$, are tabulated below.

Ring position	Diameter (cm)	Spacing (Å)	Intensity
outer	5.2 ± 0.2	3.25 ± 0.2	medium (diffuse)
middle	3.6 ± 0.01	4.50 ± 0.1	very weak (sharp)
inner	1.5 ± 0.2	10.5 ± 1.0	strong (diffuse)

There is a certain similarity between this pattern from myxomyosin and that obtained from both α - and β -myosin, but the present results are not adequate for detailed comparison.

---

* This work is done in cooperation with Dr. D. L. Caspar. The author wishes to express his thanks for permission to reproduce these results.

APPENDIX II

CYTOLOGICAL STUDIES OF MYXOMYCETE PLASMODIUM EMPLOYING THE FREEZE-DRY METHOD*

The purpose of this study is to re-examine the structure of plasmodium using material prepared by the freeze-dry technique. This technique has been shown to be superior to chemical fixation for the preservation of cytological detail (94). Because of the striking similarity between actomyosin and myxomyosin, it is of interest to look for the existence of oriented microscopic structures that may be composed of myxomyosin.

Plasmodial strands showing active streaming were frozen in isopentane cooled with liquid nitrogen (-160° C) and dehydrated in a moving air freeze-dry apparatus at -30° C. The tissue was then infiltrated with paraffin and imbedded. Sections of 5 microns and 7 microns were cut. These sections were stained with Heidenhain's hematoxylin and counter stained with safranin.

Microscopic examination of the preparation reveals striking differences between the plasmagel and plasmasol. The plasmagel appears to be less dense than the plasmasol

---

* This work is done in cooperation with Dr. W. A. Jensen. The author wishes to express his thanks for permission to reproduce these results.

on the basis of the amount of dye bound. The plasmagel contains a larger number of nuclei, mitochondria, vacuoles, and other cytoplasmic inclusions than the plasmasol. The types of inclusions bodies found and their morphology were similar to those described by Andresen and Pollock (40).

While no organization of fibers was observed analogous to muscle fibers, there are definite indications of very thin (0.3 micron or less in diameter) fibers forming a loose net work oriented approximately parallel to the longitudinal axis of the strand. The indication of these fibers is most pronounced in the longitudinal section of the plasmagel and is far less distinct in the plasmasol.

At present it is not yet possible to show that these fibers are composed of myxomyosin. Their existence, however, agrees with other observations (Chapter IX) and supports the mechanism of streaming presented in Chapter IX.

REFERENCES

1. Bonner, J. and Millerd, A., Arch. Biochem. Biophys. 42:135 (1953)
2. Millerd, A., Bonner, J., Axelrod, B., and Bandurski, R.S., Proc. Nat. Acad. Sci. 37:855 (1951)
3. Laties, G. G., Plant Physiol. 6:199 (1953)
4. Stumpf, P. K., Annual Rev. Plant Physiol. 3:17 (1953)
5. Albaum, H. G., Ibid. 3:35 (1953)
6. Ging, N. S. and Sturtevant, J. M., Jour. Amer. Chem. Soc. 76:2087 (1954)
7. Burton, K., and Krebs, H. A., Biochem. J. (London) 55:94 (1953)
8. Levintow, L. and Meister, A., Jour. Biol. Chem. 209:265 (1954)
9. Oullet, L., Laidler, K. J., and Morales, M. F., Arch. Biochem. Biophys. 39:37 (1952)
10. Lipmann, F., Advance Enzymol. 1:99 (1941)
11. Merhof, O., Ann. N. Y. Acad. Sci. 45:377 (1944)
12. Meyerhof, O. and Oesper, P., Fed. Proc. 7:174 (1948)
13. Dubuisson, M., "Muscular Contraction" Charles C. Thomas Publisher (1954)
14. Bailey, K., "Structural proteins. II. Muscle" in "The proteins" Vol. Part. B. ed. by Neurath, H., and Bailey, K., p. 952 Academic Press Inc. (1954)
15. Szent-Györgyi, A., "Chemical Physiology of Contraction in Body and Heart Muscle" Academic Press Inc. (1953)

16. Mommaerts, W. F. H. M., Ann. Rev. of Biochem. 23:381 (1954)

17. Wilkie, D. R., "Facts and Theories about Muscle" Prog. Biophysics 4:325 (1954)

18. Muralt, A. V. and Edsall, J. T., Jour. Biol. Chem. 89:315 (1930); Trans. Far. Soc. 26:837 (1930)

19. Englehardt, V. A. and Ljubimova, M. N., Nature 144:668 (1939)

20. Goldacre, R. J. and Lorch, I. J. Nature 166:497 (1950)

21. Kriszat, G., Arkiv Zool. (2), 1:477 (1950); Chem. Abstr. 10409 h (1951)

22. Kanaziv, D. and Errera, M., Bioch. Biophy. Acta 16:198 (1955)

23. Murayama, M. Ph.D. Thesis, University of Michigan (1953)

24. Runnstrom, J. and Kriszat, G. Expt. Cell Res. 1:285 (1950)

25. Seifriz, W., "Deformation and Flow in Biological Systems" ed. by A. Frey-Wyssling, p. 3, Interscience Publishers (1952)

26. Bushee, G. L., Bot. Gaz. 40:50 (1908)

27. Seifriz, W., Bot. Rev. 9:49 (1943)

28. Dubuy, H. G. and Olson, R. A., Amer. Jour. Bot. 27:401 (1940)

29. Kamiya, N., Cytologia 15:183 (1950)

30. Stalfelt, M. G., Proc. 6th Intern. Congress Exp. Cytology (Supplement 1. Exp. Cell Res.) p. 63 (1949)

31. Goldacre, R. J., Intern. Rev. of Cytology 1:135 (1952)

32. Clarke, H. T., editor "Ion Transport Across Membranes" Academic Press (1953)

33. Overstreet, R. and Jacobson, L., Ann. Rev. Plant Physiol. 3:189 (1952)

34. Davson, H. and Danielli, J. F., "The Permeability of Natural Membranes" Macmillan Company (1943)

35. Hober, R., "Physical Chemistry of Cells and Tissues" Blakiston Co. (1945)

36. Howard, F., Amer. Jour. Bot. 18:116 (1931)

37. Holter, H. and Pollock, B. M., Comptes Rendus Lab. Carlsberg Ser. Chim. 28:221 (1952)

38. Ward, J. M., Plant Physiol. 30:58 (1955)

39. Camp, W. G., Bull. Torrey Bot. Club 64:307 (1937)

40. Andresen, N. and Pollock, B. M., Comptes Rendus Lab. Carlsberg Ser. Chim. 28:247 (1952)

41. Lewis, W. H., "The protoplasmic streaming in relation to gel structure in cytoplasm" In "The Structure of Protoplasm" p. 127, ed. by W. Seifriz, monograph of Amer. Soc. Plant Physiologists (1942)

42. Seifriz, W., "Some physical properties of protoplasm" Ibid., p. 255 (1942)

43. Sponsler, O. L. and Bath, J. D., Protoplasma 44:259 (1954)

44. Marsland, D. A., "The protoplasmic streaming in relation to gel structure in cytoplasm" In "The Structure of Protoplasm" p. 127, monograph of Amer. Soc. Plant Physiologists (1942)

45. Kamiya, N., "Physical aspect of protoplasmic streaming" In Ibid., p. 237

46. Loewy, A. G., Jour. Cell. Comp. Physiol. 40:127 (1952)

47. Morris, D. L., Science 107:254 (1945)

48. Cornell, A. G., Bardawill, C. J., and David, M. M., Jour. Biol. Chem. 177:751 (1949)

49. Allen, R. J. L., Biochem. Jour. (London) 34:358 (1940)

50. Lowry, O. H. and Lopez, J. A., Jour. Biol. Chem. 162:421 (1945)

51. Brice, B. A. and Halwer, M., Jour. Optical Soc. Amer. 41:1033 (1951)

52. Wyatt, G. R., Biochem. Jour. (London) 48:584 (1951)

53. Abramson, H. A., Moyer, L. S. and Gorin, M. H., "Electronphoresis of Proteins" Reinhold Publishing Co. (1942)

54. Abramson, H. A., Gorin, M. H. and Moyer, L. S., Chem. Rev. 24:345 (1939)

55. Longsworth, L. G., Jour. Phy. Colloid Chem. 51:171 (1947)

56. Alberty, R. A., Jour. Amer. Chem. Soc. 72:2361 (1950); "Electrochemical Properties of the Proteins and Amino Acids" in "The Proteins" Vol. I, Part A, p. 461, ed. by Neurath, H. and Bailey, K., Academic Press (1954)

57. Cerf, R. and Scheraga, H. A., Chem. Rev. 51:188 (1952)

58. Edsall, J. T., Adv. Colloid Sci. 1:269 (1942)

59. Scheraga, H. A., Edsall, J. T. and Gadd, J. O., Jour. Chem. Phys. 19:1011 (1951)

60. _____ and Backus, J. K., Jour. Amer. Chem. Soc. 74:1979 (1952)

61. Sadron, C., Jour. Phys. Radium 9:381 (1938)

62. Donnet, J. B., Jour. Chim. Phys. 50:377 (1953)

63. Goldstein, M. and Reichmann, M. E., Jour. Amer. Chem. Soc. 76:3337 (1954)

64. Edsall, J. T., Rich, A. and Goldstein, M., Rev. Scientific Instru. 23:695 (1952)

65. Mehl, I. W., Oncley, J. L. and Simha, R., Science 92:132 (140)

66. Pickels, E. G., Jour. Gen. Physiol. 26:341 (1943)

67. Schachman, H. K. and Harrington, W. F., Jour. Polymer Sci. 12:379 (1954)

68. Svedberg, T. and Pedersen, K. O., "The Ultracentrifuge" Clarendon Press, Oxford (1940)

69. Koenig, V. L., Arch. Biochem. 25:241 (1950)

70. Johnston, J. P. and Ogston, A. G., Trans. Far. Soc. 42:789 (1946)

71. Trautman, R., Schumaker, V. N., Harrington, W. F. and Schachman, H. K., Jour. Chem. Phys. 22:555 (1954)

72. Wyckoff, R. W. G., "Electron Microscopy" Interscience Publishers (1949)

73. Hall, C. E., "Introduction to Electron Microscopy" McGraw-Hill Book Co. (1953)

74. Longsworth, L. G. and MacInnes, D. A., Jour. Gen. Physiol. 25:507 (1942)

75. Goldwasser, E. and Putnam, F. W., Jour. Phys. Colloid Chem. 54:79 (1950)

76. Singer, S. J., Timasheff, S. N. and Kirkwood, J. G., Jour. Amer. Chem. Soc. 74:5985 (1952)

77. Shooter, K. V. and Butler, J. A. V., Nature 175:500 (1955)

78. Seifriz, W. and Zetzmann, M., Protoplasma 23:75 (1935)

79. Wildman, S. G., Campbell, J. M. and Bonner, J., Arch. Biochem. 24:9 (1949)

80. Eggman, L., Singer, S. J. and Wildman, S. G., Jour. Biol. Chem. 205:969 (1953)

81. Fruton, J. S. and Simmonds, S., In p. 201 "General Biochemistry" Wiley Co. (1953)

82. Ouellet, L., Laidler, K. J. and Morales, M. F., Arch. Bioch. Biophy. 39:37 (1952)

83. Blum, J. J. and Morales, M. F., Ibid., 43:208 (1953)

84. Dainty, M., et al., Jour. Gen. Physiol. 27:355 (1944)

85. Mommaert, W. F. H. W., Ibid., 31:361 (1948)

86. Watanabe, S., Tonomura, Y. and Shiokawa, H, Jour. Biochem. (Japan) 40:387 (1953)

87. Blum, J. J., Arch. Biochem. Biophy. 55:486 (1955)

88. Koshland, D. E., Jr., and Budenstein, Z., Fed. Proc. 13:245 (1954)

89. Oncley, J. L., Annals New York Acad. Sci. 41:121 (1941)

90. Ardenne, V. and Weber, H. H., Kolloid-beihelfte 97:322 (1941)

91. Ziff, M. and Moore, D. H., Jour. Biol. Chem. 153:653 (1944)

92. Hall, C. E., Jakus, M. A. and Schmitt, F. O., Biol. Bull. 90:32 (1946)

92. Katchalsky, A., "Polyelectrolyte gels" 4:1 Progr. Biophysics (1954)

93. Moore, A. R., Jour. Cell Comp. Physiol. 7:113 (1935)

94. Danielli, J. F., "Cytochemistry" Wiley Co. (1953)